Pisa 9 marzo 2015

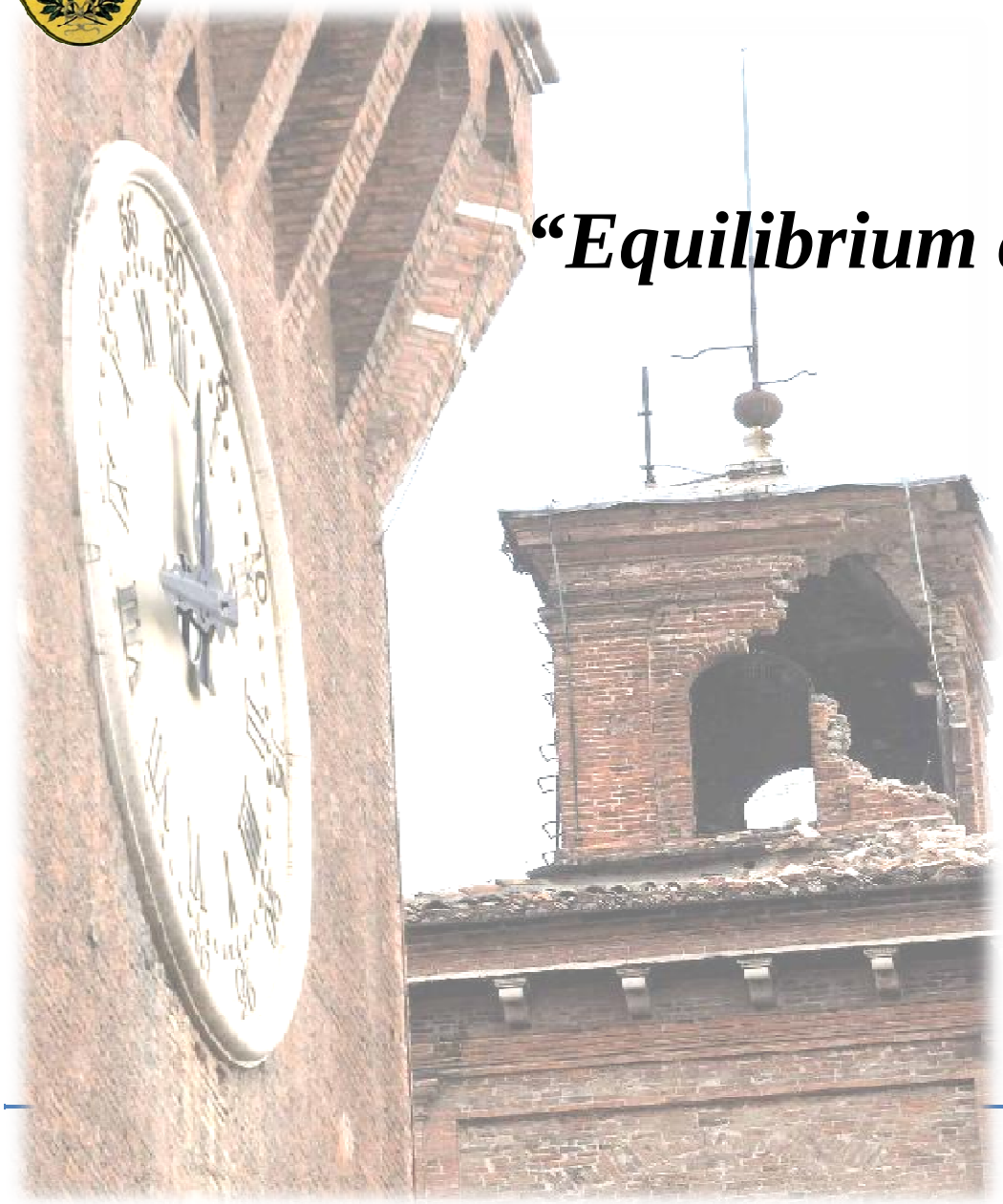

"Equilibrium and collapse of masonry vaults"

Antonio Tralli
Università di Ferrara

Summary of presentation

- *The '900 Italian masonry school*
- *A brief introduction on masonry vaults*
- *Computational methods:*

1. *Thrust network methods*
2. *F.E.M. incremental non linear analyses*
3. *F. E. M. limit and incremental analyses by rigid elements*

- *Recent (2014) papers*

Work in progress

Il materiale muratura

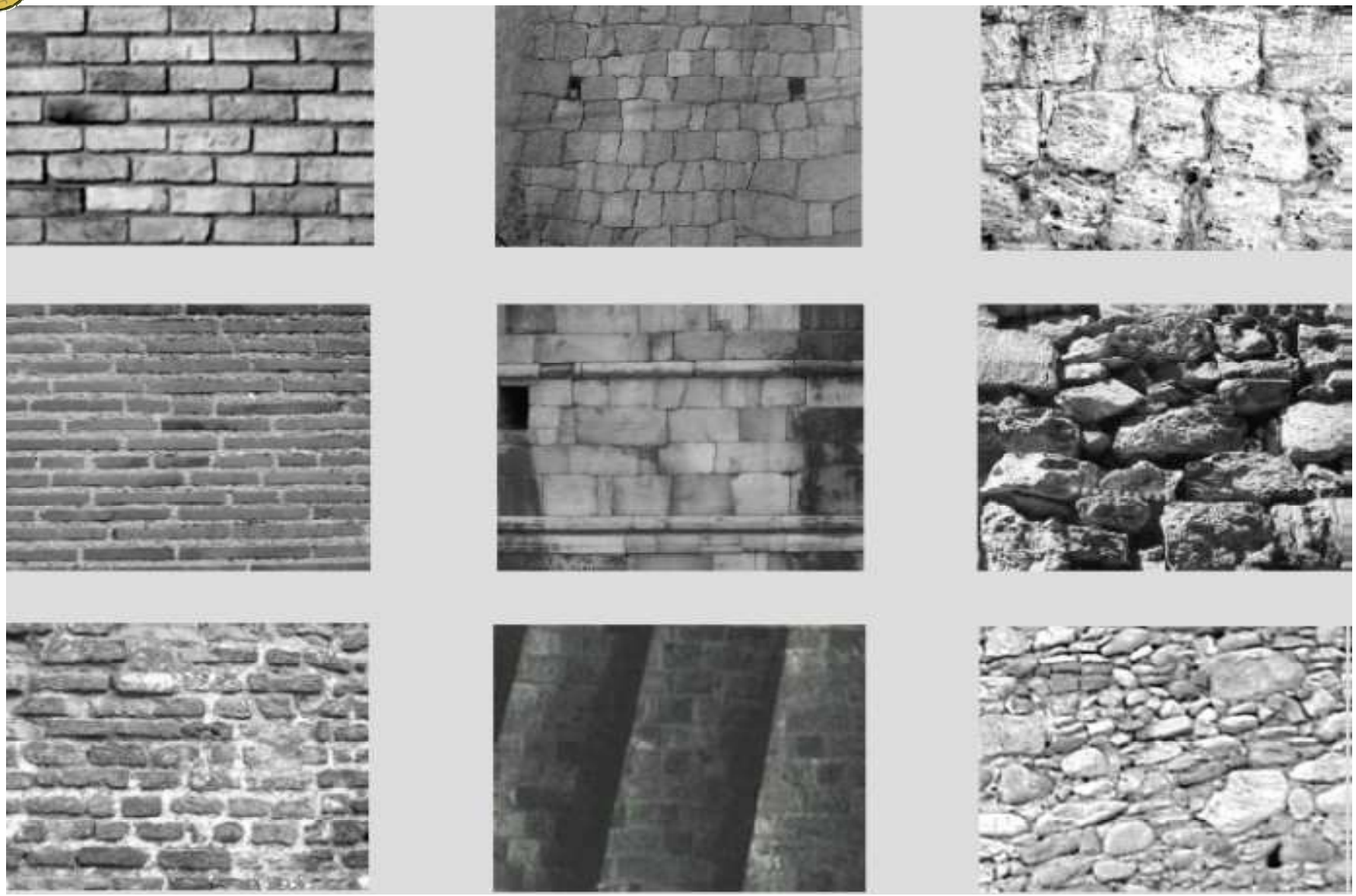

Il materiale muratura

- *Con il termine muratura si intende un materiale eterogeneo composto da più fasi solide*
- *La tipologia dell'apparato murario utilizzata in Italia è estremamente varia, si passa dalla muratura in laterizio con mattoni interi (come in Emilia) o forati alla muratura in sasso con elementi squadrati o meno (come a L'Aquila)*
- *Le caratteristiche meccaniche delle fasi componenti e del composito risultano molto diverse*
- ***La caratteristica saliente è la scarsa ed incerta resistenza a trazione che ha condizionato la forma stessa delle costruzioni***

Il materiale muratura

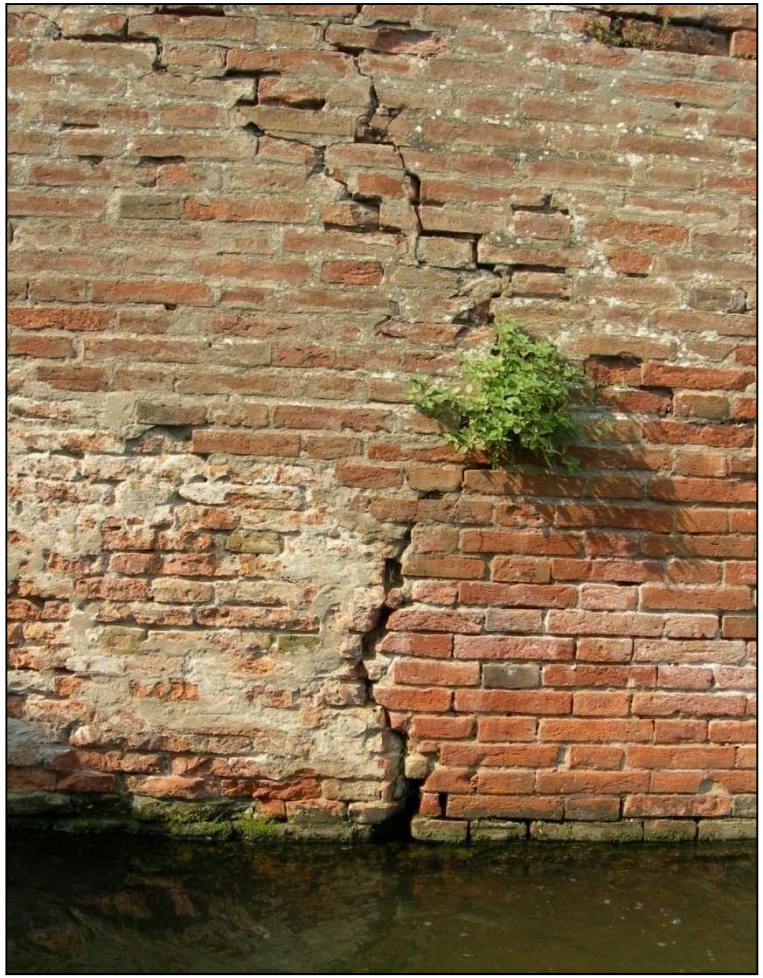

Muratura in mattoni di argilla e malta

I 3 ponti di Comacchio Ferrara **S. Francisco del Baron Valparaiso**

Il materiale muratura

Caratteristiche del "materiale" Muratura

- *Resistenza a compressione e modulo elastico (quanto mai vari).*
- ***La resistenza a trazione è esigua e comunque non affidabile**.*
- *L'eterogeneità delle caratteristiche meccaniche e dei comportamenti strutturali degli edifici in muratura, anche formalmente simili*, ***porta a prescrizioni normative assai diverse da quelle per le costruzioni in c.a. o metalliche.***
- ***Verifiche puntuali dello stato di tensione in una struttura in muratura sono prive di senso.***
- ***Pertanto, almeno bei maschi murari, verifiche allo stato limite ultimo in termini di N,M e T.***
- ***L'analisi elastica appare del tutto convenzionale.***

Le NTC08 , il D.M.del1987 e L'OPCM 3274 consentono un'analisi lineare solo al fine di valutare le caratteristiche della sollecitazione (N,M,T) nei vari elementi strutturali, mentre le verifiche sono di fatto agli stati limite.

The '900 masonry Italian school

Masonry structures do not behavior as an elastic continuum

"Something deserves to be reviewed in the mechanical baggage of the civil engineer …….between Mechanics and the chapter which is occupied by the theory of Elasticity. Due to the resulting confusion, all progress which, since the time of Cauchy, has been made with the help of modern computerized algorithms in understanding the behavior of elastic structures could be referring to "tout court" construction, and even ancient cathedrals or temples are viewed in this same light".

(**A. Giuffrè** *Letture sulla meccanica delle murature storiche. Kappa Rome1990)*

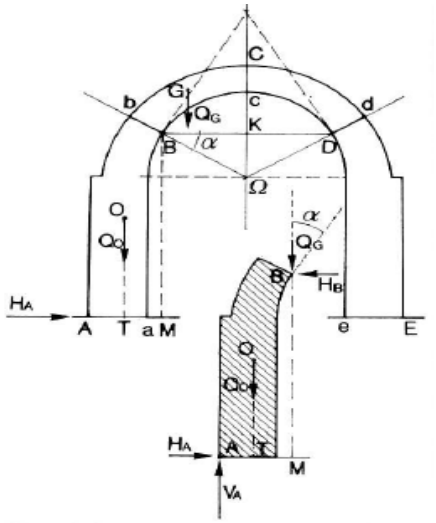

Fig. 9.44.

In masonry the form of the resistant structure depends on loads

"Una costruzione in acciaio, o in c.a., quando viene spogliata dalle parti di completamento… mette in luce l'organismo resistente, lo scheletro strutturale a cui sono affidate tutte le funzioni statiche. Questo organismo … può e deve sopportare tutte le azioni esterne,…e talvolta, le azioni sismiche. Tali azioni possono variare ma lo scheletro resistente è sempre lo stesso. Viceversa nelle costruzioni in muratura lo scheletro resistente, la struttura, non è mai fissa ma dipende dalle azioni esterne, salvo che non sia stata concepita essa stessa come struttura resistente: è il caso unico, e diffuso in zone non sismiche, del gotico."

(**S. Di Pasquale** *The Building art* (in Italian) Marsilio Venice 1996)

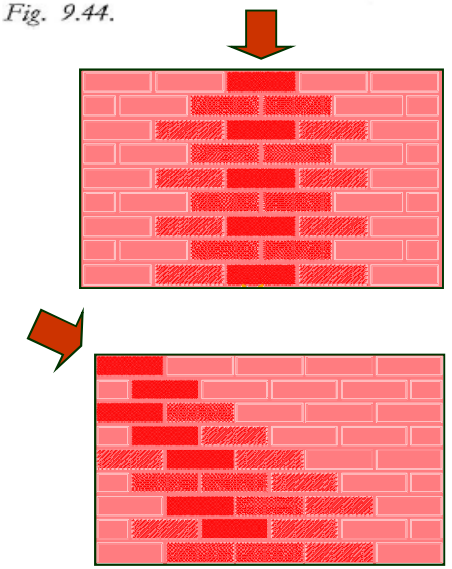

Materiale Elastico non Lineare (non resistente a trazione)

E' il metodo classico proposto negli anni 80 del secolo scorso (Di Pasquale, Como,Villaggio, G. Romano….etc.)

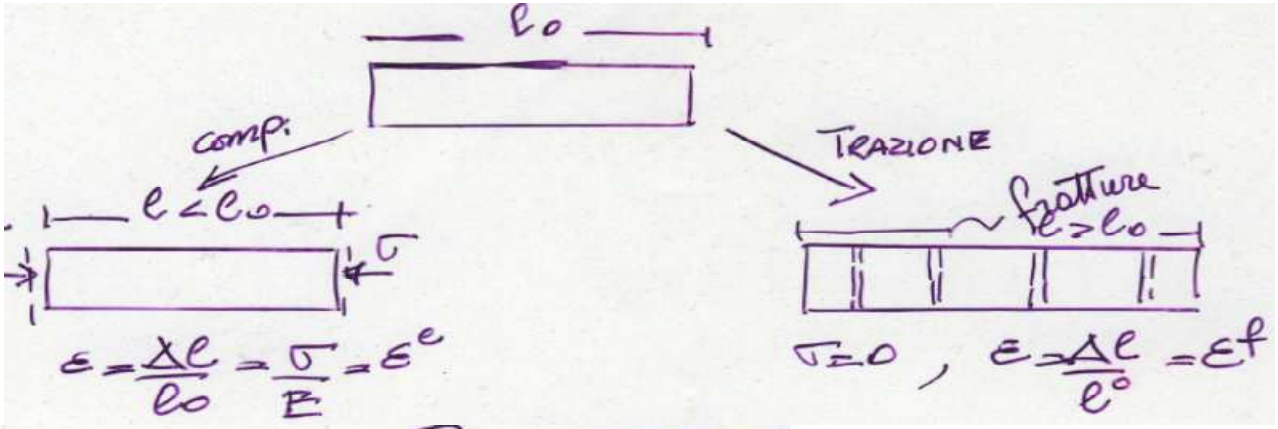

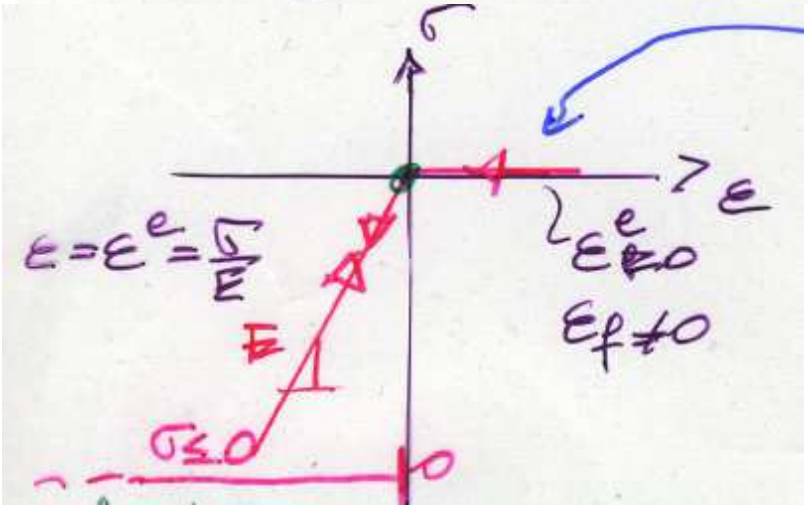

NO TENSION MATERIAL

La muratura è considerata un materiale elastico non lineare (**olonomo**) (la lesione si deve richiudere prima di trasmettere sforzi)

La resistenza a trazione è supposta nulla

A compressione si ha un comportamento elastico (eventualmente elasto-plastico). Vale il principio della massima dissipazione e valgono i teoremi dell'analisi limite (Del Piero 1991)

The ‘900 masonry Italian school

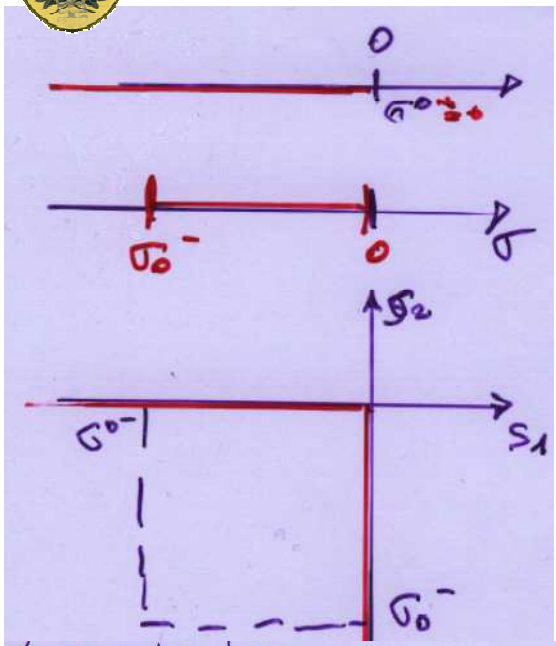

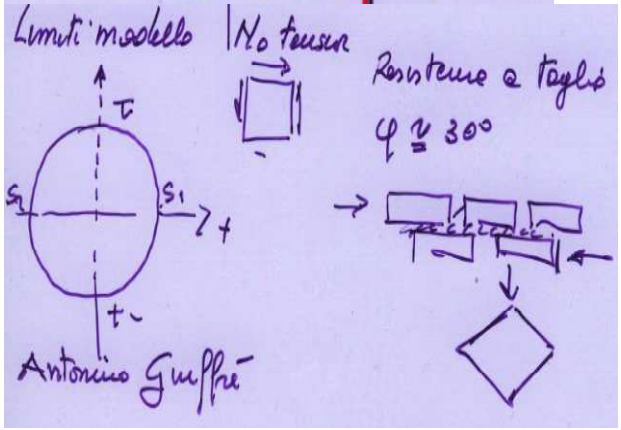

Dominio di ammissibilità per NTM

•Lo stato scarico non è all’interno del dominio

•Il problema è formulabile all’interno della teoria delle diseguaglianze variazionali di Lions e Stampacchia (Giusti, Giaquinta, Anzellotti, Dal Maso etc..)

•Non è garantita l’esistenza della soluzione per qualunque condizione di carico

•All’eleganza di questa formulazione corrisponde una grande difficoltà di ottenere formulazioni numeriche efficienti e con queste di ottenere risultati di utilità tecnica.

•Nelle strutture in muratura gli spostamenti in campo elastico sono molto piccoli e non significativi

Anisotropia dello yield locus e dipendenza dalla inclinazione del carico rispetto ai giunti orizzontali - PAGE 1981, DHANASEKAR PAGE E KLEEMAN 1985

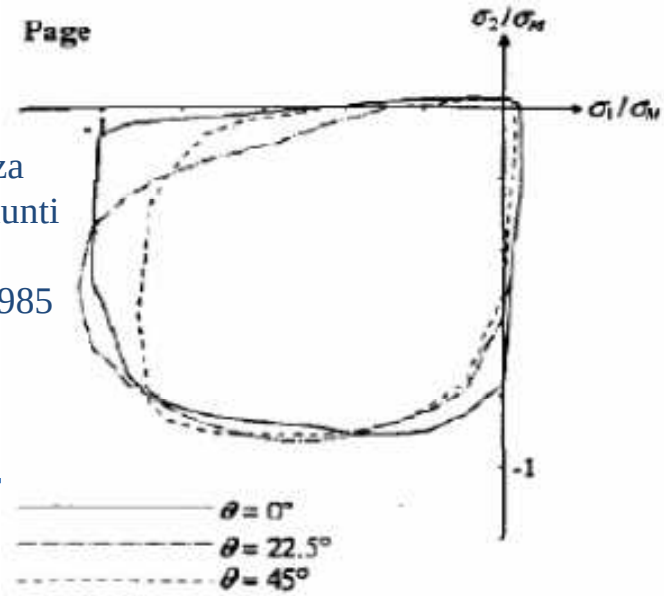

Già Antonino Giuffrè sottolineava il limite essenziale dell’impossibilità di mettere in conto l’attrito

The ‘900 masonry Italian school

a)

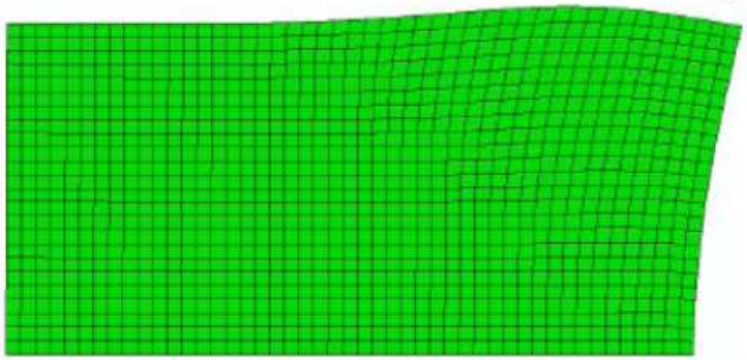

b)

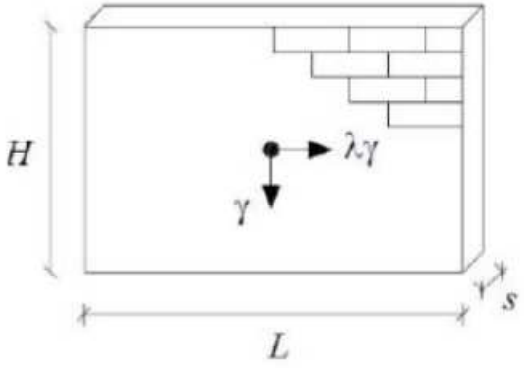

a)

b)

Figure 5.21 Masonry walls under uniform vertical and horizontal accelerations:(a) view of the walls,(b) system of application of the load adopted by Ceradini (1992).

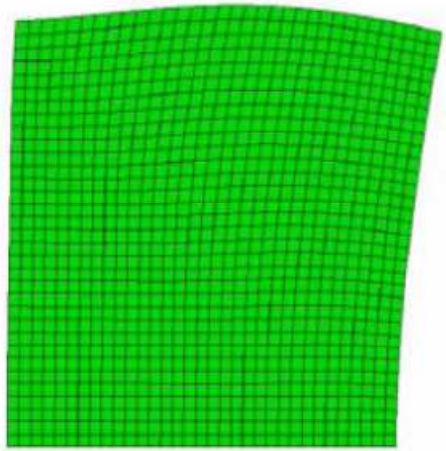

Confronto fra modellazione FEM (deformata Elastica) e le prove svolte a Roma La Sapienza 1992-1993 nell’ambito della tesi di dottorato di Ceradini sotto la direzione di Antonino Giuffré

- *A brief historical introduction on masonry vaults*
- *Things that have to be taken into account*

E. Benvenuto *-An Introduction to the History of Structural Mechanics, Springer-Verlag, New York 1991.; vol. II: Vaulted Structures and Elastic Systems, pp. I-XXII, 307-554.*

Masonry curved elements – as for instance arches, domes and vaults – represent one of the most diffused structural typologies in historical buildings of both Eastern and Western architecture. Moreover, the growing interest in the preservation and rehabilitation of historic constructions has created a need for the development of new efficient tools for the analysis and the evaluation of load-bearing capacity of these structures but we can not ignore the knowledge of the their methods of design and construction technologies

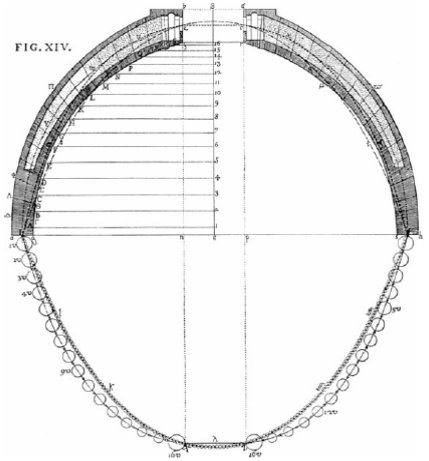

Poleni 's solution describing the Equilibrium of S. Peter's dome as the inverted shape of a catenary- Poleni. G. 1743 Padua

The XVII century English approach

"Ut pendet continuum flexile, sic stabit contiguum rigidum inversum" as hangs a flexible cable, so inverted, stand the touching pieces of an arch" R.Hooke (1676,1705), D. Gregory (1698)

The XVIII French contributions

The first "scientific" graphical attempts for the study of the equilibrium of masonry domes go back to the early 18th century and are due to, e.g. Bouguer (1734), Bossut (1778), Coulomb (1773- also taking into account friction), stated mono-dimensional equilibrium equations, neglecting the role of circumferential forces. Also Italian scholars as Mascheroni (1785) gave significant contributions.

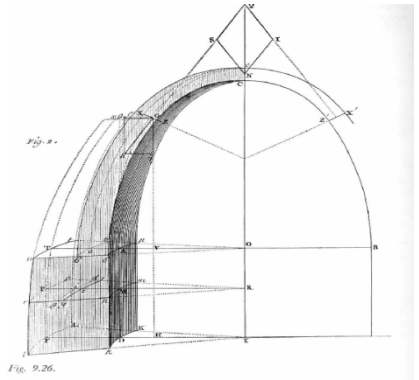

A brief historical introduction on masonry vaults

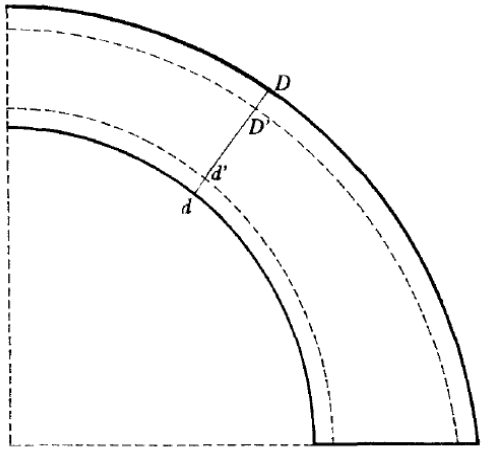

During the 19th century the theory of elasticity was developed and a new look was given to the statics of arches (C. Navier 1826); after that, for almost fifty years, the researchers – for instance Mery (1840)- tried to conciliate the traditional approach in terms of rigid body analysis with the new claims in the name of strength and elasticity . The elastic solution is admissible following limits that are fixed by Méry on the basis of the very personal criterium for which the distance of he thrust line from the extrados and intrados «doit etre assez grand pour supporter les deux tiers de la pression totale».
Consequently a number of Thrust lines are possible and is possible to check the existence of admissible solutions without requiring to find the true one: as Durand-Claye (1867) writes, ***«de la possibilité de l' équilibre, nous concluons a la stabilité».***

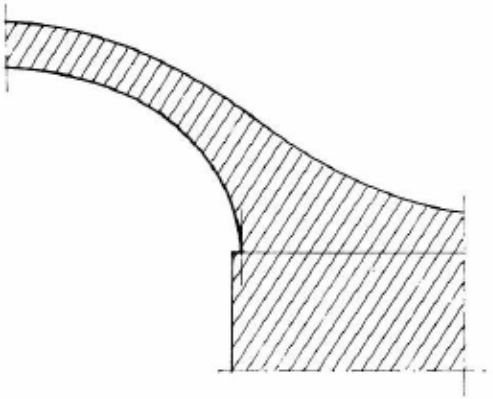

Anyway, what appeared clear from the beginning, was that cracking occurs on curved masonry elements in presence of self-weight and of very low tensile stresses (hoop membrane stresses = 0 for f = 51,8° in spherical domes).
In this context, a considerable improvement in the analysis of spherical domes was achieved when Levy (1888) proposed a graphical analysis aimed at finding the circle on which circumferential forces vanish.

C.PESCIULLESI et al."On optimal spherical masonry domes of uniform strength" J. ST. ENG. ASCE 123, pp. 203-209, 2 Feb. 1997.

The XX century main contributions

As regards masonry arches and vaults (made of stone blocks or solid clay bricks), a sound theoretical framework exists and nowadays - following S. Huerta or M. Como - it can be affirmed that the modern theory of limit analysis of masonry structures, which has been developed mainly by **J. Heyman**, is the most reliable tool to understand and analyze masonry curved structures. For the sake of completeness, it is worth citing also the previous papers of Pippard and Ashby (1936) on the analysis of masonry arch bridges and the Ph. D. thesis of A. Kooharian in 1952 at Brown University where the basic idea appeared for the first time.

According to Heyman formulation, the limit theorems of plasticity can be applied to masonry structures provided the following conditions are verified:

(1) The compression strength of the material is infinite;

(2) Sliding between parts is impossible;

(3) The tensile strength of masonry is null.

These conditions enable the application of the well known limit theorems of Plasticity- **static** (lower bound) and **kinematic** (upper bound) theorems. The possibility of extending limit analysis theorems to no tension materials has been completely proved by Del Piero (1991).

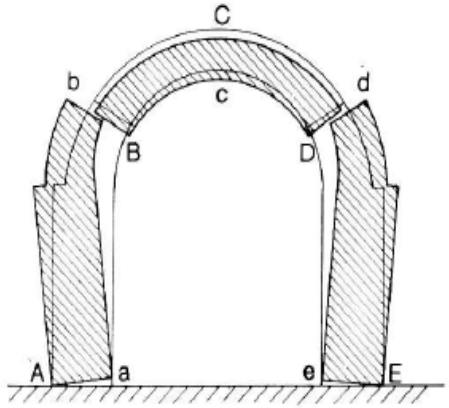

Fig. 9.43.

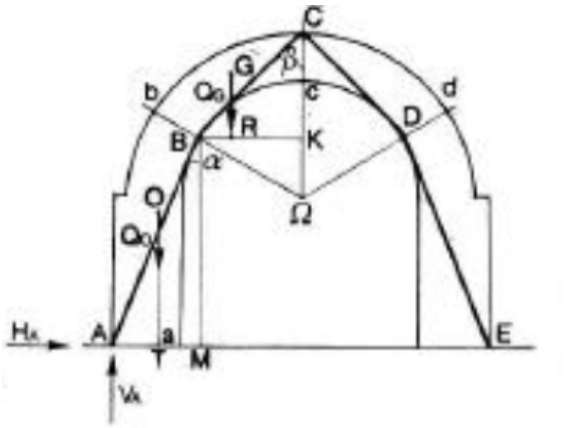

The contribution of Mascheroni
According to Benvenuto

A brief historical introduction on masonry vaults

Static -The structure is safe, meaning that the collapse will not occur, if a statically admissible state of equilibrium can be found. This occurs when a thrust line can be determined in equilibrium with the external loads .

Kinematic- if a kinematically admissible mechanism can be found, for which the work developed by external forces is positive or zero, then the arch will collapse.

However in the technical literature the Heyman's limit analysis solutions are limited to 1-d case such as arches or barrel vaults (Lucchesi et al 1997 etc..) unreinforced, steel reinforced (Roca et al., 2007) FRP reinforced (Briccoli Bati et al 2007, Caporale et al 2006-2013), or simplified models for studying geometrical complex domes (Bagicalupo et al. 2013)

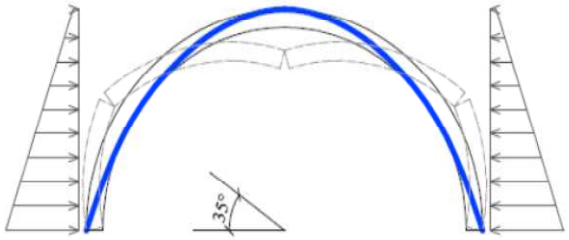

Curva delle pressioni (linea continua blu) dell'arco 8 lunetta 'A' e relativo cinematismo

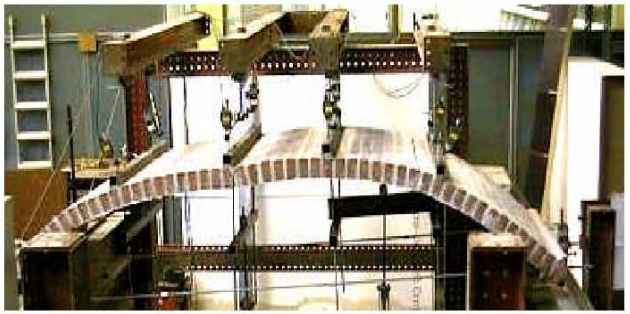

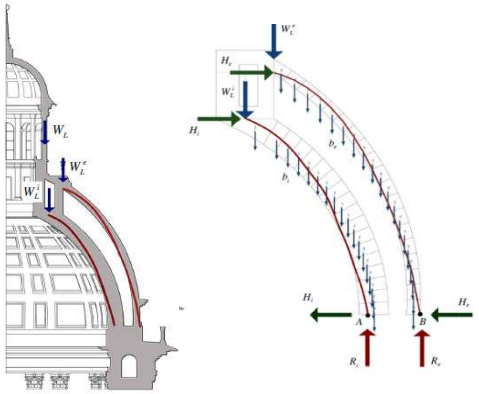

A. Bacigalupo, A. Brenchich, L. Gambarotta "A simplified assessment of the dome and drum .." Eng. Struct., 56,749-765,2013

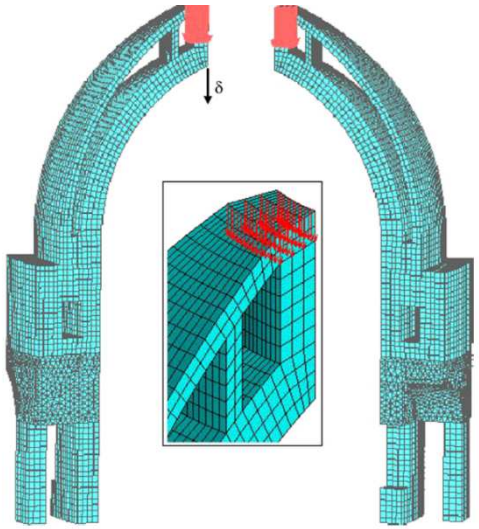

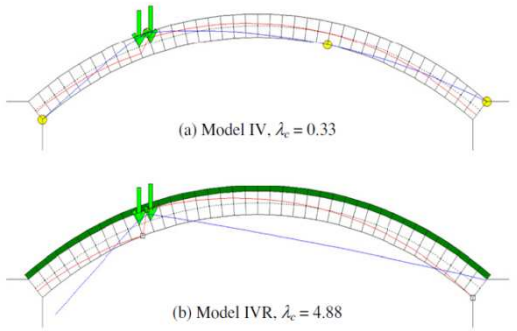

Fig. 22. Collapse mechanisms and collapse multipliers of the models IV and IVR for $t = 100$ mm.

Caporale and Luciano Composites part B 2013

Things that we must take into account

The study of masonry vaults should take into account the essentials of the material “masonry”:

1.Heterogeneity

2.Almost no resistance to tension and good compressive strength

3.High friction coefficient

4.Overall importance of geometry for achieving the equilibrium

The modern theory of limit analysis of masonry structures , which has been developed mainly by J. Heyman, is the tool to understand and analyze masonry vaults. (S. Huerta *Mechanics of masonry vaults: the equilibrium approach. In: Lourenço PB, Roca P, editors. Proc. III International seminar on structural analysis of historical constructions, Guimaraes, 2001.Balkema)*

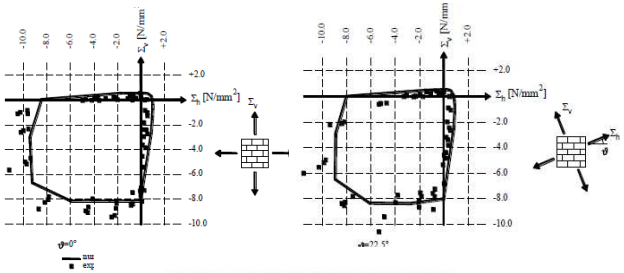

COMPRESSIONE-COMPRESSIONE

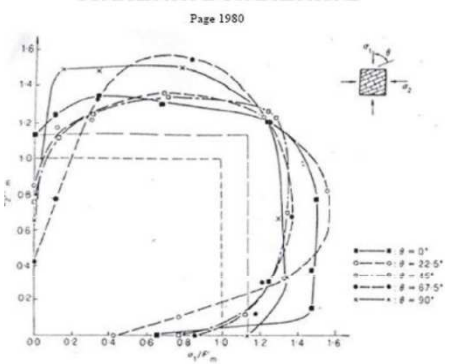

Page 1980, Dhanasekar, Page and Kleeman 1985

1. ***Heterogeneity***-The masonry it is obviously in any case an heterogeneous composite material (made by clay bricks or stone blocks and mortar) and would have a non isotropic behavior either in the elastic field and at collapse. Moreover in the case of vaults the texture can be completely different in the different parts.

Courtesy of prof. A. Cazzani, Cagliari

2.Almost no resistance to tension and good compressive strength

The traction strength it is quite variable and uncertain, usually the crisis occurs in the interface between mortar and brick which is modeled according to Lourenço and Rots (1997),Sutcliff and Page (2001) . As it concerns compression see previous slide.

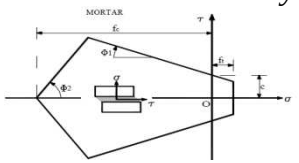

Tension test on brick

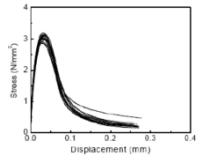

3.High friction coefficient

According to Vasconcelos and Lourenço (2006) the friction coefficient for historical masonry is $\mu = 0{,}4\text{-}0{,}6$. However the normality is loss and the flow rule is not associate, in this case, as it well known Radenkovic (1960) or Salençon (1977), the limit analysis theorems do not hold and LP methods cannot be used. A number of authors proposed different numerical methods (Livesley (1978), Orduna and Lourenço(2005) ,Tangaramvong and Tin-Loi .

The effects of friction on static behavior of masonry vaults has been studied by D'Ayala and coworkers, (D'Ayala and Casapulla 2001, D'Ayala and Tomasoni 2011) who assert that limit state analysis with finite friction allows investigating two aspects previously neglected for masonry vaults: the possibility of sliding mechanisms between the blocks and the importance of three-dimensional stress fields in the equilibrium of complex vaults. Particularly the analysis has been able to show that for values of the coefficient of friction smaller than 0.5, sliding becomes a critical failure mode and further increases in thickness are necessary to re-establish equilibrium.

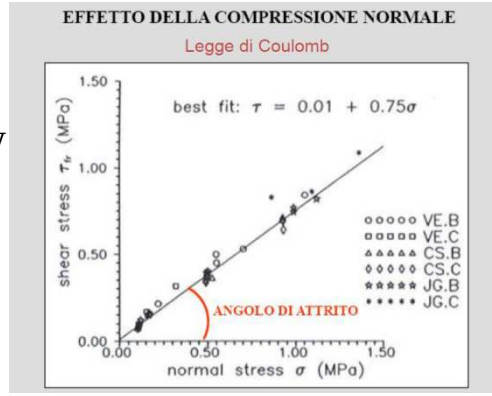

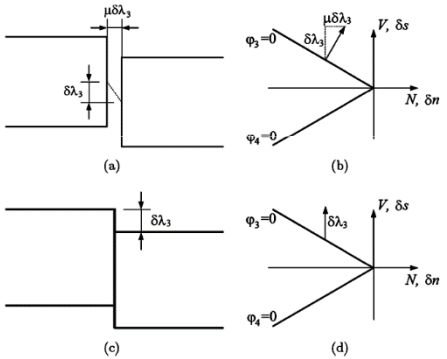

Associated flow rule (*top) with* $\mu = \tan = \tan\psi$, *and* non-associated flow rule (below), with null dilatancy ($\tan\psi = 0$). The yield criterion is represented as relationship between the normal (*N)* and shear forces (*V)*

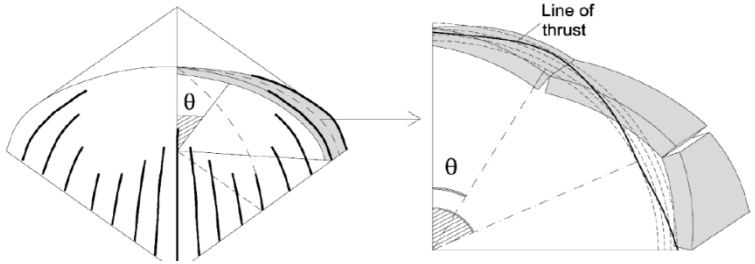

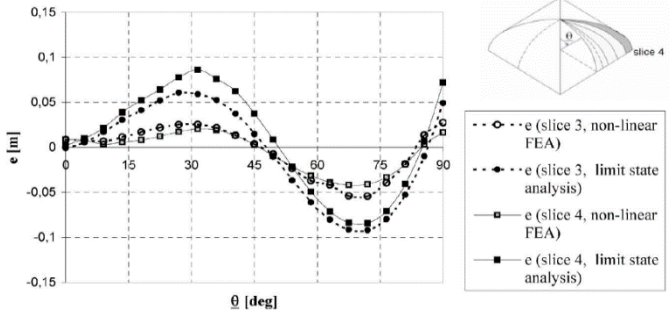

4. Overall importance of geometry for achieving the equilibrium

Nowadays new laser scanner techniques are available for accurate geometric surveys of actual masonry vaults (Schueremans and Van Genechten 2009). Obviously the evaluation of gravity loads and of their work in the kinematic limit analysis or of the thrust line in the static approach depends on the way the geometry is taken into account. For instance, an example of this effect can be appreciated by looking at the difference between the limit load multipliers evaluated by curved six-noded elements and by plane triangular elements, as shown in Figure 7, in the case of a hemispherical dome. Either the thrust line or the evaluation of gravity loads and of theirs work depends on the geometry. (The difference between the load multiplier evaluated by curved and plane triangular elements is shown.

Carini and Genna (2012) for a particular case study (a old masonry vaults under compressive longitudinal loads) state: in the case of the Drucker Prager modeling, this imperfection causes a reduction of collapse load,with respect to the perfect case, of about 65% (from 14.93 to 5.45 MN). This gives good evidence of the extreme importance of the correct definition of the starting geometry for t class of problems.

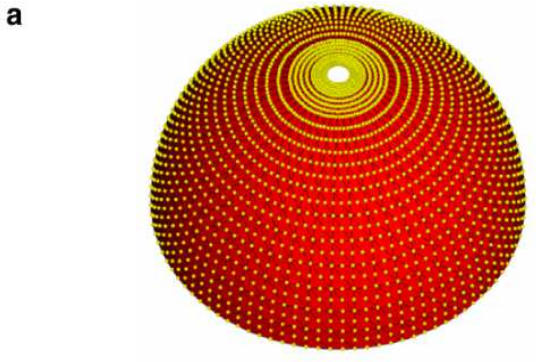

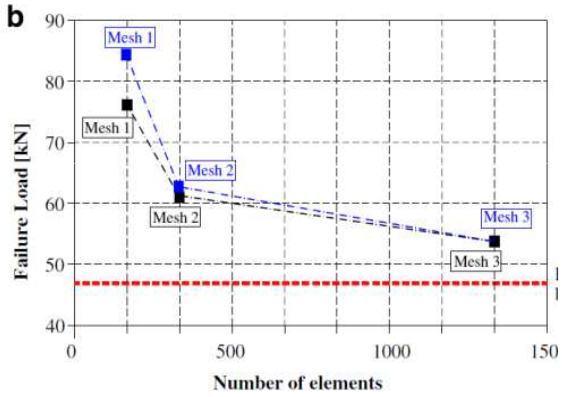

Solid geometry of the nave vault as produced by the software JRC 3D Reconstructor

Things that we must take into account

5.- The importance of taking into account the fill-in. A large amount of technical literature deals with masonry arch bridges due also to the consistent number of railway masonry arch bridges that are still in service . In this context the importance of taking into account the back fill has long been recognized. Recently Cavicchi and Gambarotta (2005) have rigorously investigated the role played by the backfill in the determination of the actual bearing capacity of 2D bridges and Milani and Lourenço (2012) have presented a 3D limit analysis study of a skew masonry arch bridge by taking into account transversal effects..

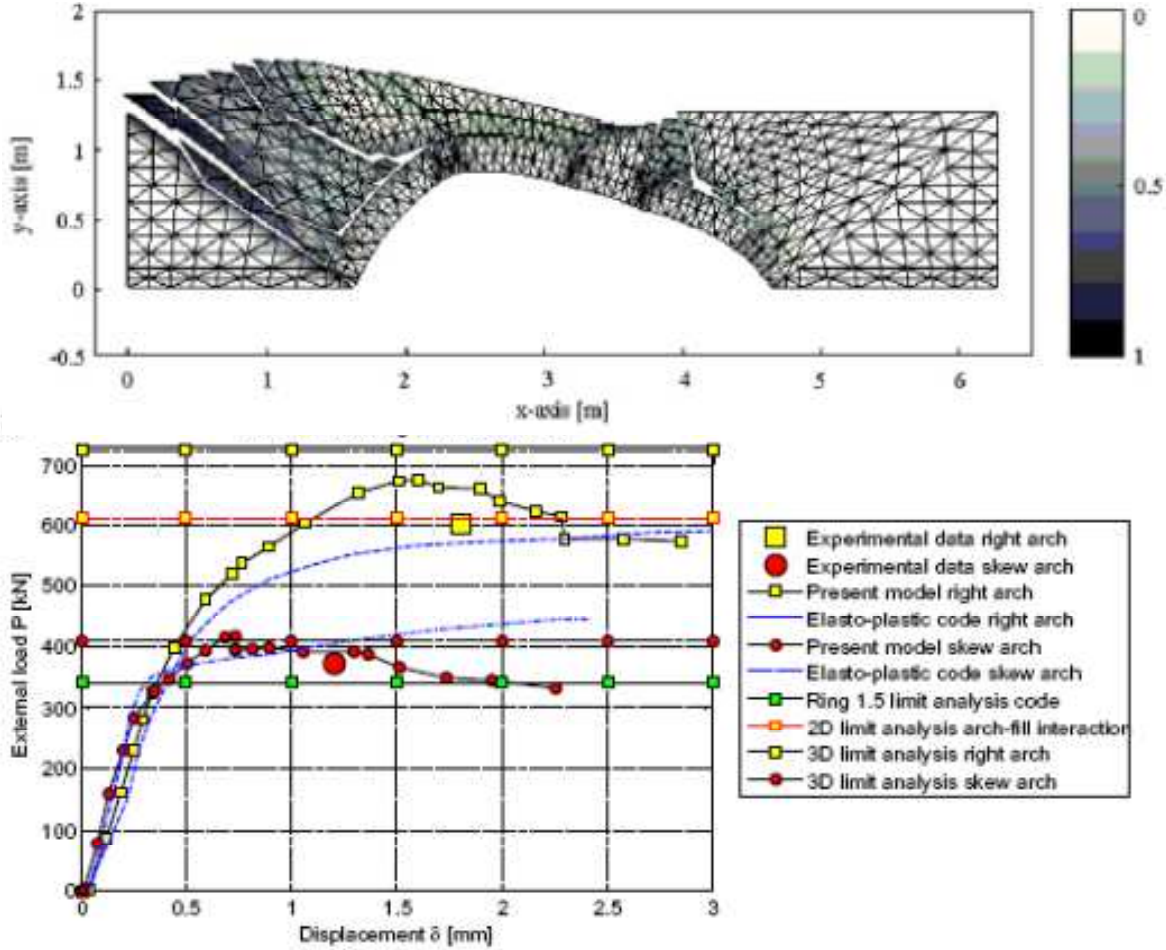

Vertical load-maximum vertical displacement curves obtained in Milani et al.. In the figure experimental data available, collapse loads provided by Ring program, 2D FE limit analysis with arch–fill interaction, 3D FE limit analysis and elastic-plastic FE models are also represented. (b) Deformed shape at collapse obtained by using the 2D limit analysis code with arch–fill interaction.

Things that we must take into account

6.- Importance of taking account the existing cracks- Actual masonry vaults present generally a diffused crack pattern due too many and mostly unknown factors (building sequence, settlement of foundations, seismic events, wrong consolidation works etc.). The crack pattern obviously affects the structural behavior and should be considered in the analysis. It can be observed that, at least in masonry vaults built with regular stones or solid clay bricks, the cracks are evident and clearly separated from each other; moreover treating cracks as distributed distortions appears still questionable.

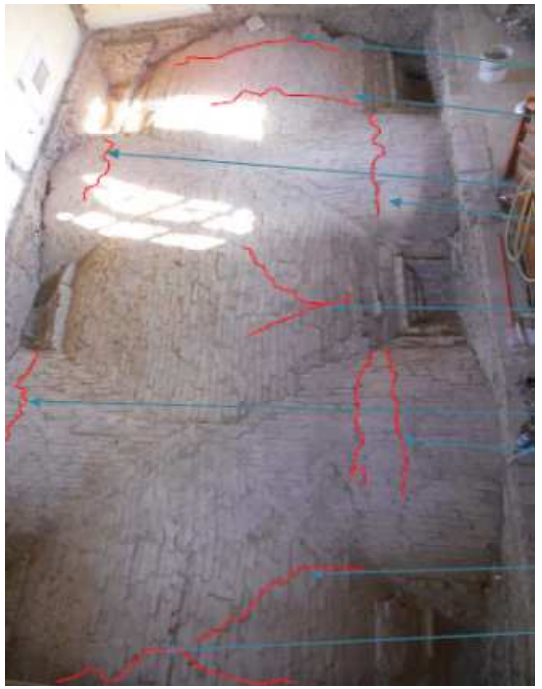

Chile 2010 – Valparaiso S. Francisco del Baron damaged by an old seismic event, Santiago SS. Sacramento . Both of Arch. Provasoli 1880-1890, Torre Fornasini XII century Emilia 2012

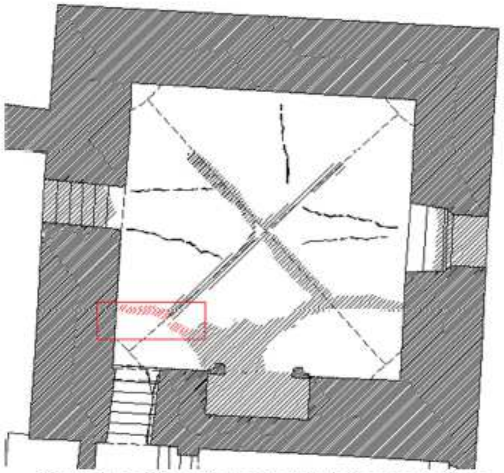

Figura 7: Posizione in pianta della lesione esaminata

La muratura della volta è disposta per ogni unghia a filari normali alle linee di perimetro della stanza, parallela alle generatrici.
Lo spessore della volta sembra di 3 teste con i mattoni disposti di coltello (Figura 9) e qualche mattone disposto di testa (diatoni) come a creare un collegamento tra gli strati di muratura ma senza un ordine preciso (Figura 10). Tale disposizione si è notata osservando la tessitura presente tra le fessure più grandi (Figure 7 e 8). Al di sopra della volta sono presenti ancora mattoni ma con una disposizione molto confusa, probabilmente utilizzati con la funzione di riempimento (Figure 11 e 12).

Figura 8: Localizzazione della lesione studiata

Figura 9: Dettaglio dello spessore e tessitura della volta

Figura 10: Presenza di diatoni

Figura 11: Probabile riempimento della volta con mattoni

Figura 12: Dettaglio tessitura volta nella zona della lesione

S. Felice sul Panaro

Stanza di Giulio II

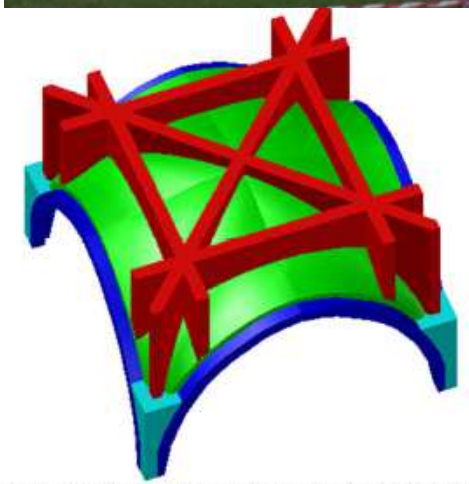

Figura 39:Modello 3d della volta; si sono indicati: in verde la volta a crociera, in blu gli archi perimetrali, in rosso i frenelli, in ciano i pilastri della volta su cui scaricano le pressioni gli elementi costituenti la volta

Computational methods

Thrust network methods

In order to extend thrust line to spatial structures, O'Dwyer (1999) introduced the use of 3D funicular force networks defined in plan. Even though the fixed network in plan still inherently gives rise to conservative results, these 3D networks give a much better understanding of vaults than the previous simplified analysis that combines one-dimensional thrust line analyses. Building on O'Dwyer's seminal work, thrust network analysis (Block and Ochsendorf 2006-7) addressed the first issue by introducing Maxwell reciprocal force diagrams, which describe the possible horizontal equilibria of compressive funicular networks, named thrust networks, under vertical loading. An important drawback of the original thrust networks framework, as presented in the abovementioned references, was the lack of a general algorithm and the necessity of the manual manipulation of the reciprocal force Diagrams. The extensions that overcome this limitation are discussed in Block and Lachauer (2014).

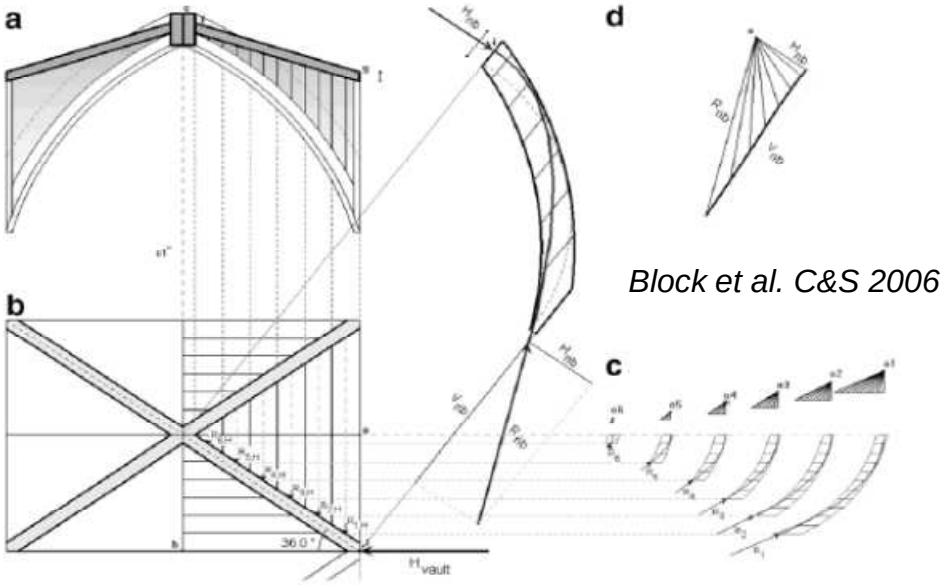

Block et al. C&S 2006

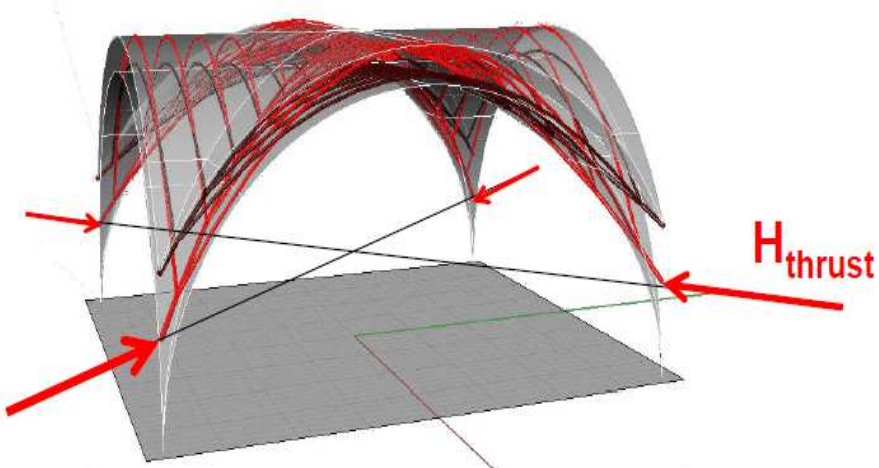

Block P, Ochserdorf J (2007) Thrust network analysis: a new methodology for three-dimensional equilibrium. IASS 48(3):155

Thrust network methods

Another recent approach for 3D equilibrium analysis based on funicular networks and inspired to Gaudi's hanging models has been proposed by Andreu, Gil, and Roca (2007, 2010).
A different approach to TNA for generating funicular networks in the presence of vertical loading has been proposed by Fraternali (2010), as a specific 3D extension of the lumped stress method (Fraternali , Angelillo et al.2002). It can be showed that their equilibrium conditions and global framework, separating horizontal and vertical equilibrium, was entirely equivalent to thrust network analysis, but in contrast, this approach, based on the discretization of Airy stress functions, presented some challenges with respect to singularities in the boundary conditions and loading, or discontinuities, such as cracks or openings, in the discretized equilibrium surfaces and the supports (Babilio et al. 2008, Angelillo et a. 2013). Such structures are unilateral membranes, whose geometry is described *a la Monge*, and the equilibrium of them, under vertical loads, is formulated in the Pucher form. The unilateral restrictions require that the membrane surface lies in between the extrados and intrados surfaces of the vault and that the stress function be concave. The unilateral assumption renders the membrane an underdetermined structure that must adapt its shape in order to satisfy the unilateral restrictions

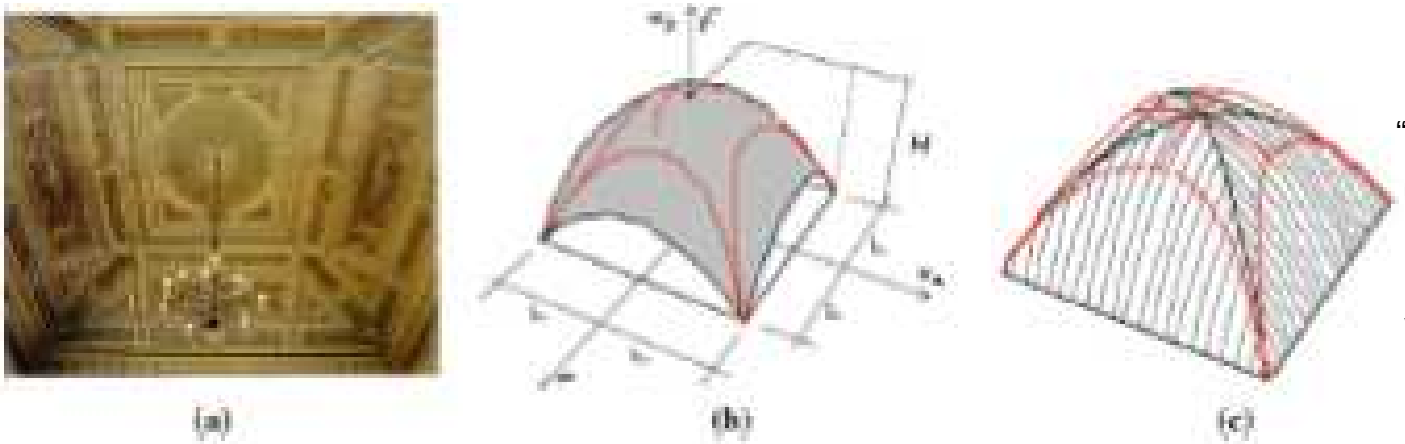

Angellillo et al. 2013
Cloister vault, "Soffitto Verde", in "Palazzo del Pozzo della Cisterna", Torino. *Parabolic shape* of the thrust membrane (**b**) and comparison with the intrados surface of the cloister vault: (**c**). A reduced portion of the *parabolic shape*, that is, inside the masonry is shown in **b** and **c**,

Thrust network methods

A different approach based on a selection of membrane stress surfaces and obeying equilibrium and a no tension masonry constitutive equation has been recently presented by Baratta and Corbi (IJSS 2007,2010). The problem is expressed in terms of a suitably defined stress function allowing some simplification. The solution is then sought by using a complementary energy approach Haar-Karman 1915- Cuomo and Ventura 2000)

. In general it is also proved that under gravitational loads the equilibrium of the vault implies its admissibility. This result is quite significant because it explains why it is possible to build up masonry vaults by simply hypothesizing a resistant shape under the assigned loads.

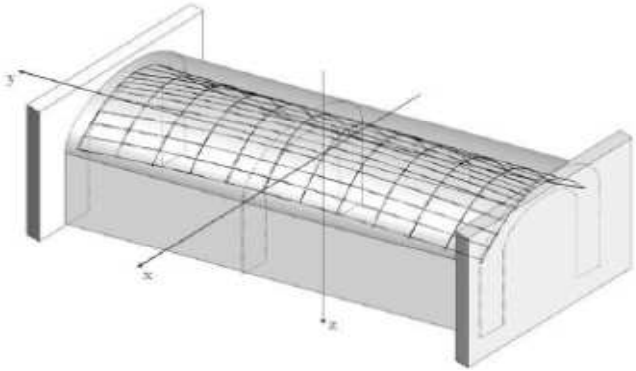

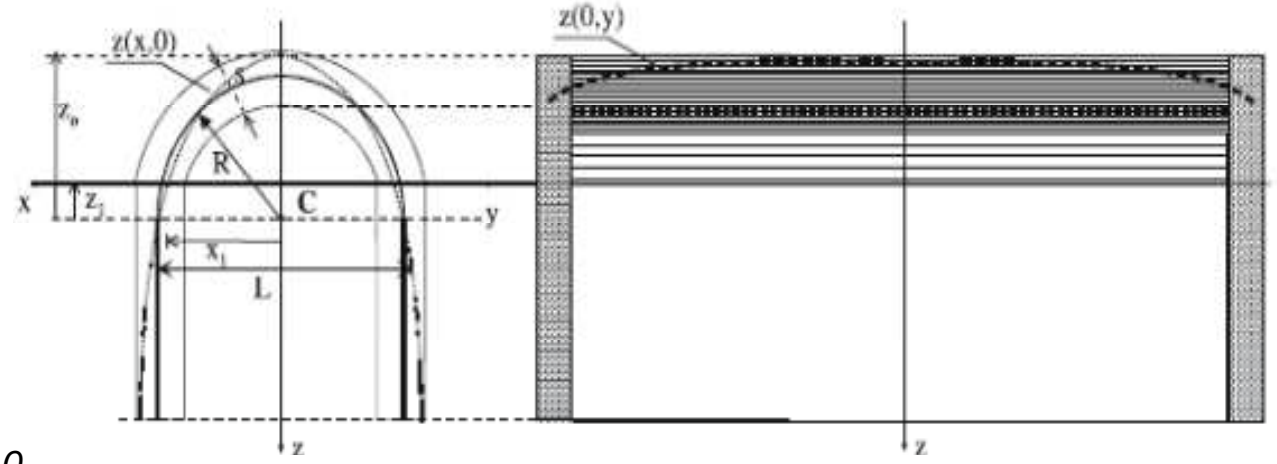

Baratta and Corbi 2010

2D representation of a confined barrel vault with the trace of a possible membrane surface.

FE programs for masonry vaults

Unsurprisingly, ancient masonry vaults have been studied since long time ago by using the most advanced tools available for structural assessment. The first researches on the static behavior of these structures began in the late 80s of the last century for instance at the University of Florence Chiarugi et al.(1993) studied the Brunelleschi Dome of S. Maria del Fiore . A complete report of these studies is in Roca et al. (2010)

A number of FE commercial programs are used in the technical literature for modeling masonry vaults e.g. Carini an Genna (2012) and Bagicalupo et al. (2013) used ANSYS with elastic-plastic material models (either Drucker-Prager or Willam-Wranke with low tension strength), D'Ayala and Tomasoni (2011) used Algor V21 with contact elements, Abaqus is used at Polimi, Midas (CSP-FEA) with the so called concrete model, ADINA etc.

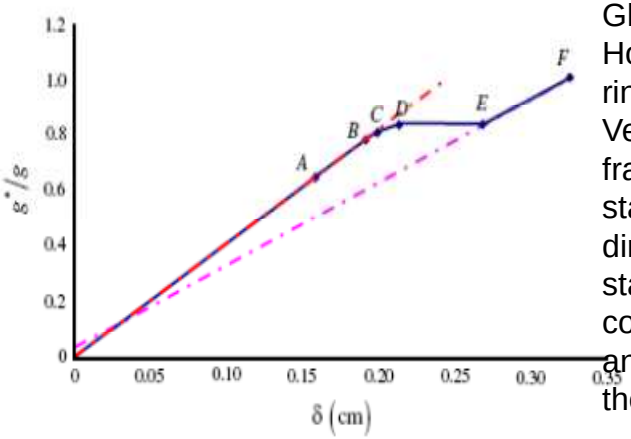

Bagicalupo et al. 2013
Global response of the dome–drum system. Horizontal axis: vertical displacement of the upper ring of the dome (positive means downwards). Vertical axis: fraction of the dead loads. Point – fraction of the dead loads: (A) 65% cracking started, (B) 78% cracks aligned in the meridian direction, (C) 80% non-linear global response starts, (D and E) 84% before and after crack coalescence and fracture on meridian direction and (F) approx 100% + convergence tolerance of the non-linear analysis

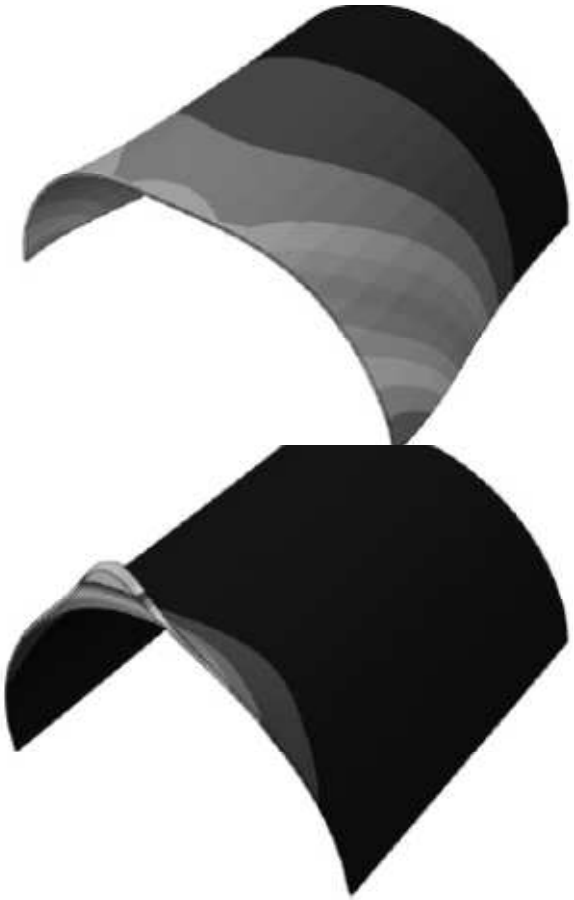

Carini and Genna_2012 Up FE analysis with linear elastic material; down with Drucker–Prager no tension-like material.

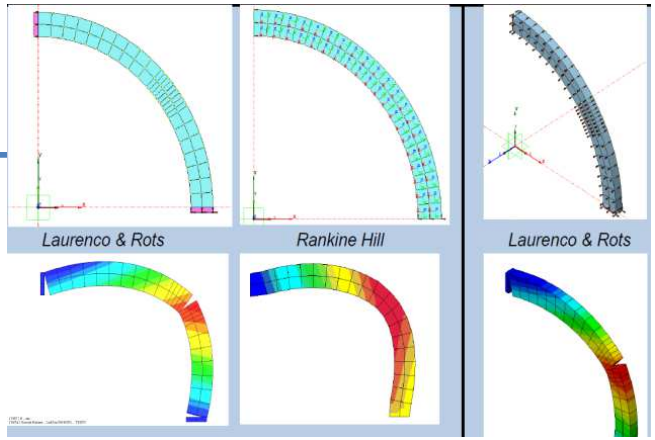

To my Knowledge only 2 programs contain specific software developed for study masonry curved structures DIANA TNO Delft (Lourenço 1996 and Lourenço et al. 1997-2000) and NOSA CNUCE Pisa (Lucchesi et al. 2007)

DIANA refers to the Ph. D. thesis of P.B. Lourenço at Delft University, is based on an accurate modeling of the masonry mechanical behaviour which requires a thorough experimental description of the material

A basic notion is introduced, named softening, to represent the gradual decrease of the mechanical resistance under a continuous increase of the deformation imposed on a material specimen or a structure. DIANA recovers, if necessary, the mesh independence by some numerical procedures derived from brittle fracture Mechanics and allows to use contact-gap element

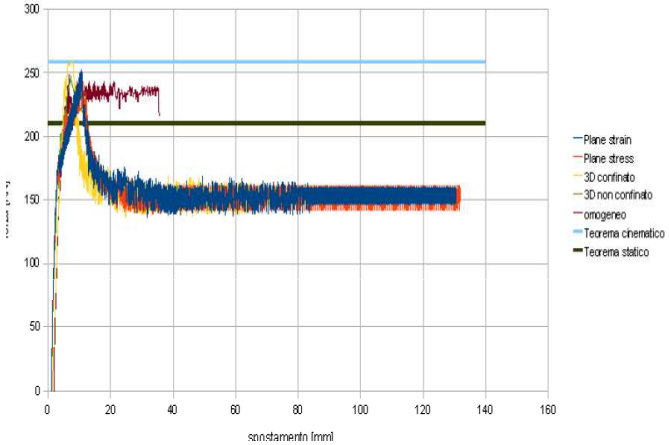

Main drawbacks encountered:

- *It is very difficult to set material parameters properly*
- *Often the procedure do not converge, always do not converge if more than 20-30 gap elements are active.*
- *The solution obviously depend on the load history.*
- *The presence of smeared cracks is not physical*
- *It is not so easy to interpret the results so obtained*

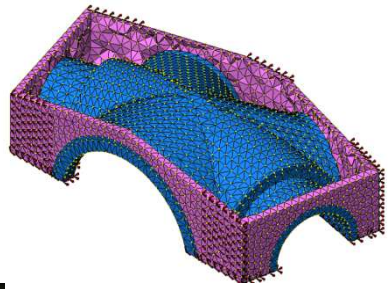

Pizzolato et al. SAHC 2011

FE programs for masonry vaults :*Elastic no tension material*

Following the suggestions of Di Pasquale a number of mathematicians studied masonry like materials in the context of the variational inequalities theory of Lions and Stampacchia (Giusti e Giaquinta, Anzellotti …) and formulated the proper functional setting (BV functions). At the end of the last century a lot of work has been done in this field (Villaggio, Del Piero, Panagiotopoulos, Shilavy, Lucchesi…). The main hypotheses are that *masonry behaves as nonlinear hyperelastic (homogeneous isotropic), no tension i.e. with zero tensile strength and infinite compressive and the cracks are dealt as distributed distortions (BD).* The infinitesimal strain E is the sum of an elastic part and a positive semidefinite fracture part: in symbols, **E = Ee + Ef** .

As far as masonry shells are concerned have to be cited: CNUCE Group (**NOSA** code- Lucchesi et al. 2007)

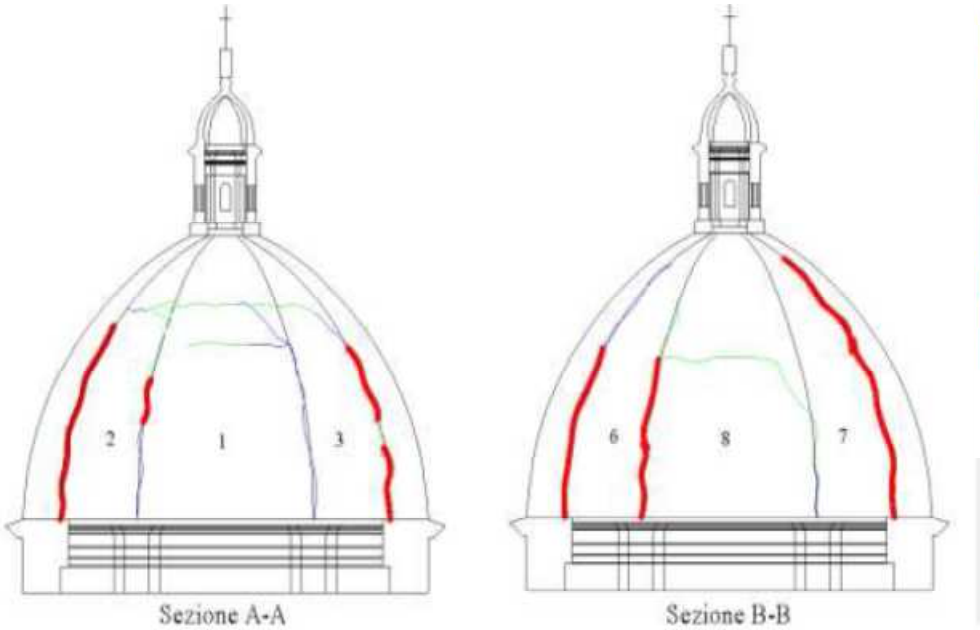

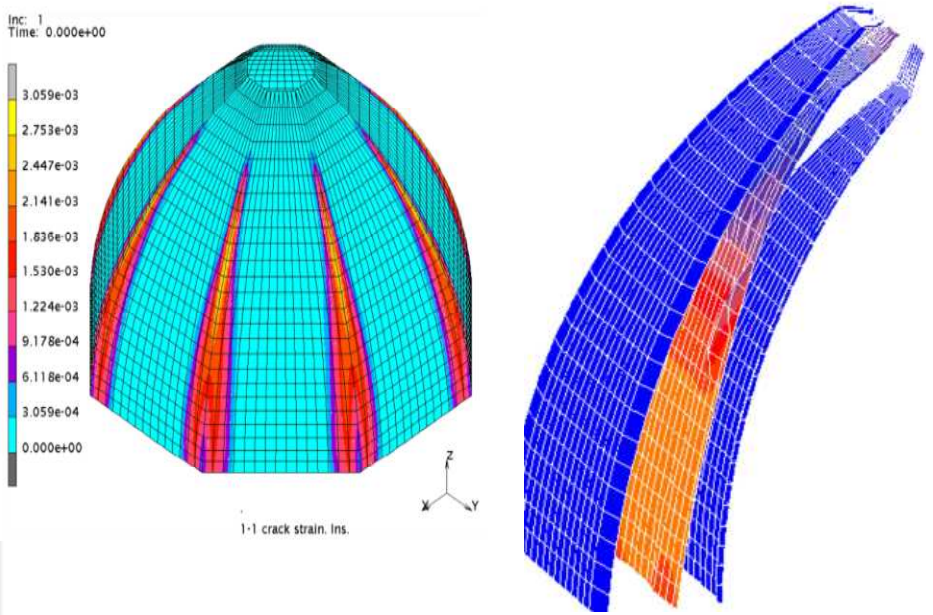

Right: Maximum modulus eccentricity surface in a web.

The dome of the church of Santa Maria Maddalena in Morano Calabro

F. E. M. limit and incremental analyses by rigid elements

3D FEM limit analysis

Main features of proposed limit analysis approach

- *Very few material parameter to set*
- *Relatively easy to program rigid elements either curved, flat triangular or 3d brick*
- *Accurate evaluation of the work of loads*
- *The masonry cracks lumped on lines and not smeared (the dissipation or internal work is defined only at the interface between elements)*
- *The material parameters are defined starting from those of mortar and brick according a homogenization approach Which takes into account the curvature of the surface and the texture.*
- *Efficient internal point algorithms are adopted for solving the LP problem*

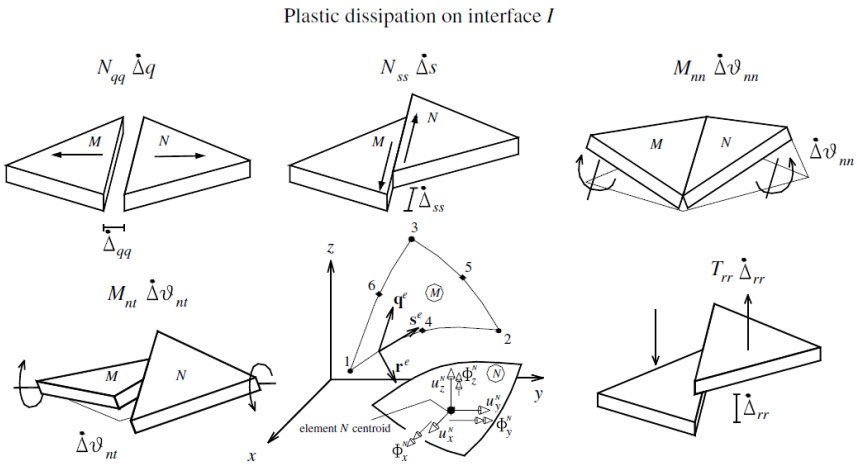

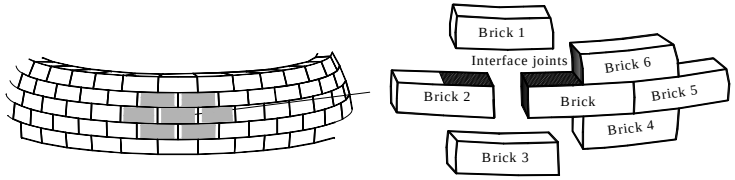

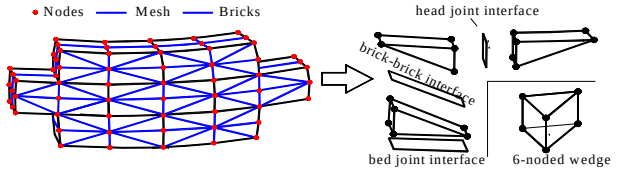

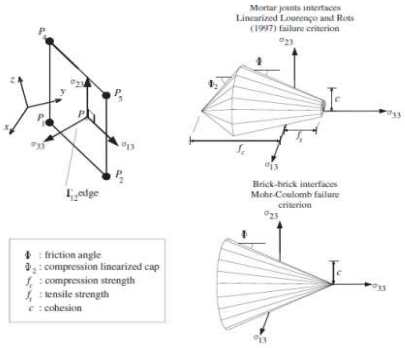

E. MILANI, G. MILANI, A. TRALLI "Limit analysis of masonry vaults by means of curved inite elements and homogenization" INT. J. SOLIDS & STUCTURES (IJSS) vol. 45, n. 20, pp.5258-5288, 2008.

G. MILANI, E. MILANI, A. TRALLI " Upper bound homogenized limit analysis of FRP-reinforced masonry curved structures. Part I : unreinforced masonry failure surfaces" COMPUTERS & STRUCTURES, vol. 87, 23-24,pp. 1516-1533, 2009.

Part II : structural analysis" COMPUTERS & STRUCTURES, vol. 87, 23-24,pp. 1534-1558, 2009.

3 D F.E.M. Limit analysis - Homogenized failure surfaces Vermelfoort barrel vault

Homogenization consists in extracting a REV which generates the whole structure by repetition, in solving a b.v.p. on the REV and in substituting the assemblage of bricks and mortar with a fictitious orthotropic equivalent material, with mechanical properties evaluated at a cell level.

$$S^{hom} \equiv (\mathbf{N}\ \mathbf{T}\ \mathbf{M}) \left\{ \begin{array}{l} \mathbf{N}/t = \langle \boldsymbol{\sigma} \rangle = \frac{1}{V} \int_V \boldsymbol{\sigma} dV \\ \mathbf{M}/t = \langle \boldsymbol{\sigma} y_3 \rangle = \frac{1}{V} \int_V \boldsymbol{\sigma} y_3 dV \\ \mathbf{T}_3/t = \langle \tau_3 \rangle = \frac{1}{V} \int_V \tau_3 dV \\ div\boldsymbol{\sigma} = \mathbf{0} \\ [\boldsymbol{\sigma}]\mathbf{n}^{int} = \mathbf{0} \\ \boldsymbol{\sigma}\mathbf{n} \quad \text{anti-periodic} \quad \text{on} \quad \partial Y \\ \boldsymbol{\sigma}(\mathbf{y}) \in S^m \quad \forall \mathbf{y} \in Y^m ; \boldsymbol{\sigma}(\mathbf{y}) \in S^b \quad \forall \mathbf{y} \in \end{array} \right.$$

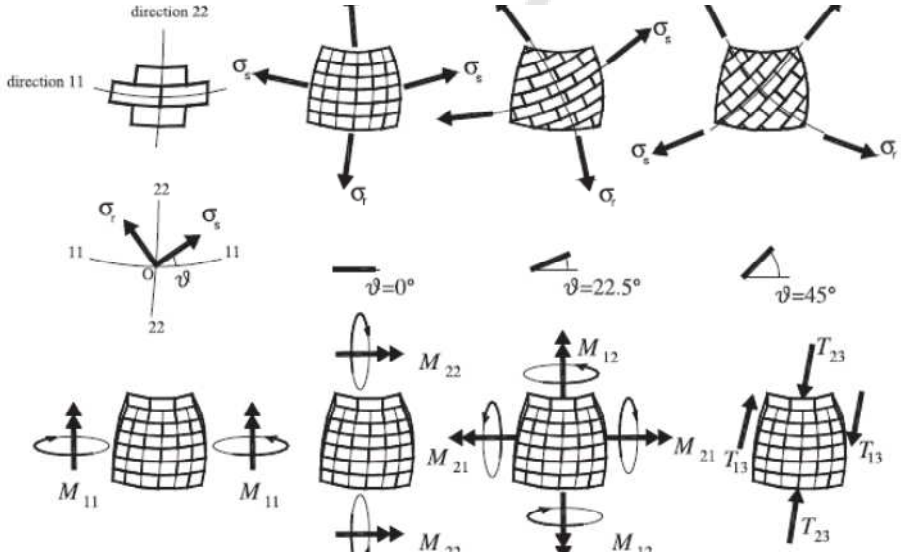

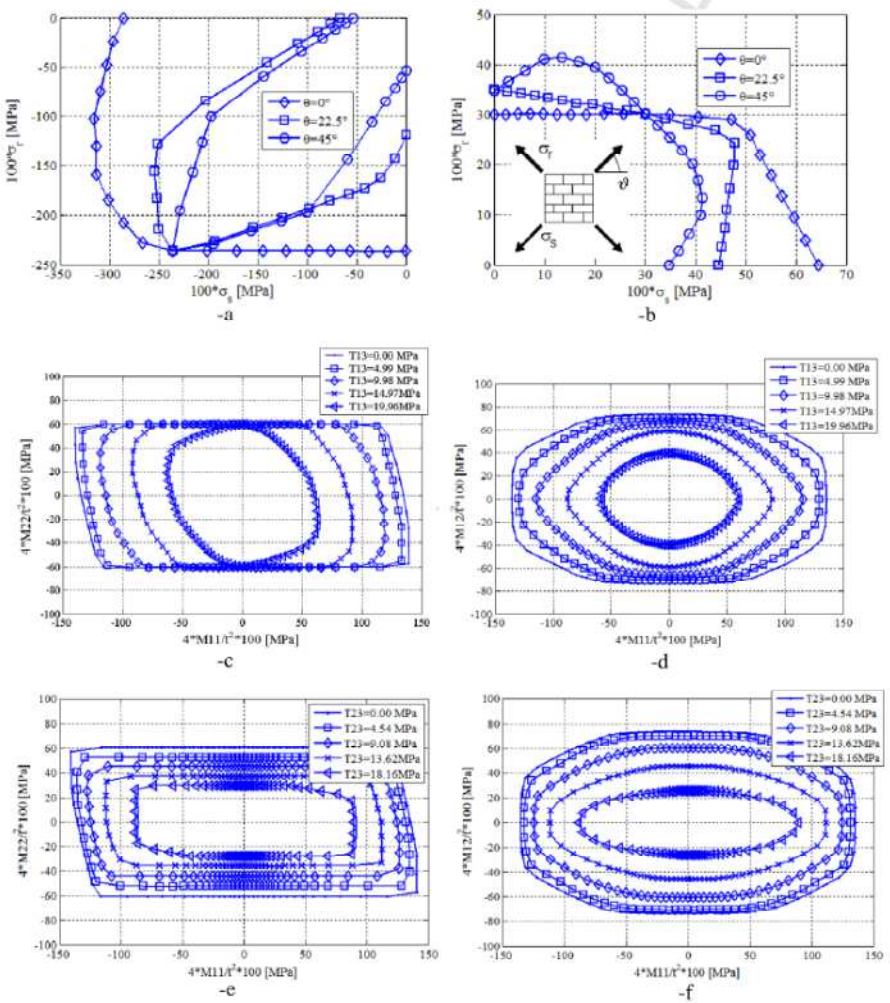

11. Vermeltfoort masonry arches. (a) and (b) In-plane homogenized failure surface ((a) compression region, (b) tension region) at different orientations of the load with ect to bed joint ϑ direction. c and d: M11–M22 (c) and M11–M12 (d) failure surfaces at different values of out-of-plane shear T13. e and f: M11–M22 (c) and M11–M12 (d) re surfaces at different values of out-of-plane shear T23.

3 D F.E.M. Limit analysis - Barrel rectangular vault

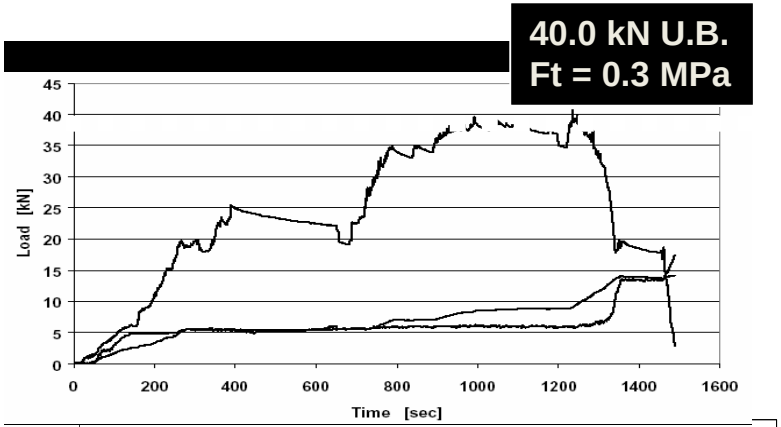

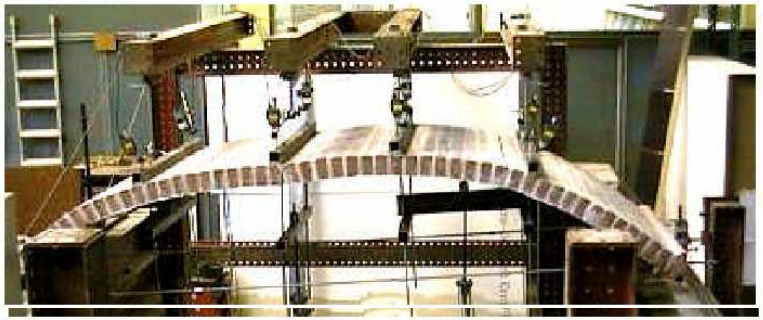

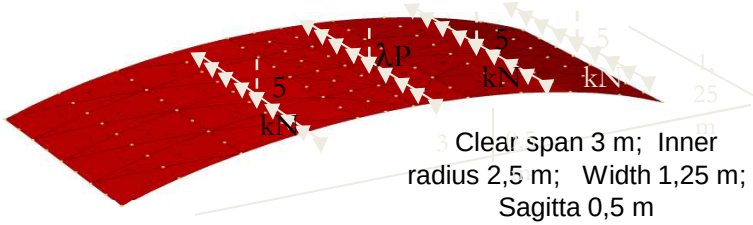

Clear span 3 m; Inner radius 2,5 m; Width 1,25 m; Sagitta 0,5 m

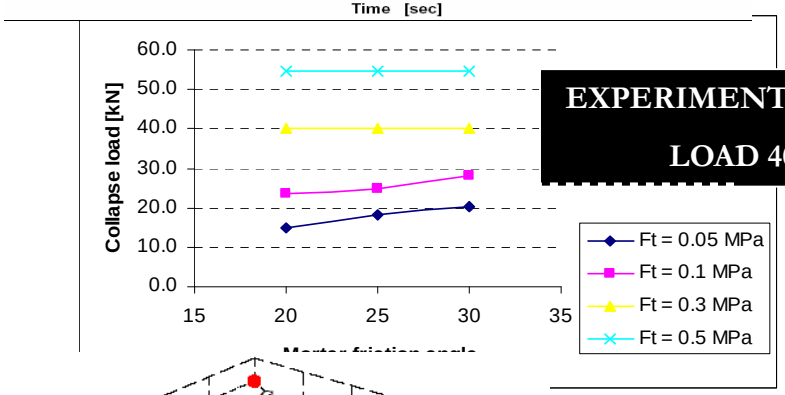

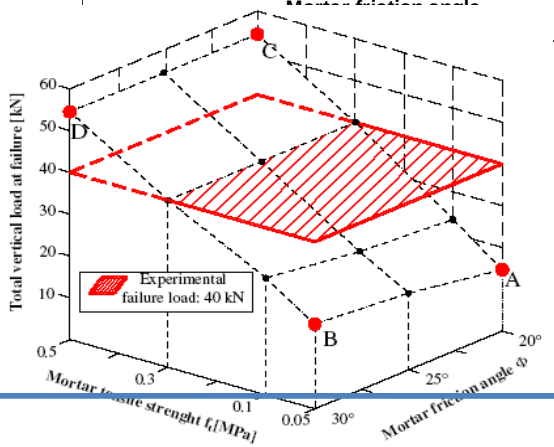

Mesh 4: Sensitive analysis

Ft: 0.05 – 0.1 – 0.3 – 0.5 Mpa

Φ: 20° – 25° – 30°

Experimental data from Vermelfoort 2001

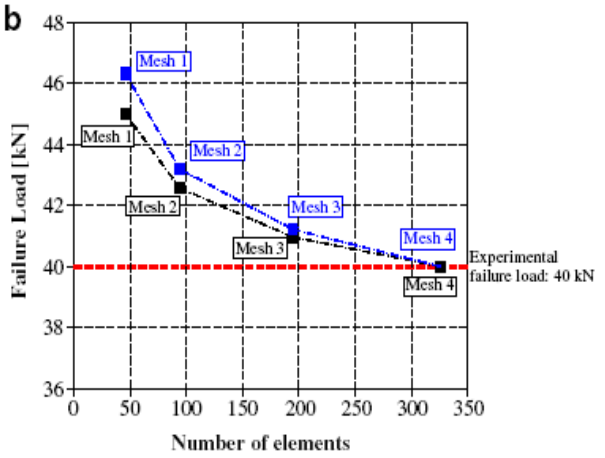

Barrel rectangular vault
Compressive stress eccentricity (dual solution)

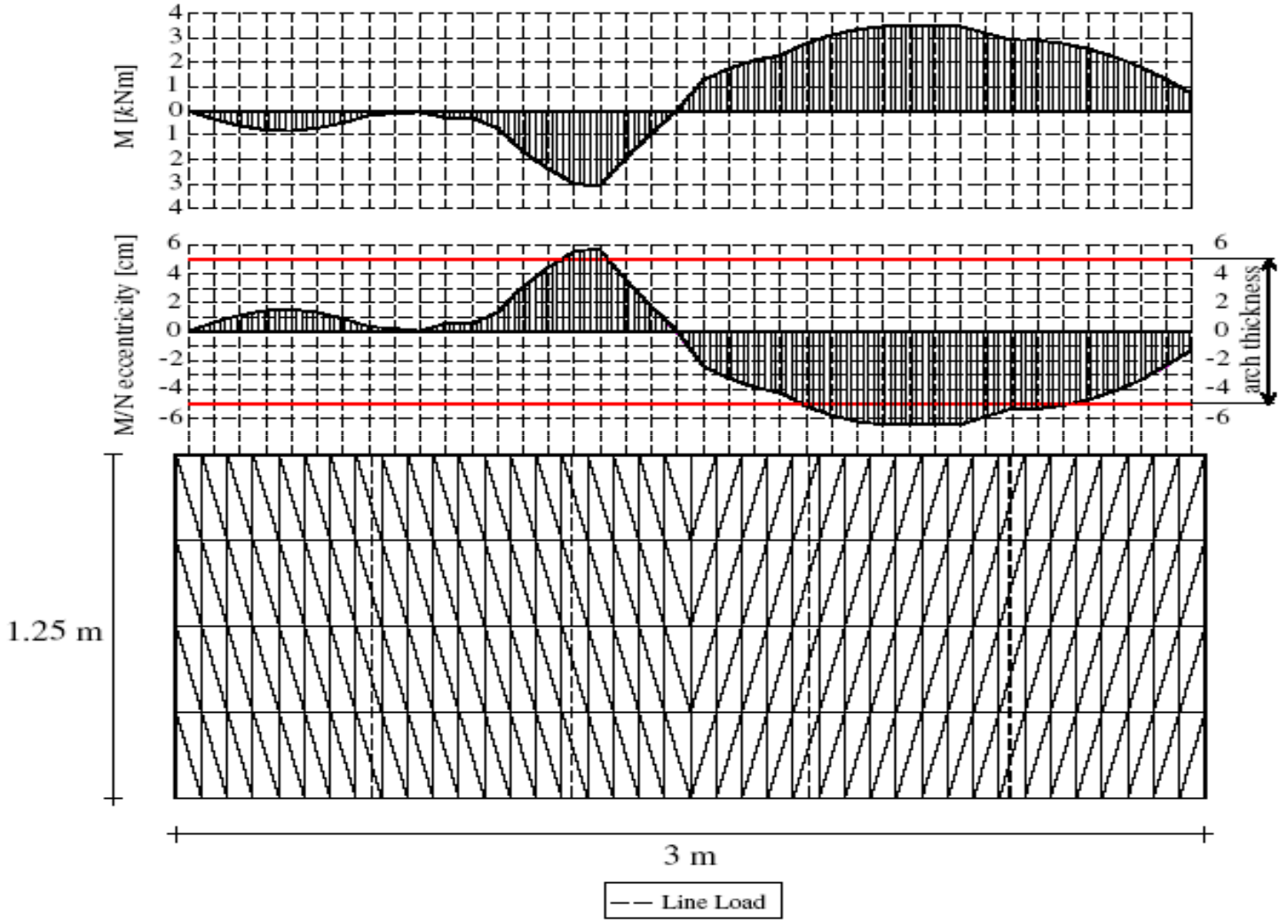

FRP reinforced barrel rectangular vault

2D FRP - masonry interface has been implemented

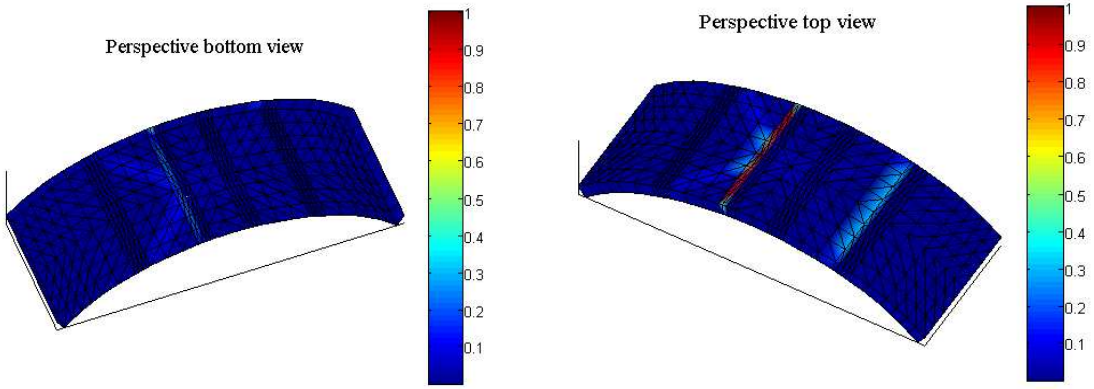

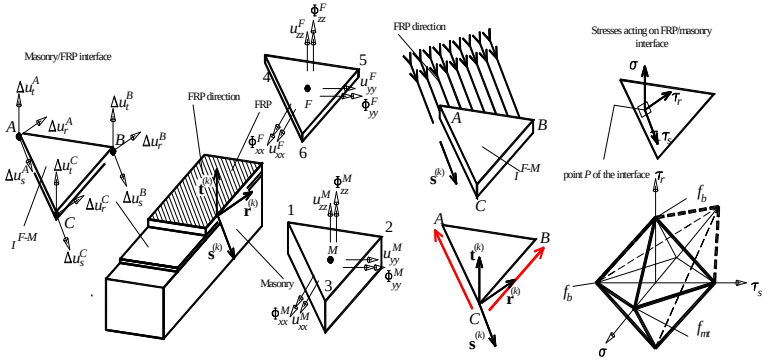

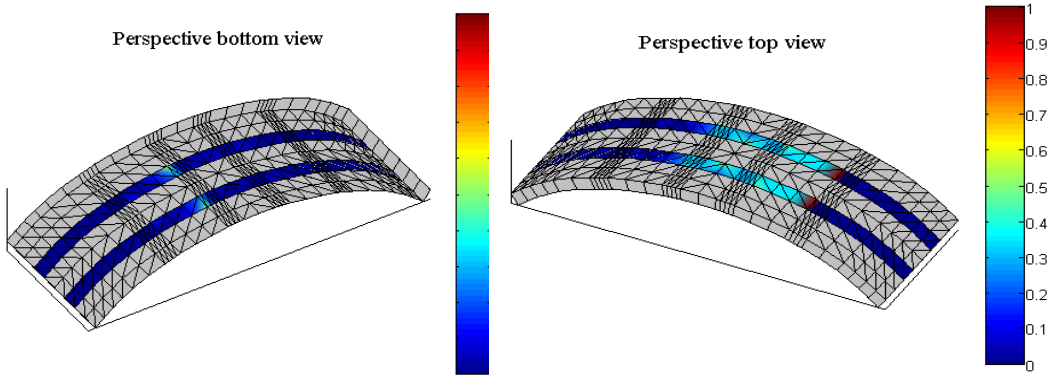

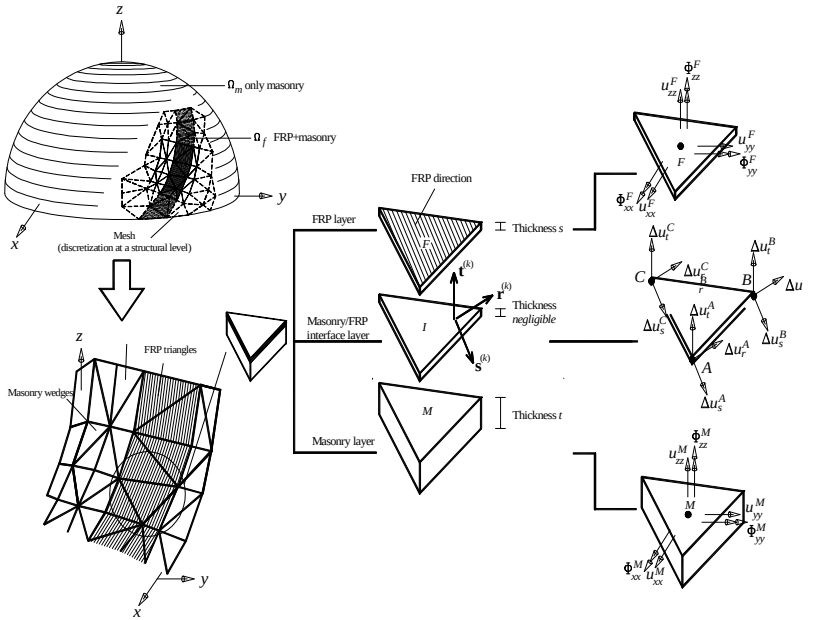

FRP reinforced parabolic arch

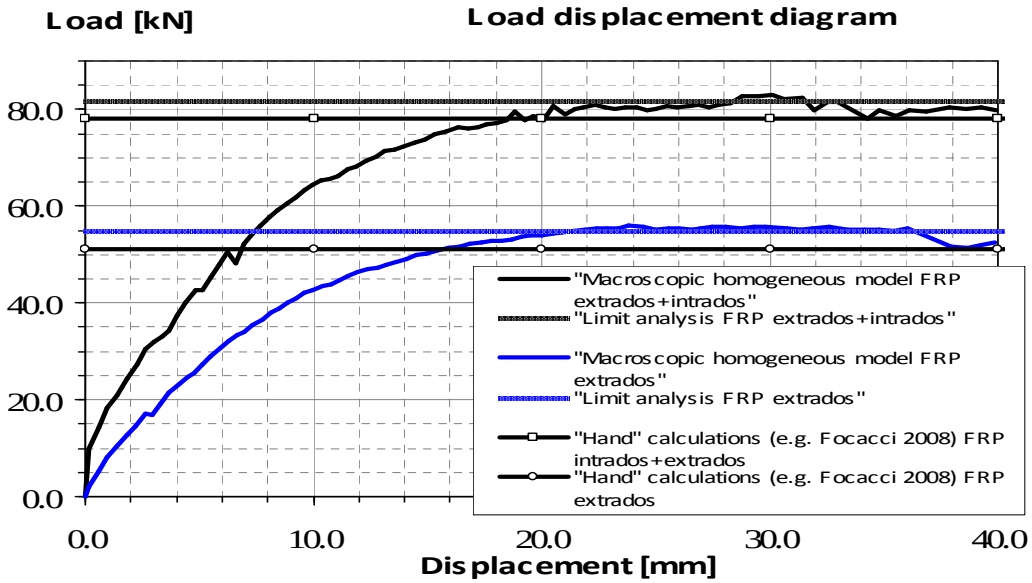

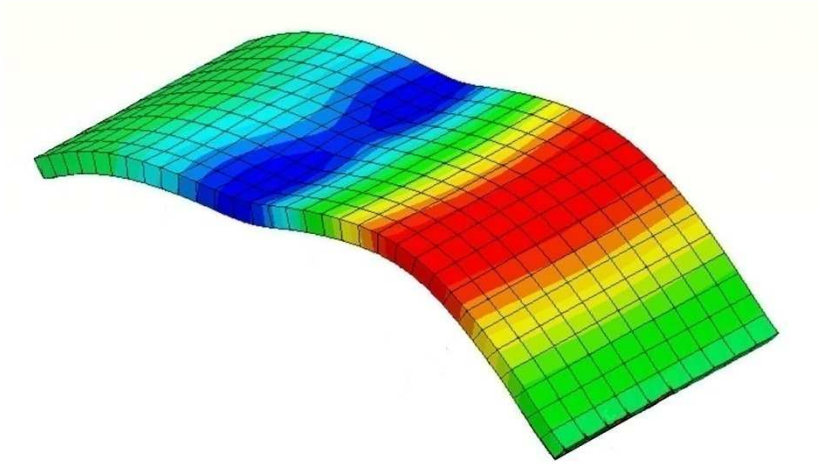

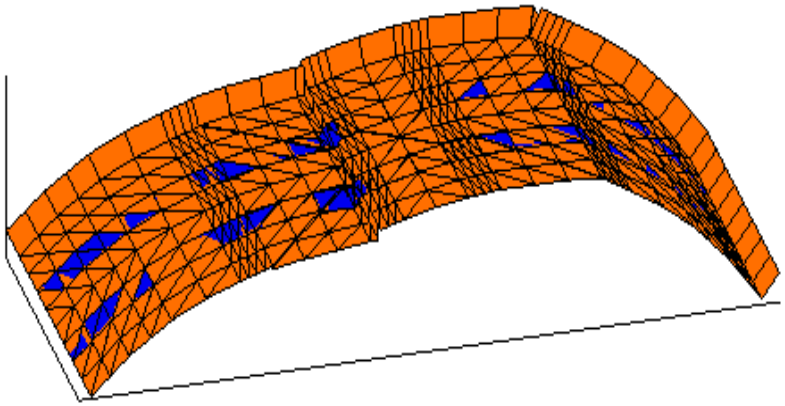

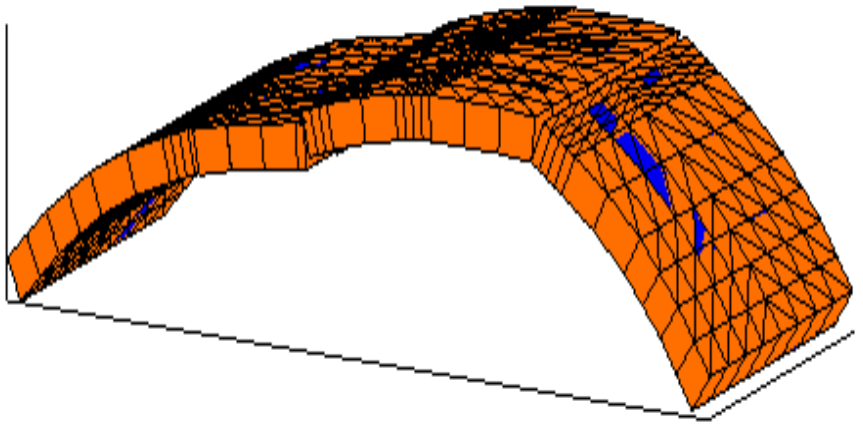

Unreinforced skew barrel vault

Experimental data Vermelfoort 2001

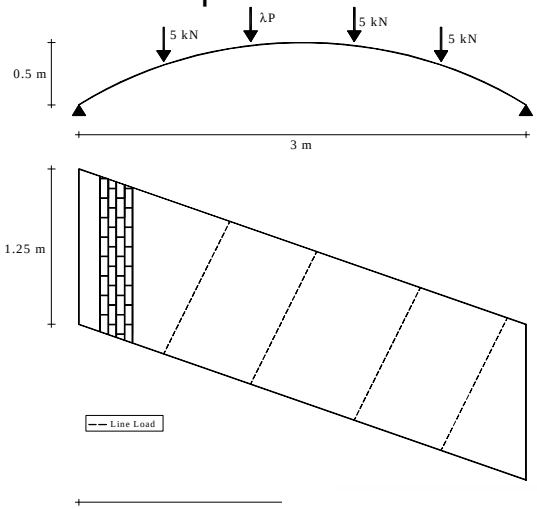

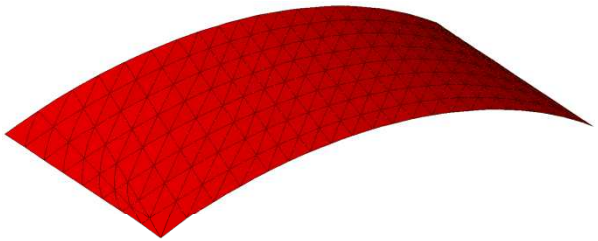

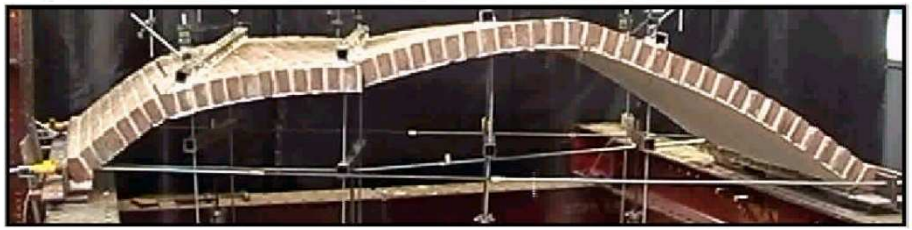

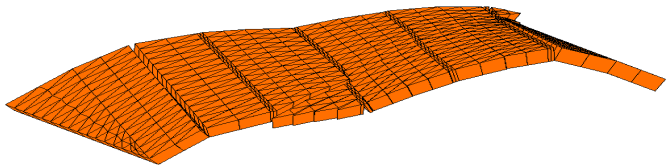

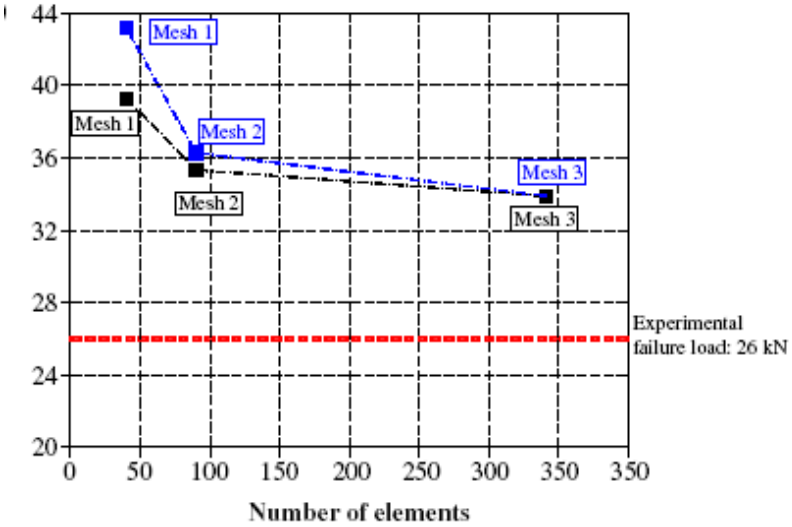

Unreinforced skew barrel vault

a

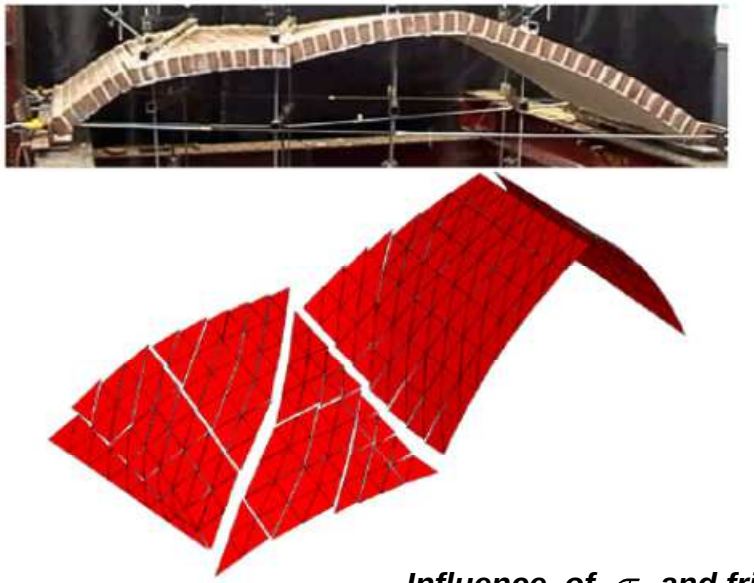

a

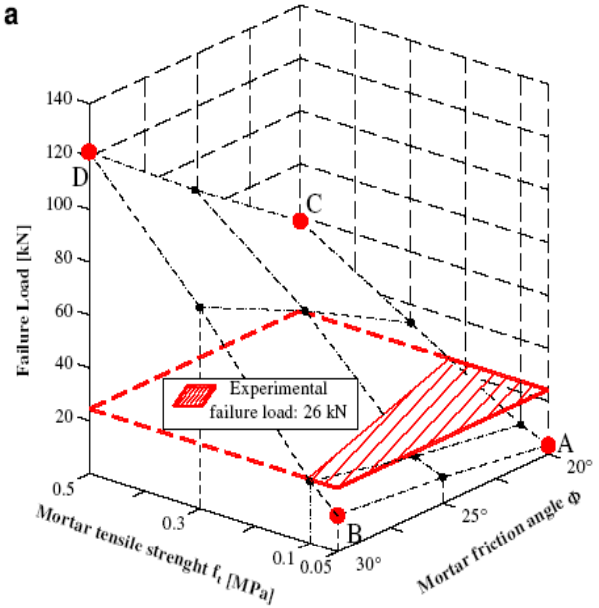

Influence of τ and friction on collapse multiplier and mechanism

b

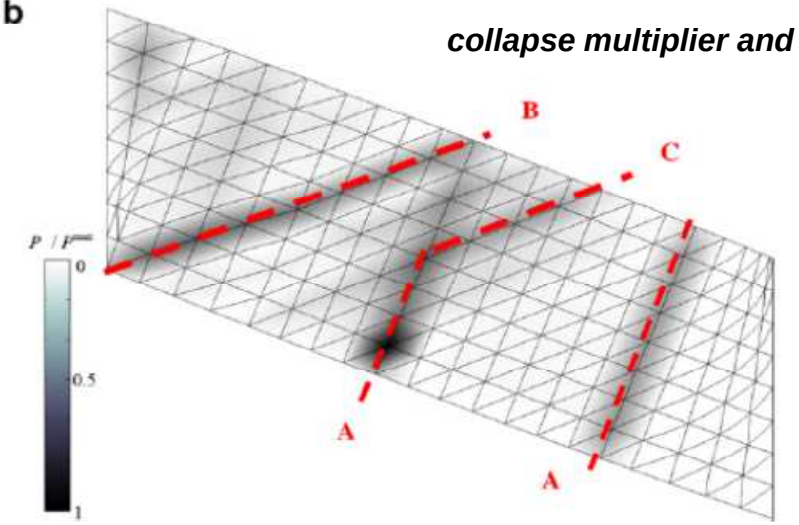

b

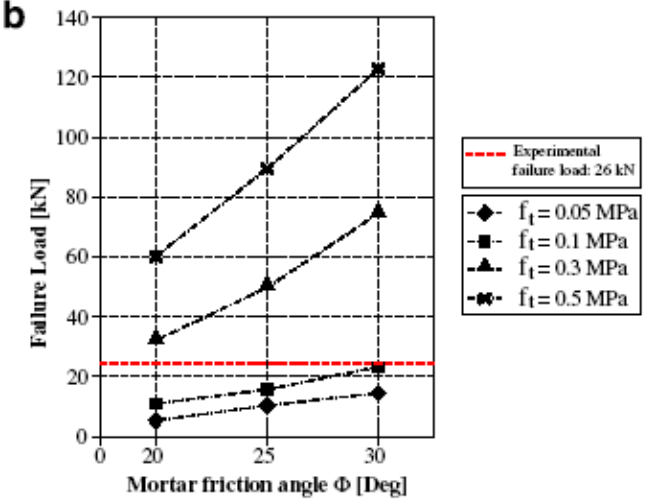

Cross vaults

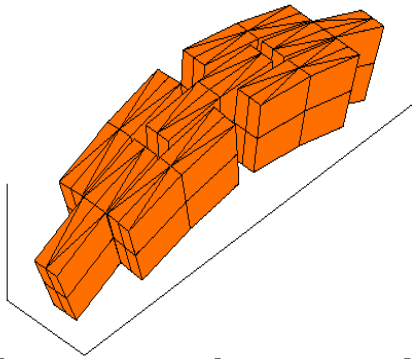

(-a) N11 membrane action

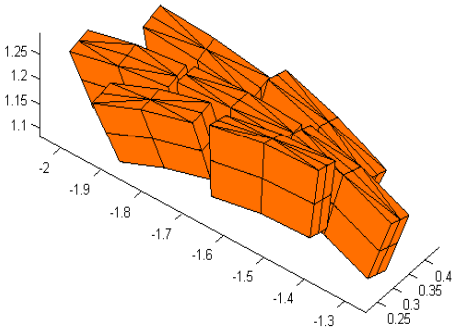

(-b) pure M12 torsion

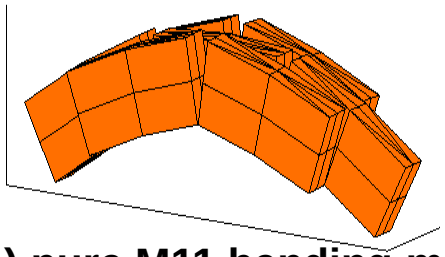

(-c) pure M11 bending moment

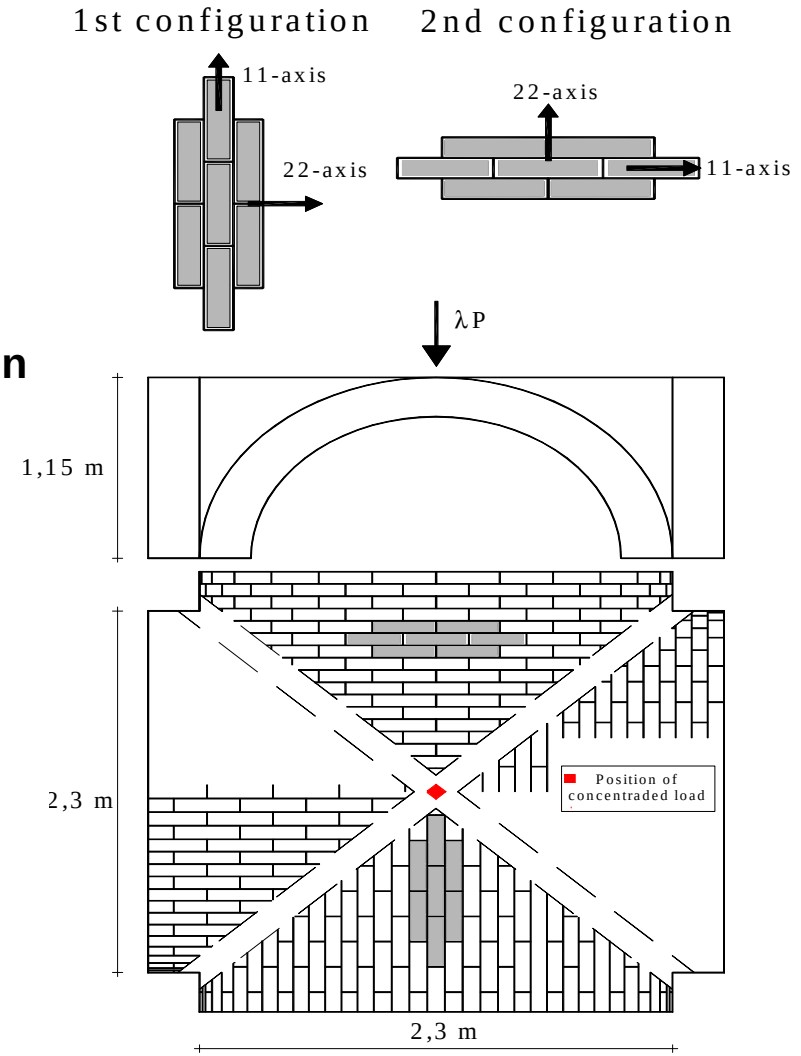

Ribbed cross vault
experimental data from Creazza et al. 2002

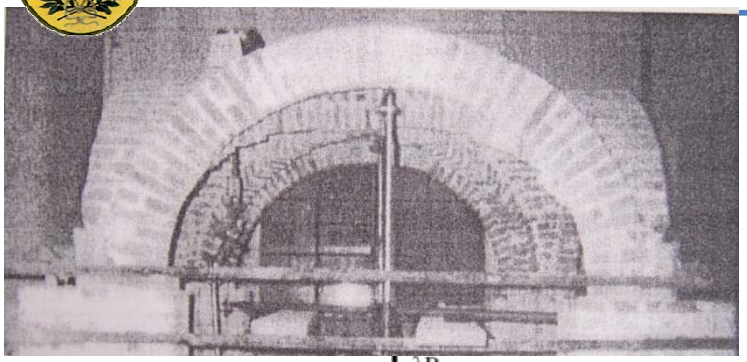

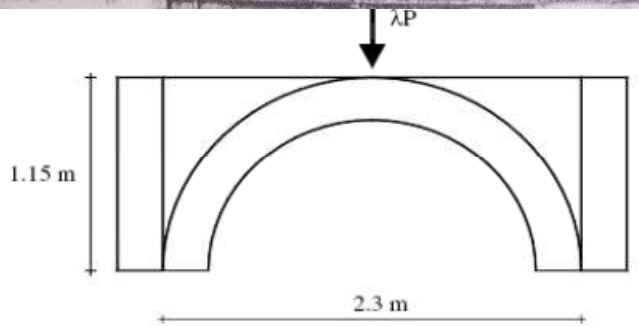

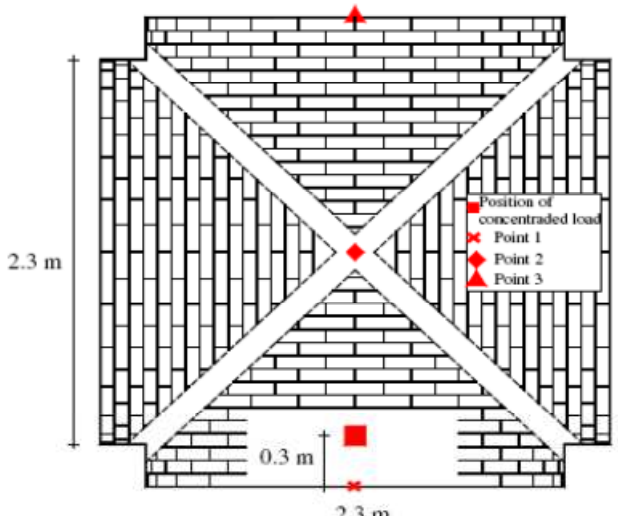

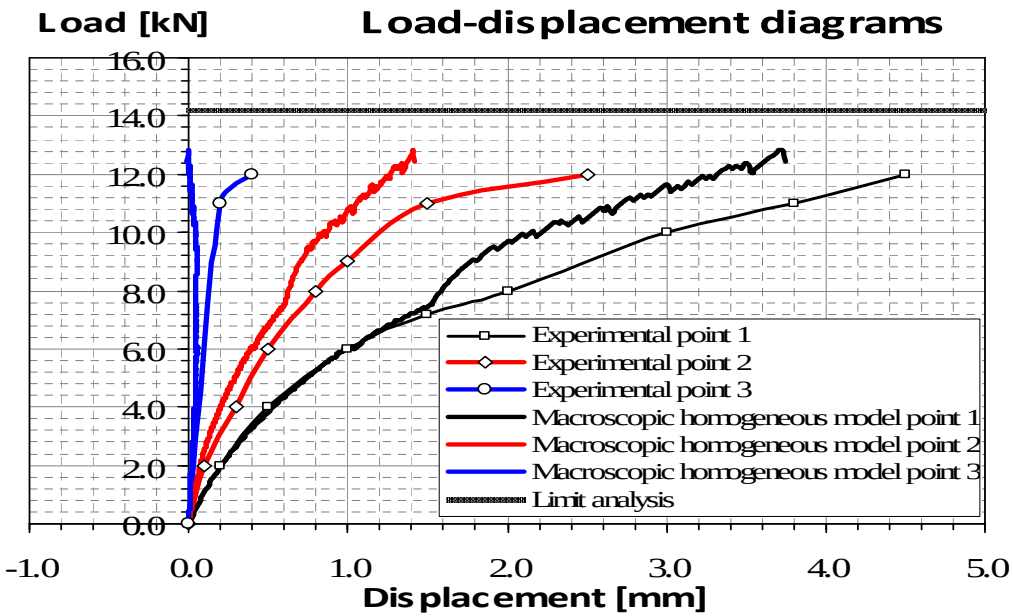

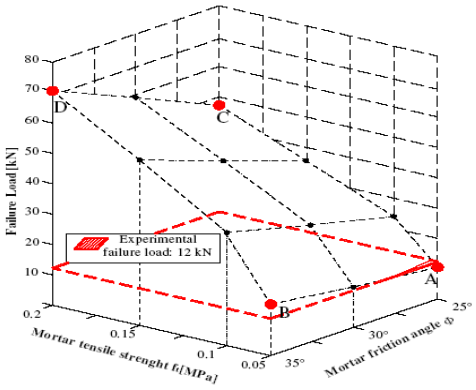

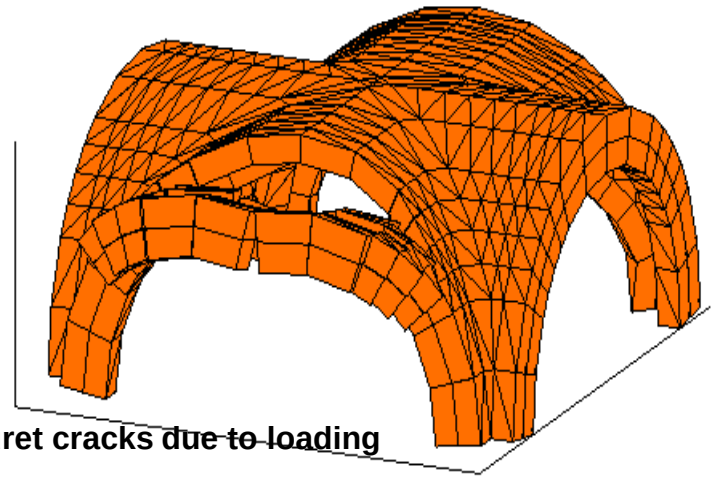

Do not appear Sabouret cracks due to loading

Hemispherical dome

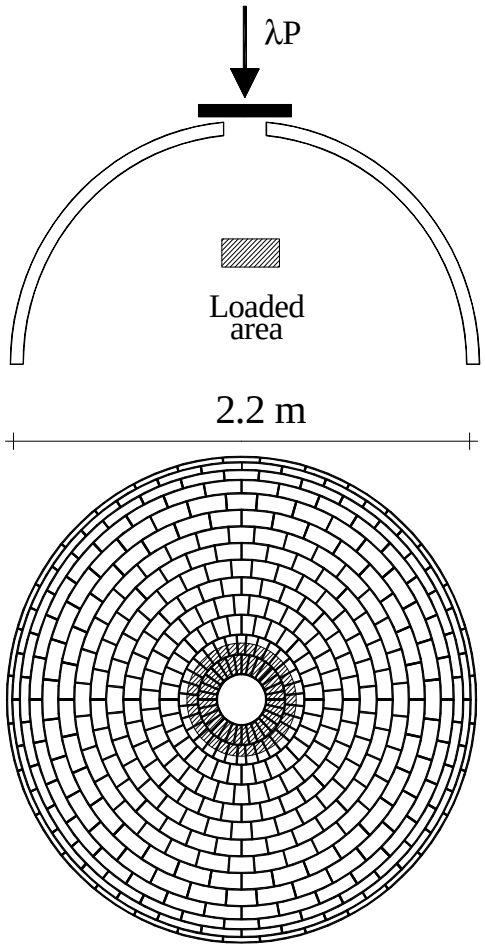

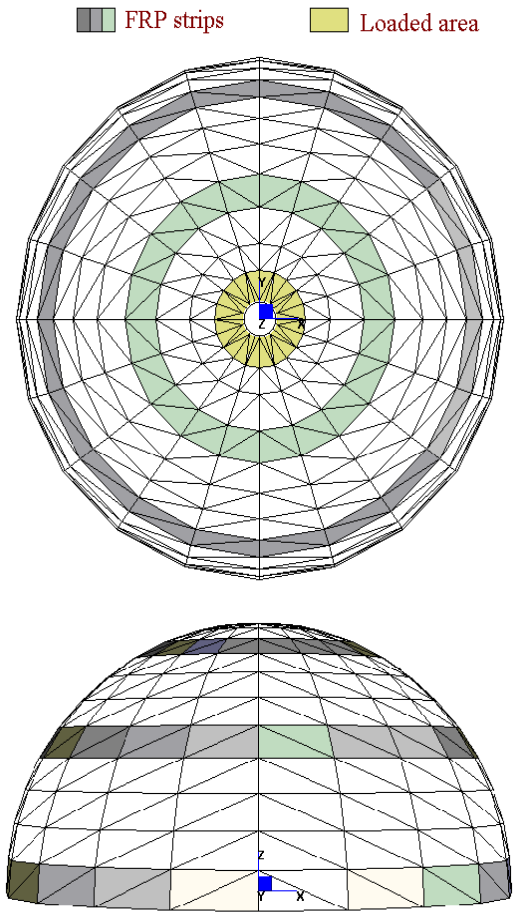

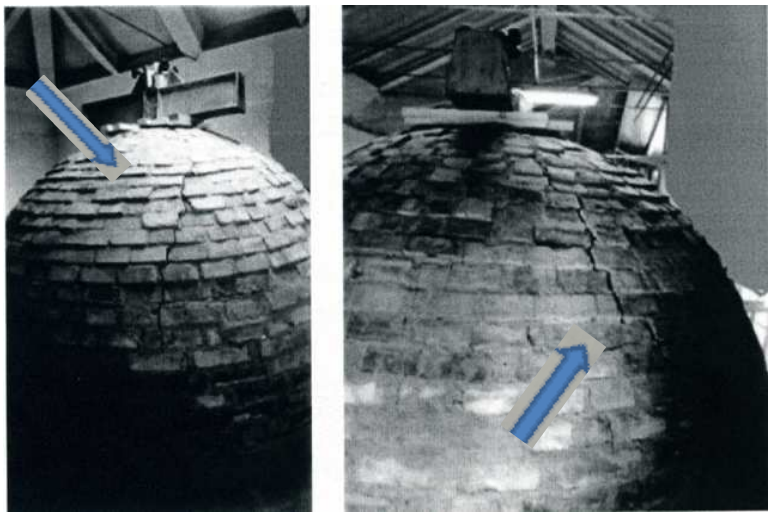

meridian cracks

Experimental data from Creazza et al. 2002 and from Foraboschi 2006

Unreinforced hemispherical dome

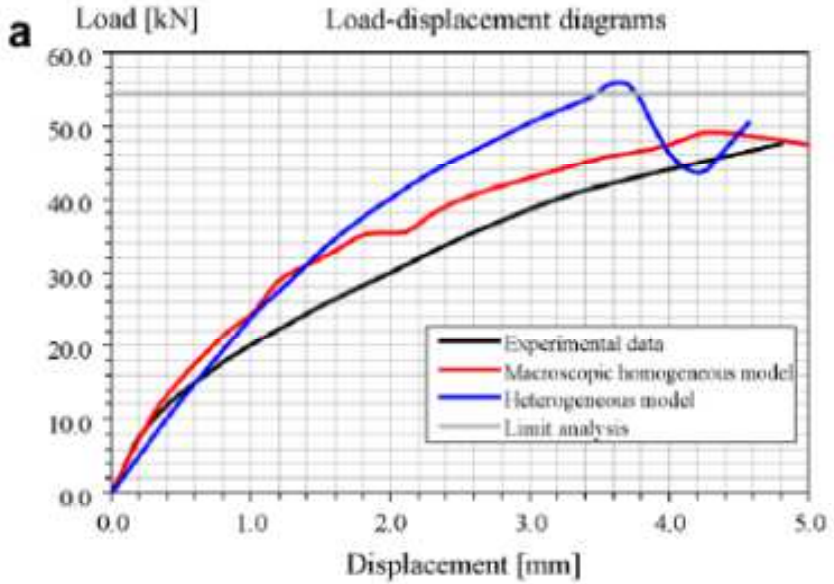

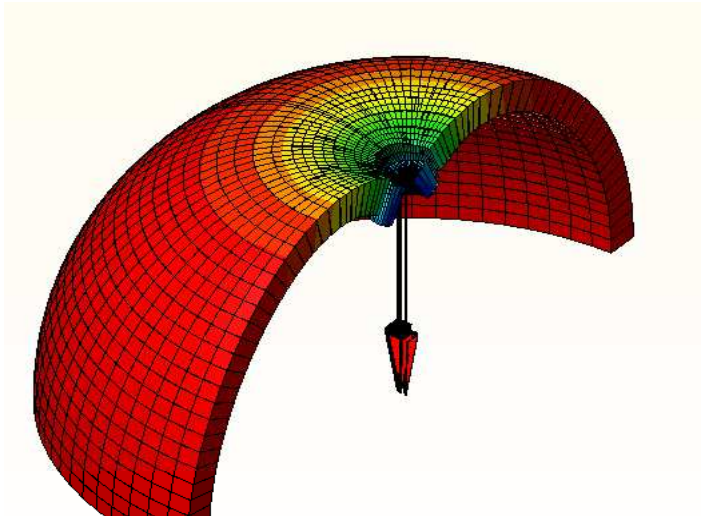

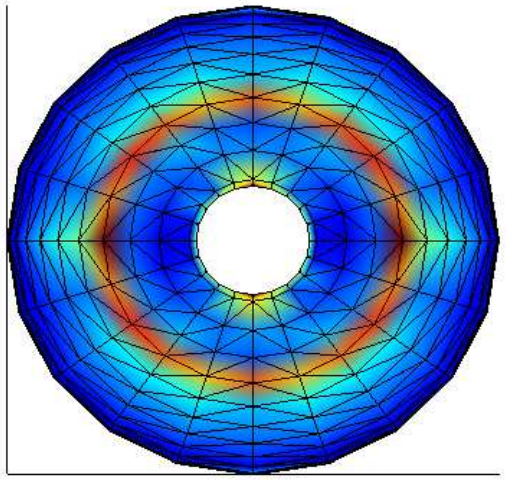

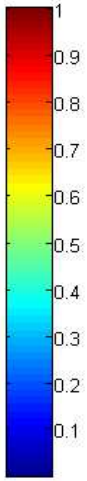

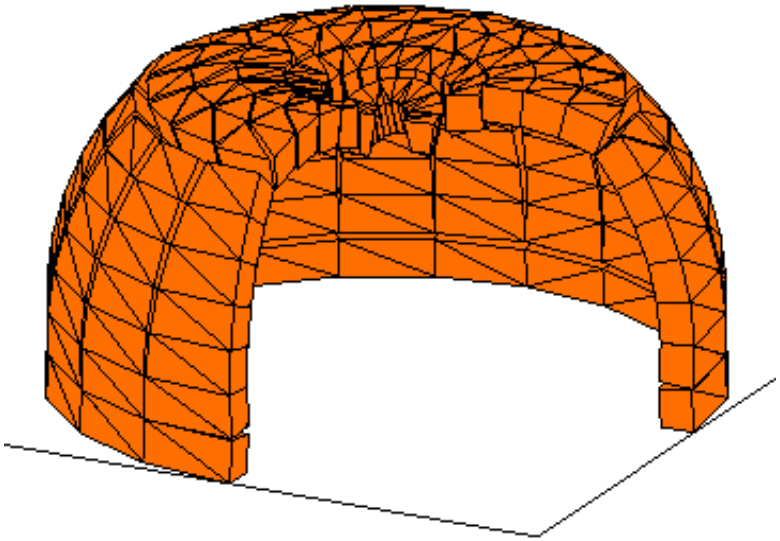

Hemispherical dome

Unreinforced case

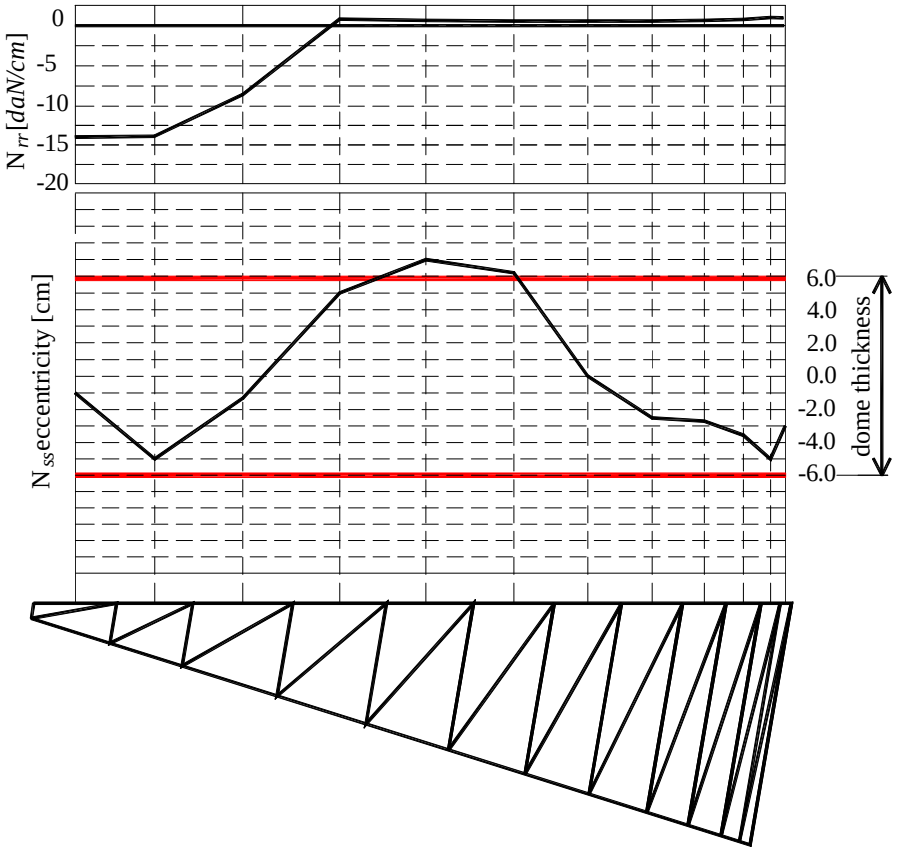

FRP reinforced case

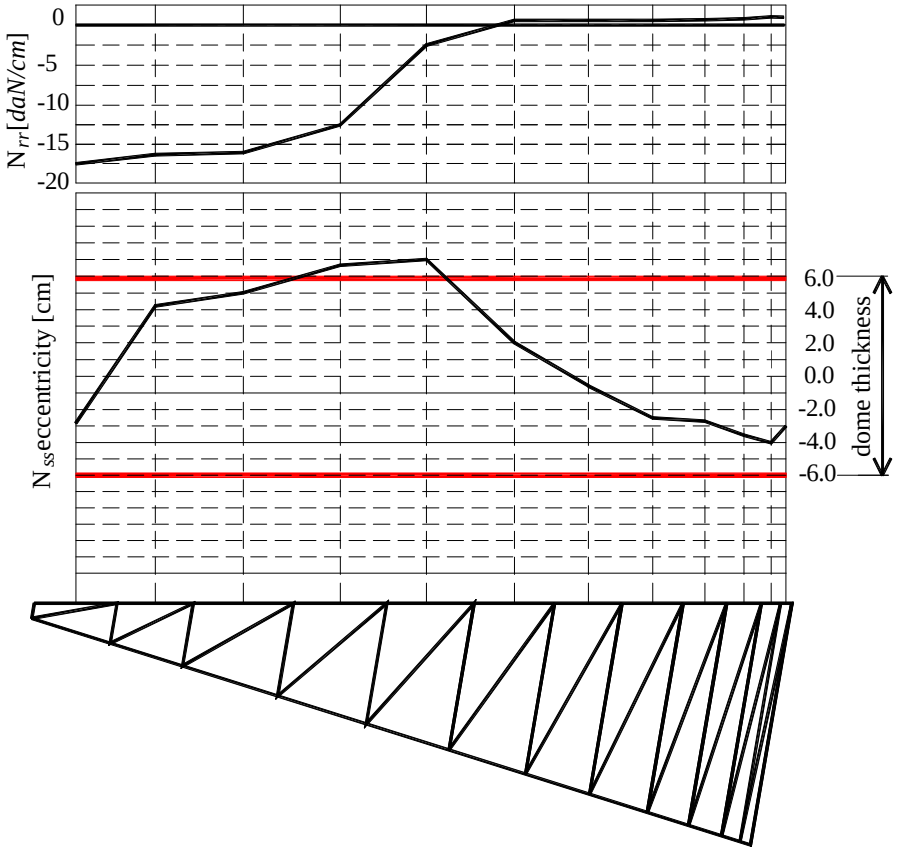

FRP reinforced masonry vaults

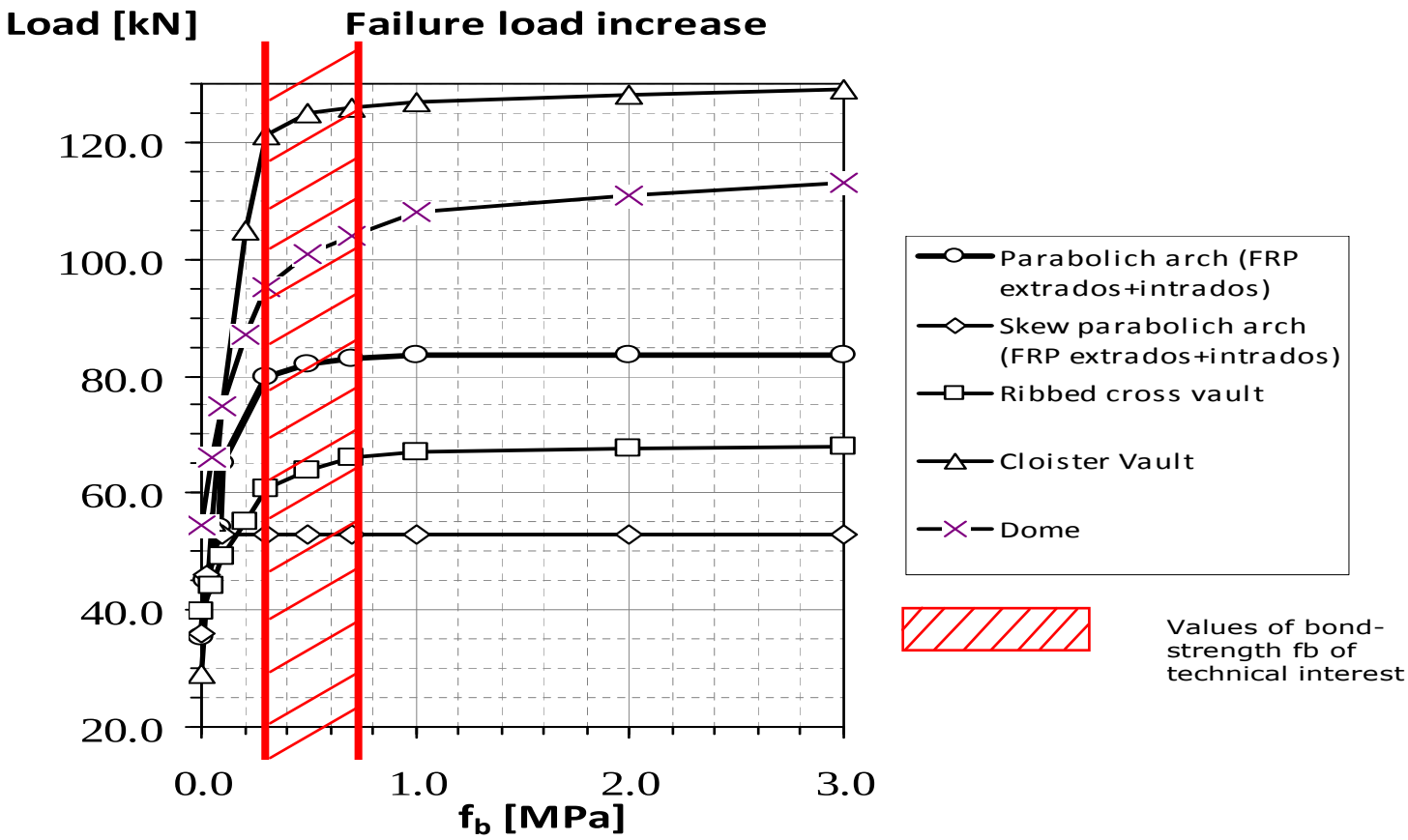

Synopsis of sensitivity analyses for different values of tangential bond stresses

F.E. non-linear analysis of masonry double curvature structures

Non-linear analysis of masonry double curvature structures

Main features of proposed non linear analysis

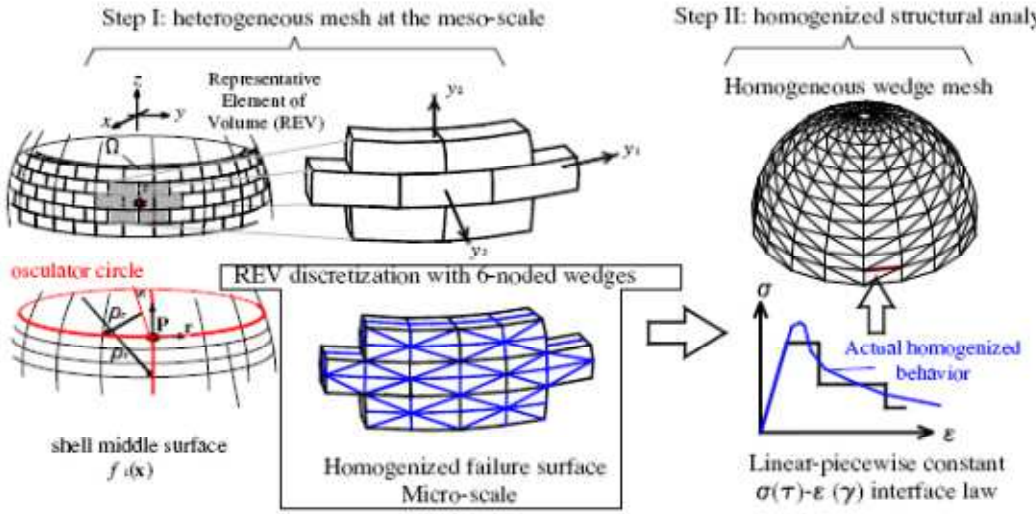

G.MILANI, A. TRALLI " Simple SQP approach for out-of-plane loaded homogenized brickwork panels, accounting for softening" COMPS & STR vol. 89, 1-2, pp. 201-215, 2011.
G. MILANI, A. TRALLI "A simple meso-macro model based on SQP for the non-linear analysis of masonry double curvature structures" IJSS vol. 49, pp.808-834, 2012.
G. MILANI, M. PIZZOLATO, A. TRALLI "Simple numerical model with second order effects for out-of-plane loaded masonry walls" ENG. STR. vol. 48, pp. 98-120, 2013**.**

1- The material parameters are defined starting from those of mortar and brick according a homogenization approach

(At the meso-scale, a curved running bond representative REV constituted by a central block interconnected with its 6 neighbors is discretized through of a few 6-nodes rigid wedge elements and rectangular interfaces)

2- Non linearity is concentrated exclusively on joints reduced to interface, exhibiting a frictional behavior with limited tensile and compressive strength with softening.

The macroscopic homogenous masonry behavior is evaluated on the REV imposing separately increasing internal actions (in-plane membrane actions, meridian and parallel bending, torsion and out-of-plane shear)
This simplified approach allows to estimate heuristically the macroscopic stress–strain behavior of masonry at the meso-scale.

3- Rigid infinitely resistant 6-nodes wedge elements and non-linear interfaces, exhibiting deterioration of the mechanical properties.

4- Physically consistent line cracks (the dissipation or internal work is defined only at the interface between elements)

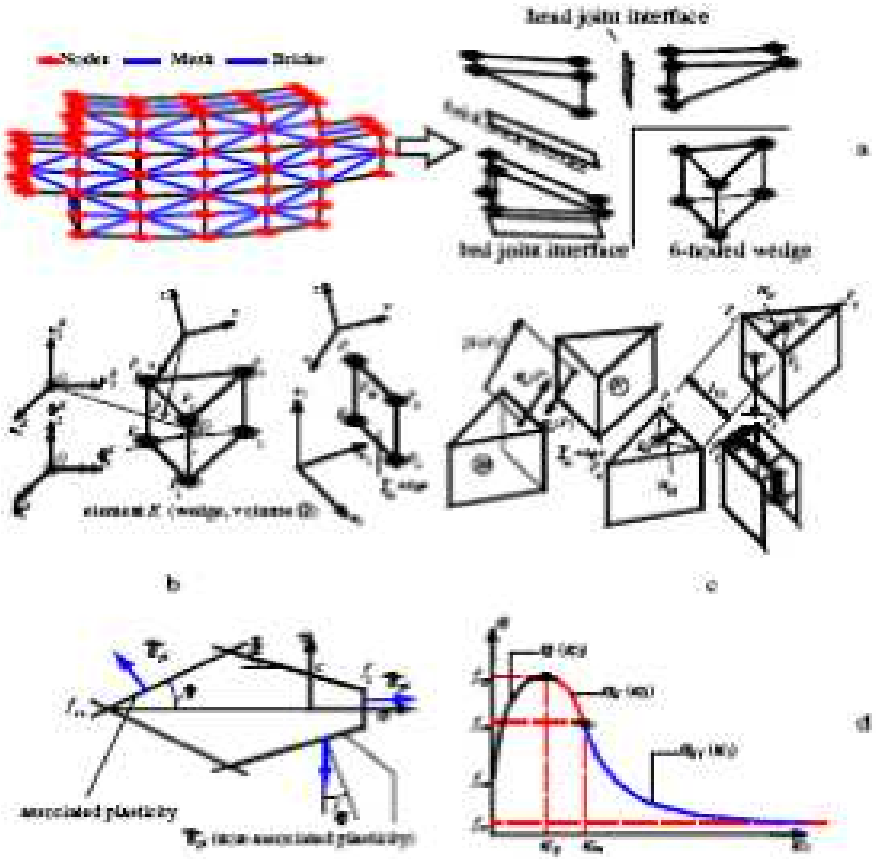

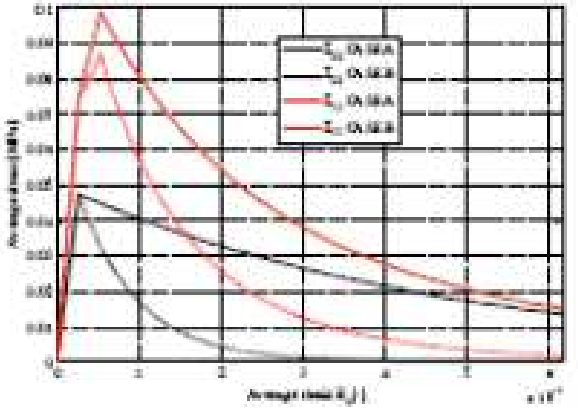

Fig. 6. Uniaxial response of masonry along horizontal and vertical tensions for some values of fracture energies

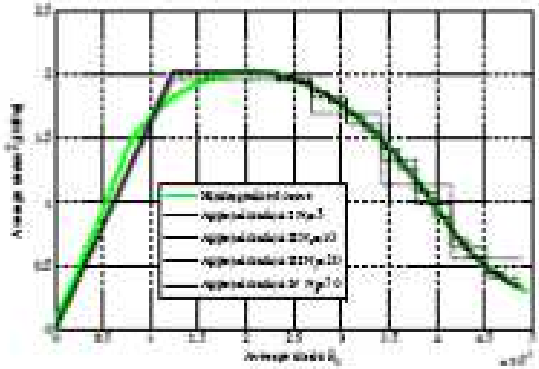

Fig. 7. Uniaxial response of masonry in meridian compression (with the linear plane-stress constant approximation used at a structural level).

Simplified Kinematic approach: flexural behavior of REV

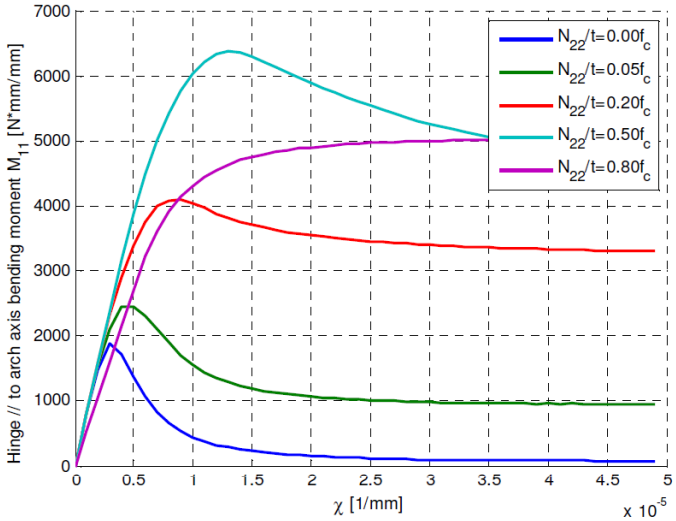

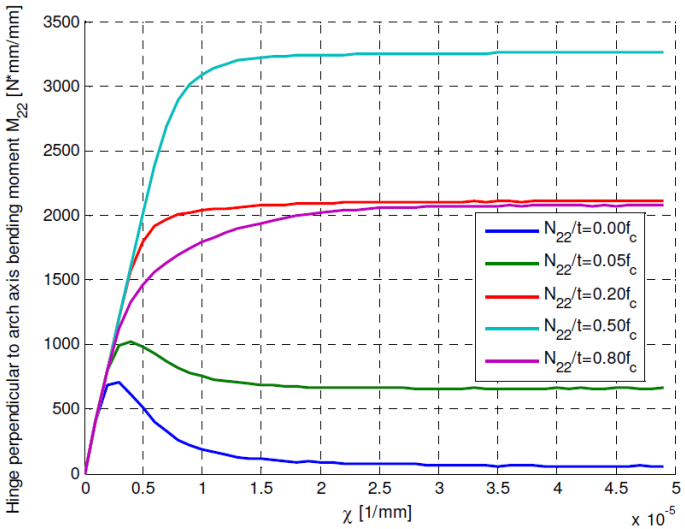

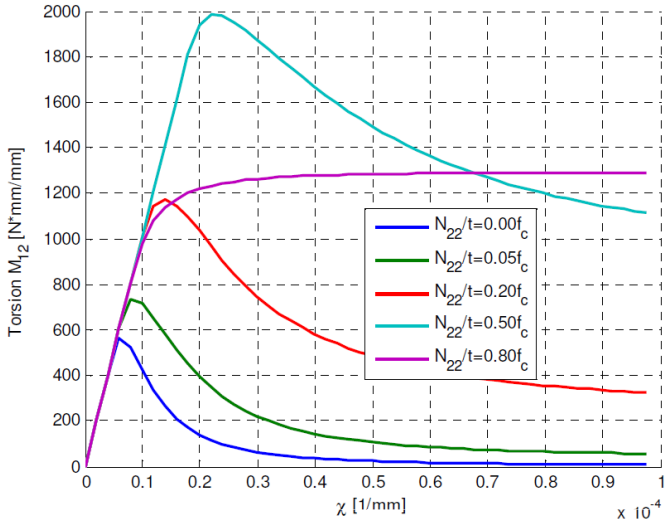

-c

Flexural behavior of the REV. Parabolic Arch Bending curvature diagrams at increasing Normal force compressive:
a)Axis bending moment parallel arch axis
b) Axis bending moment orthogonal arch axis
c)Torsion

-b

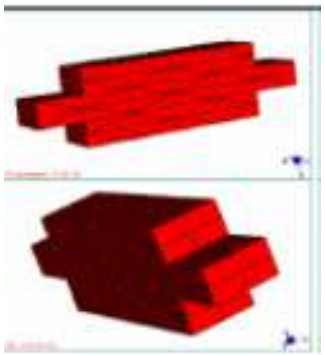

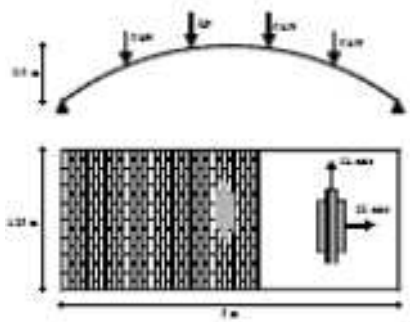

Parabolic arch: nonlinear incremental analysis

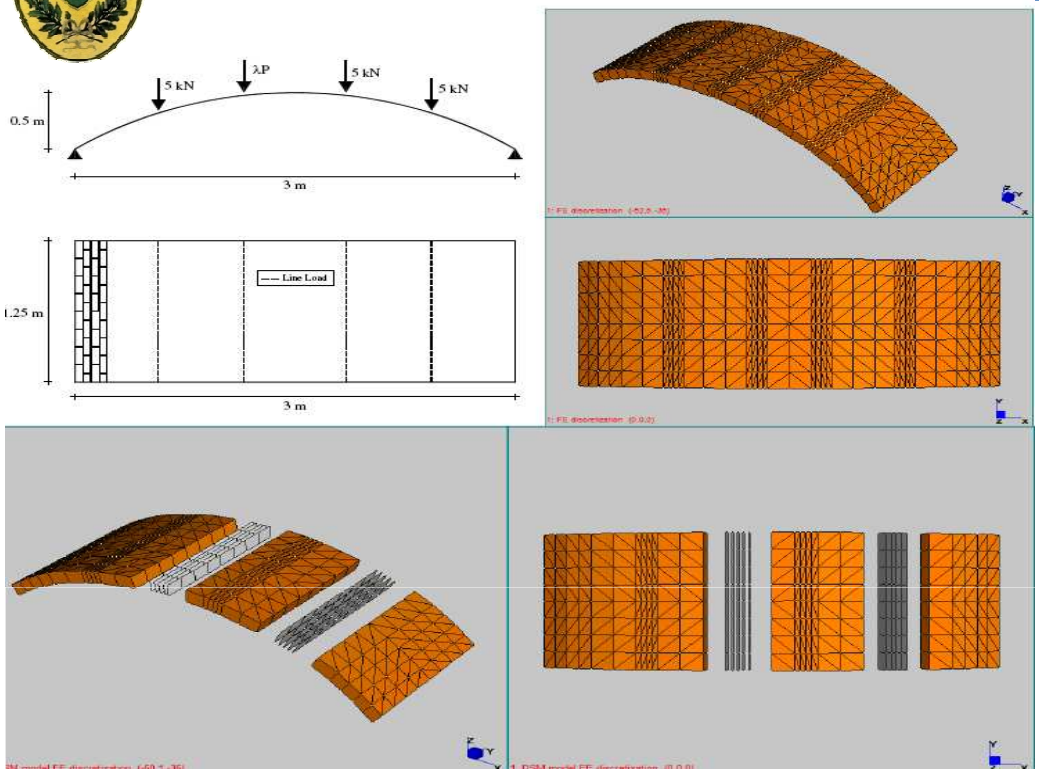

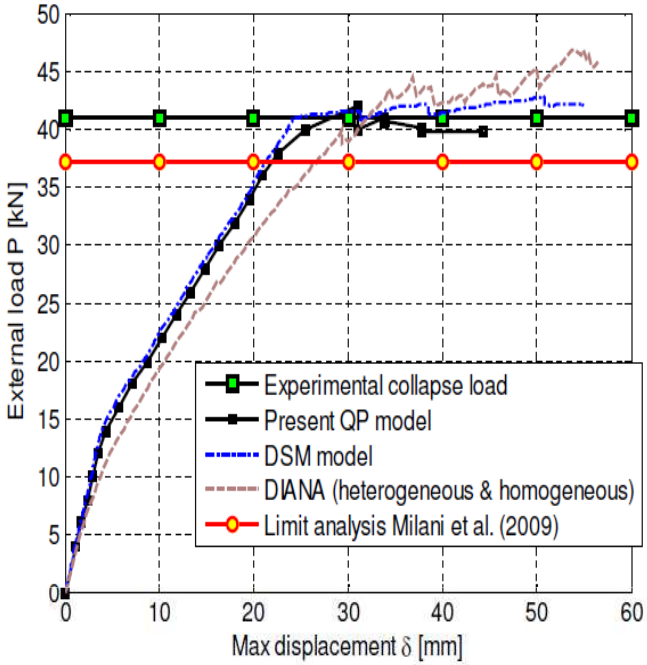

: 15: Parabolic arch. Comparison among load-displacement curves or collapse loads provided by experimentation, limit analysis and non-linear FE code.

Deteriorating simplified model (DSM), is non-commercial and seems the most suited to be used in common design. It consists into a preliminary homogenized limit analysis of the structure in order to identify the failure mechanism and in the subsequent FE non linear analysis of the whole structure assuming that all the non-linearity is concentrated on the interfaces defining the failure mechanism. The analysis is performed through a non-commercial software equipped with a standard arc-length algorithm, suitable to follow the drop of the load bearing capacity due to interfaces deterioration. The advantage interms of processing time is remarkable only if the number of non-linear interfaces is small. That occurs always for out-of-plane loaded panels which fail systematically for the formation of well-defined yield lines, where as for curved shells the convenience may be less evident in some applications, especially when regions at diffused deterioration can be, rarely. present (membrane crushing).

Ribbed cross vault: incremental nonlinear analysis

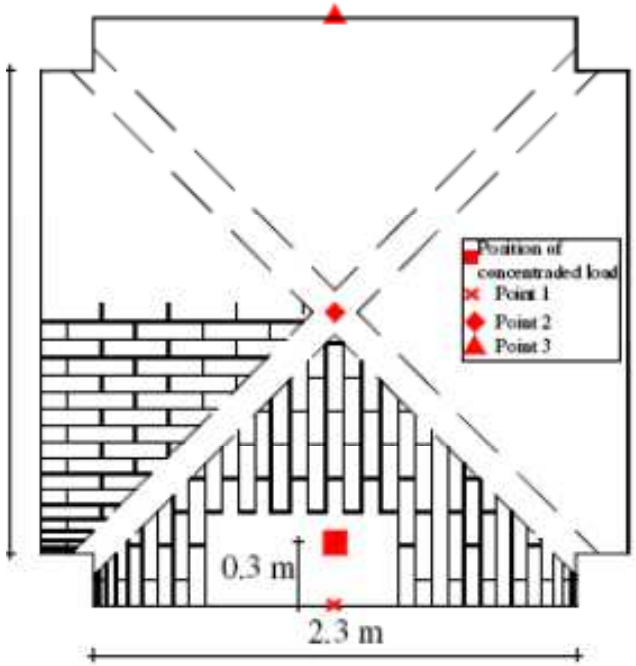

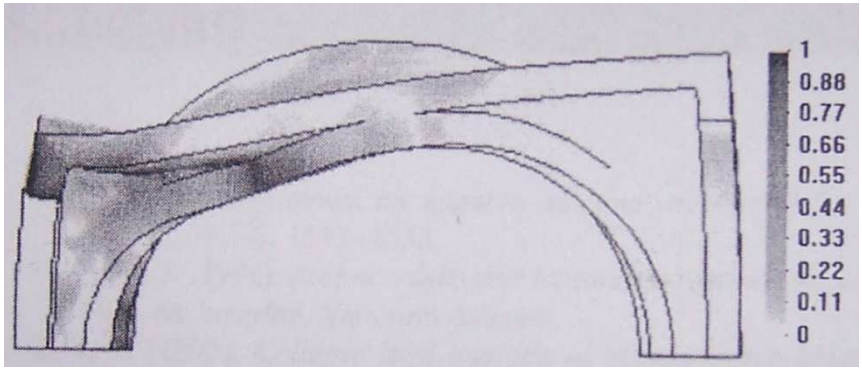

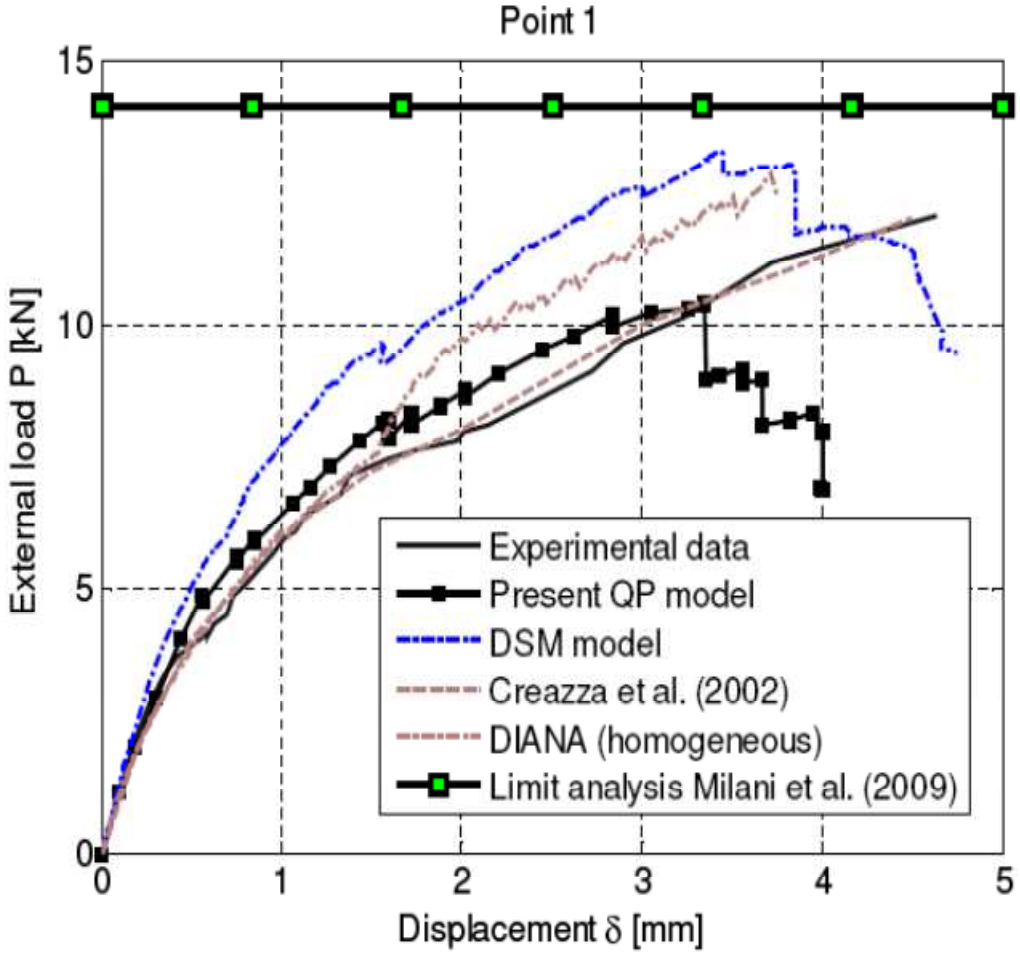

Ribbed cross vault: incremental nonlinear analysis

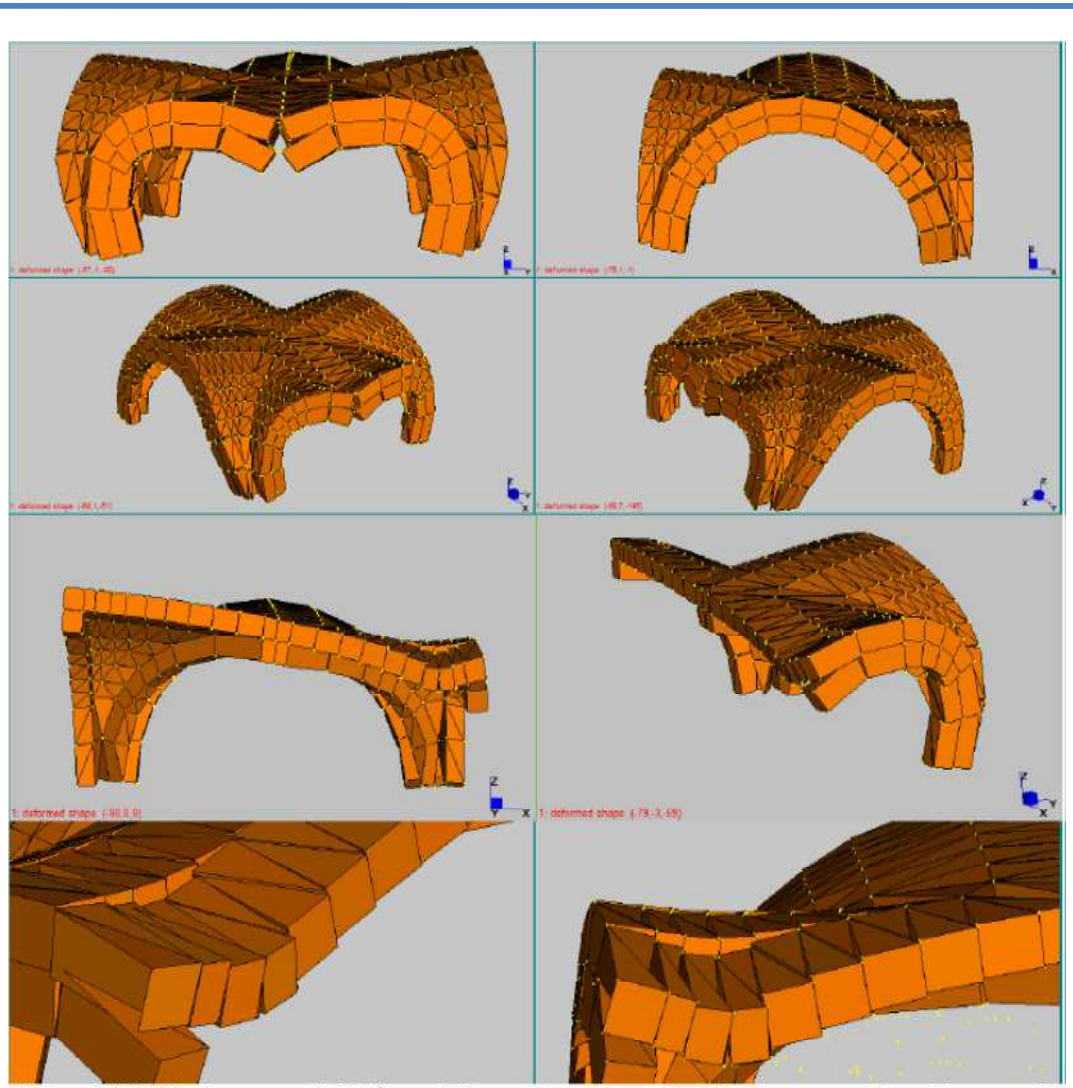

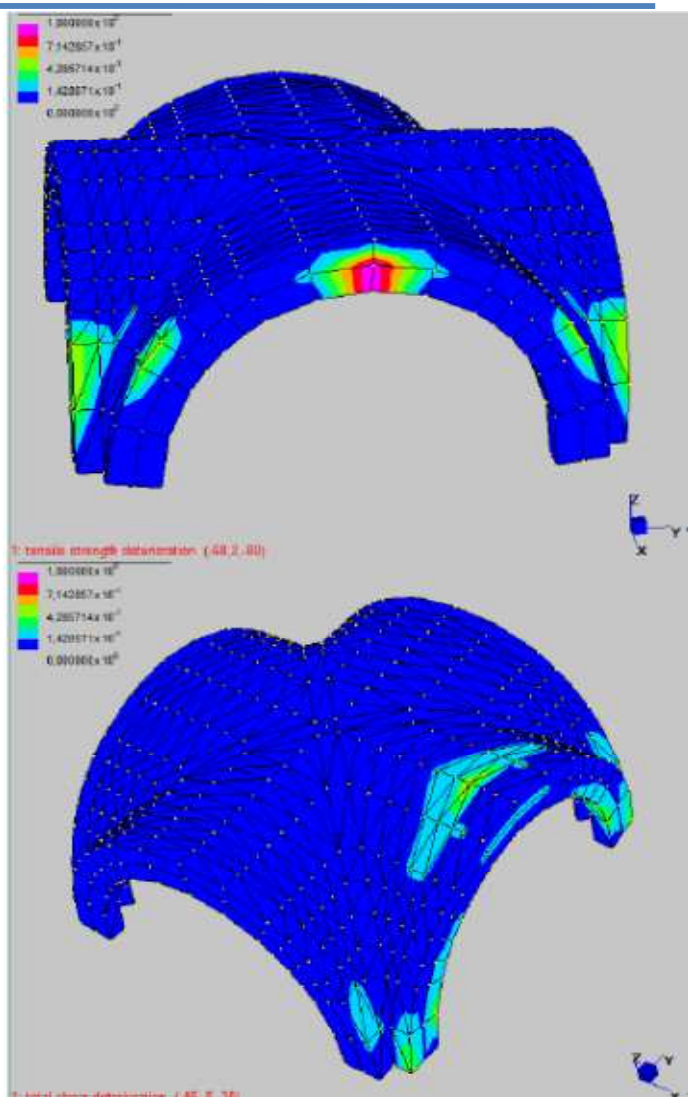

Figure 24: Ribbed cross vault. Deformed shapes at peak provided by the proposed non-linear code and detail of the out-of-plane sliding.

Hemispherical dome

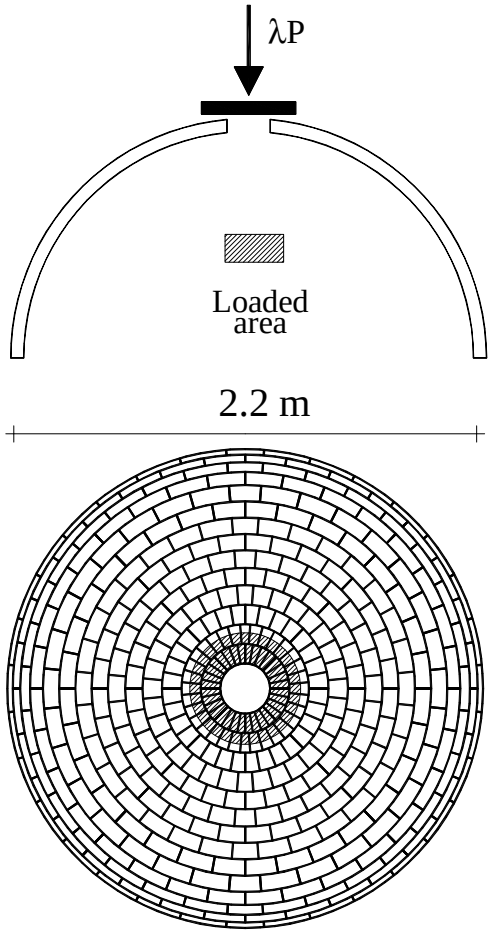

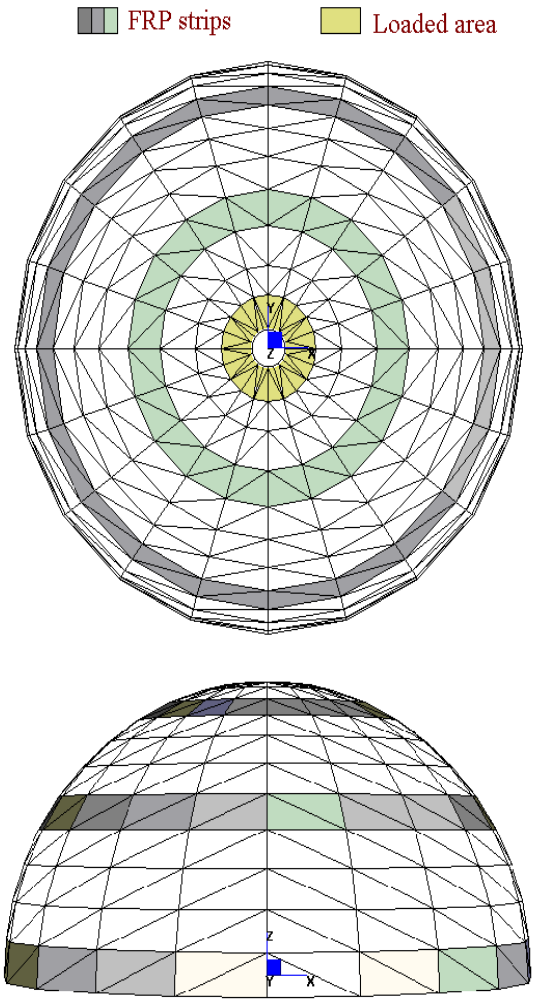

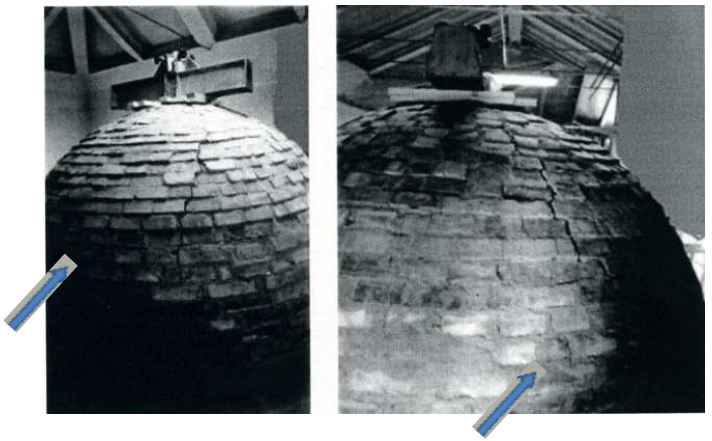

Experimental data from Creazza et al. 2002 and from Foraboschi 2006

Hemispherical dome: nonlinear incremental analysis

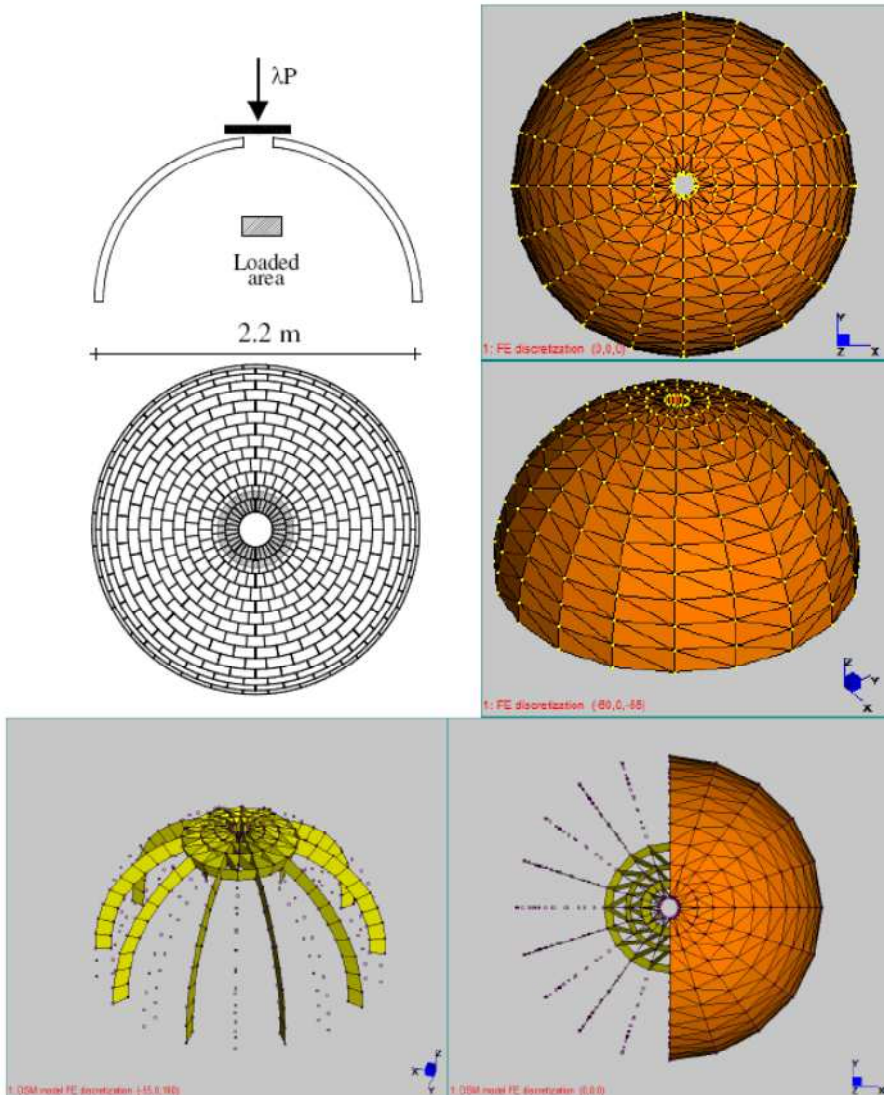

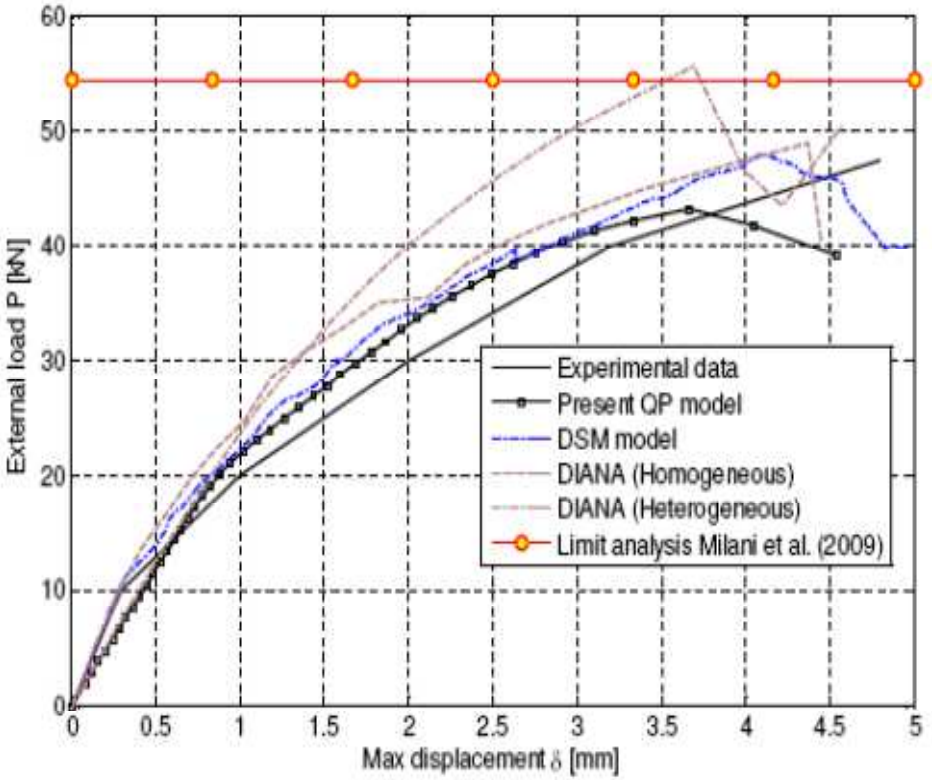

e 27: Hemispherical dome. Comparison among load-displacement curves or collapse loads provided by experimentation, limit analysis and non-linear FE code.

Cloister vault

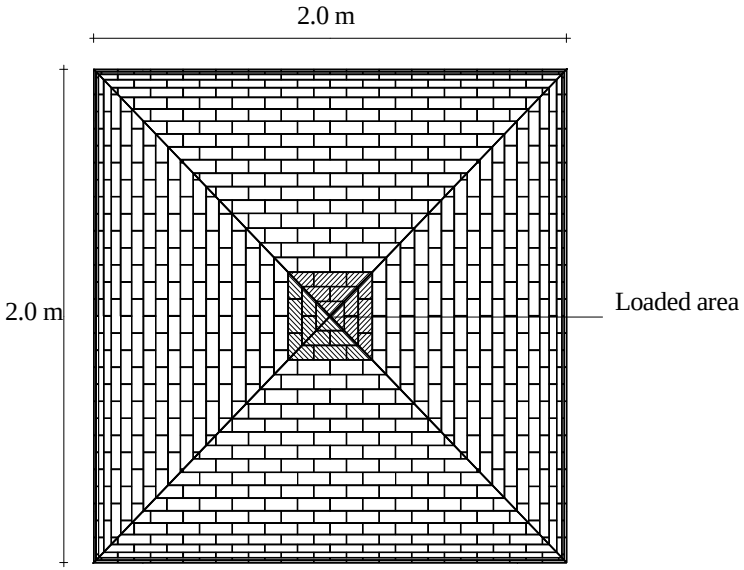

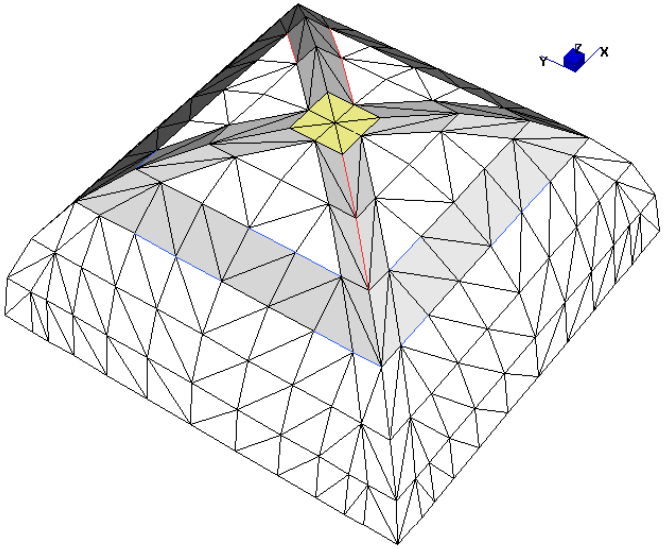

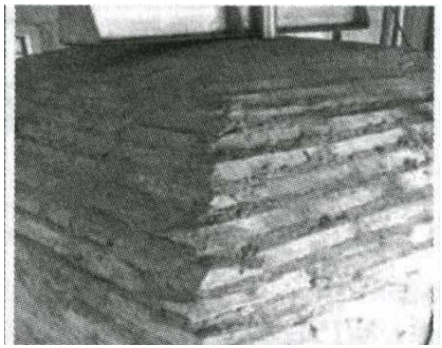

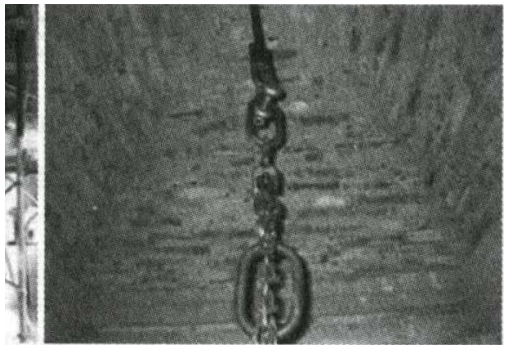

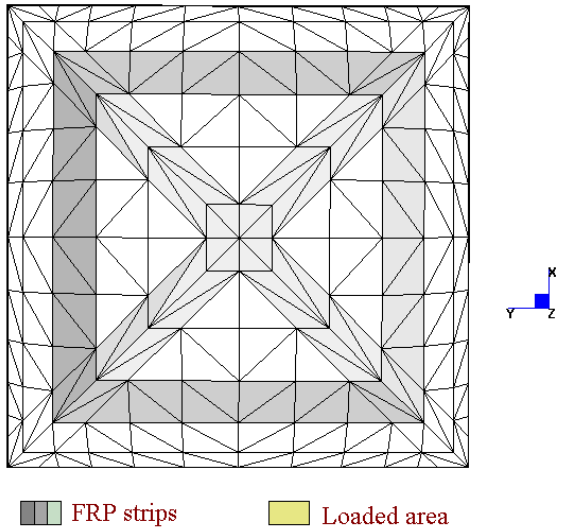

Experimental data from Foraboschi 2006

Unreinforced cloister vault

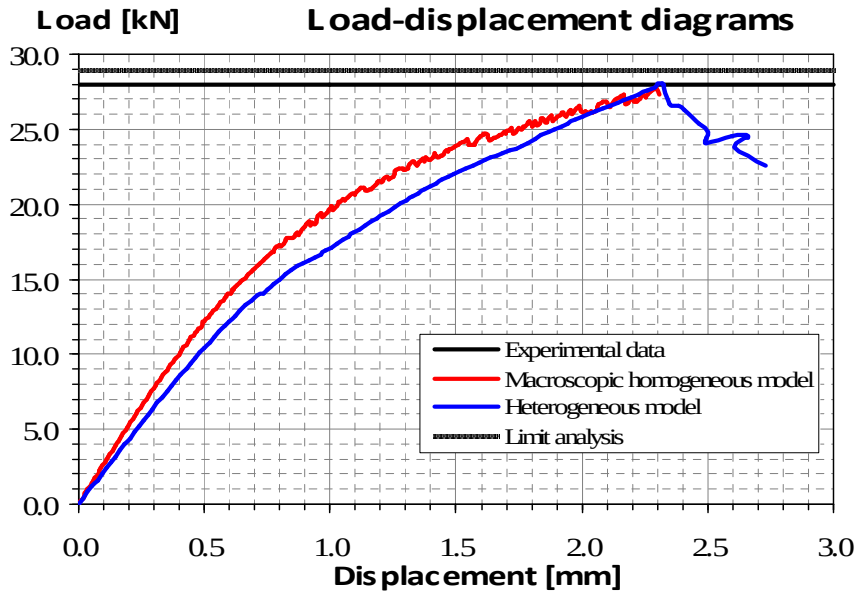

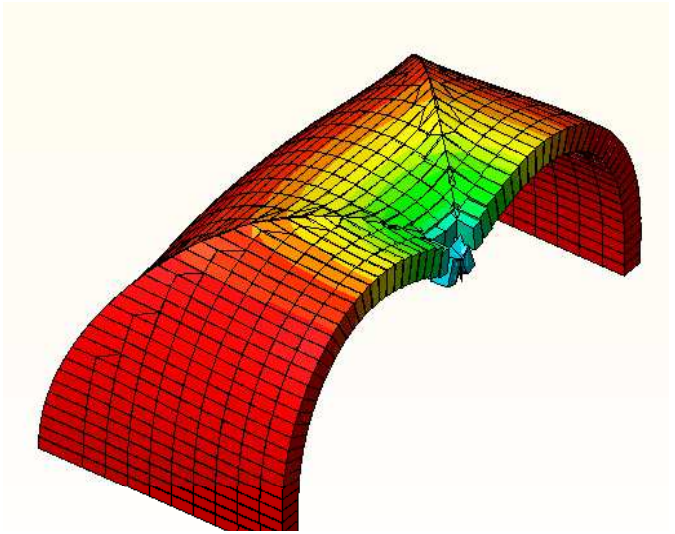

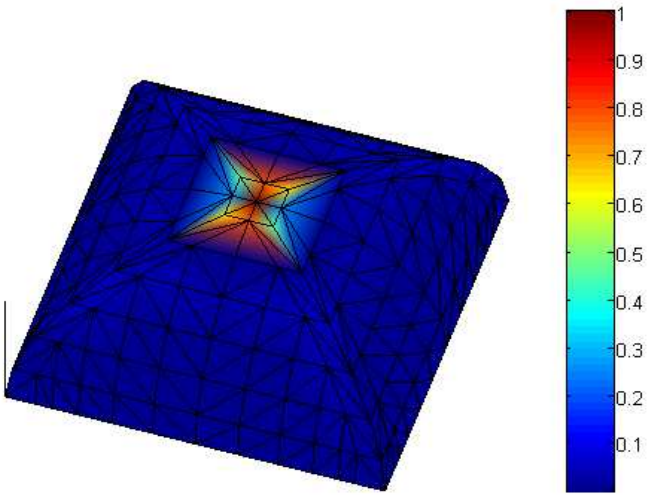

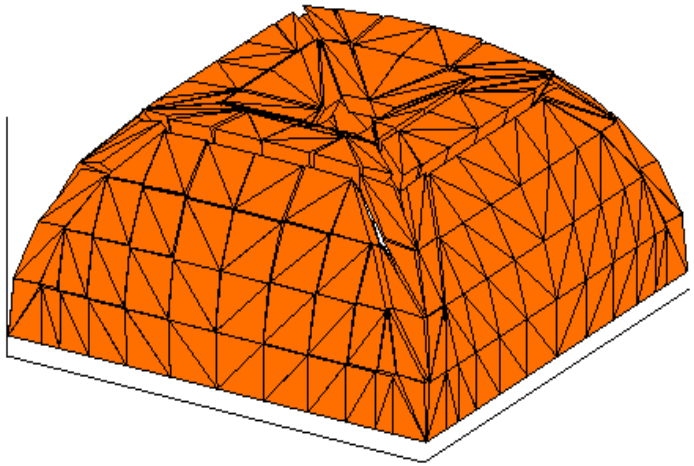

Cloister vault: nonlinear incremental analysis

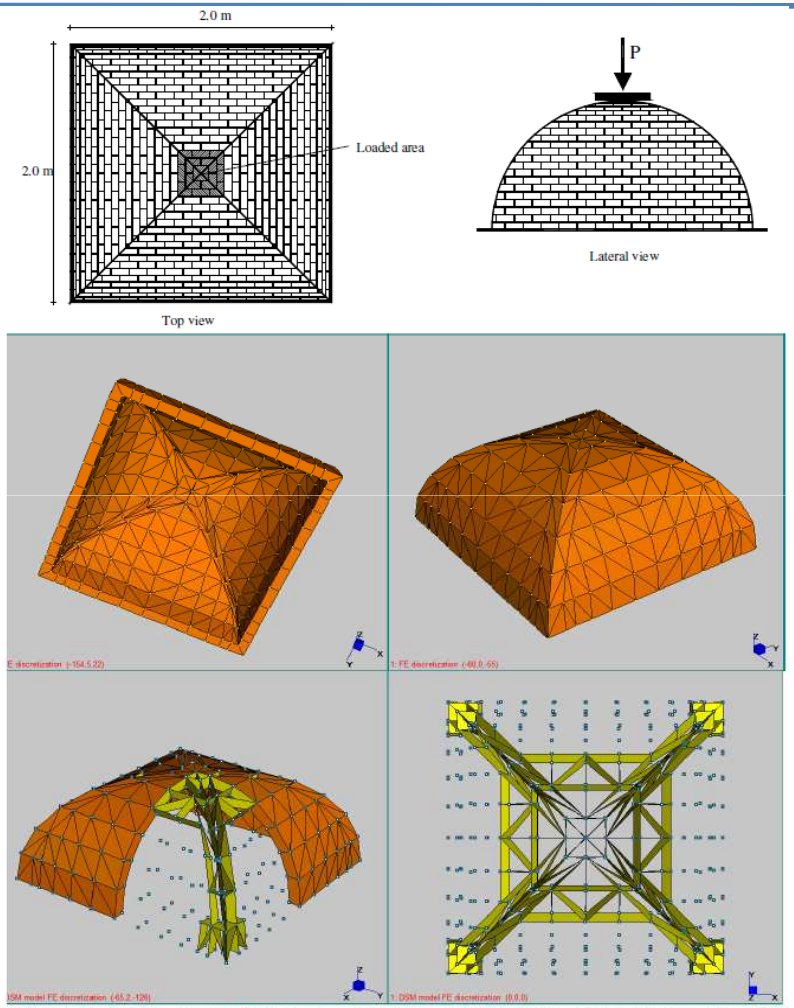

Figure 30: Cloister vault. Geometry, loading condition and FE discretization adopted for the numerical analyses. Non-linear interfaces considered in the DSM model are also indicated

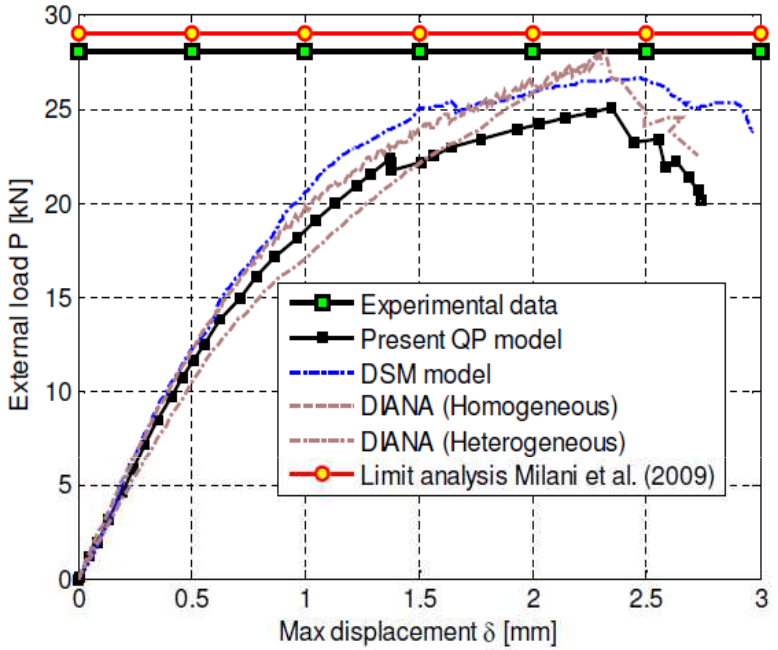

Figure 31: Cloister vault. Parabolic arch. Comparison among load-displacement curves or collapse loads provided by experimentation, limit analysis and non-linear FE code.

Cloister vault: nonlinear incremental analysis

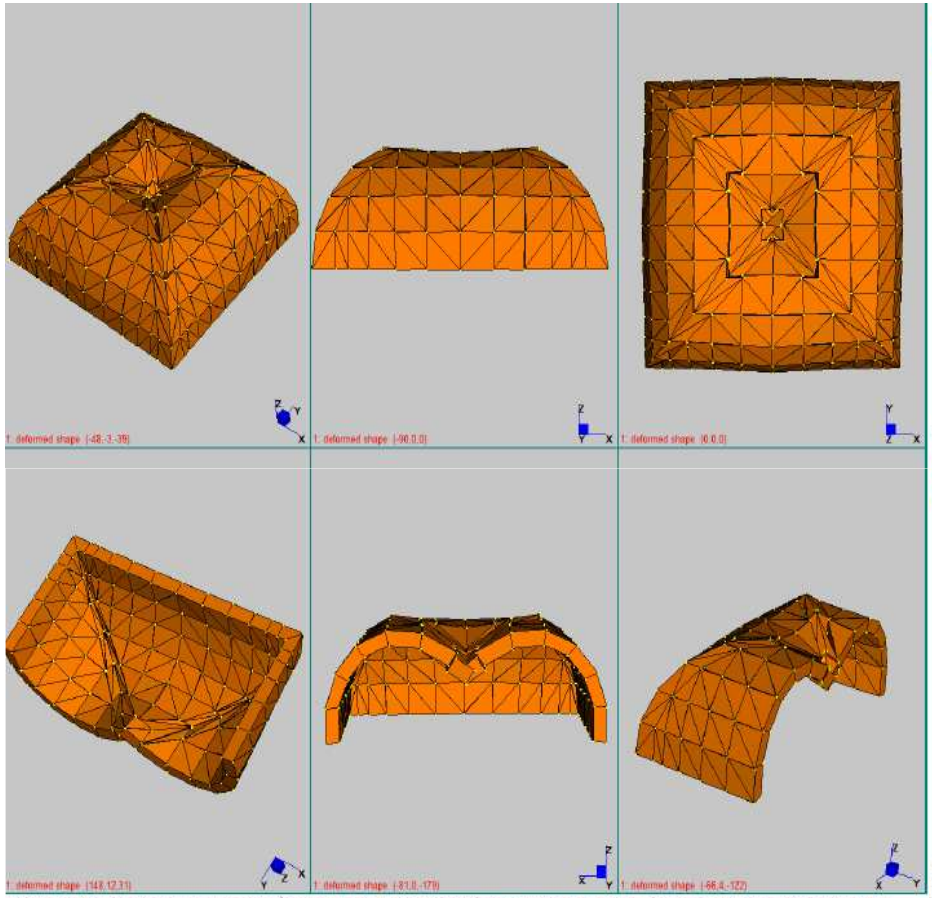

Figure 32: Cloister vault. Deformed shapes at peak provided by the proposed non-linear code.

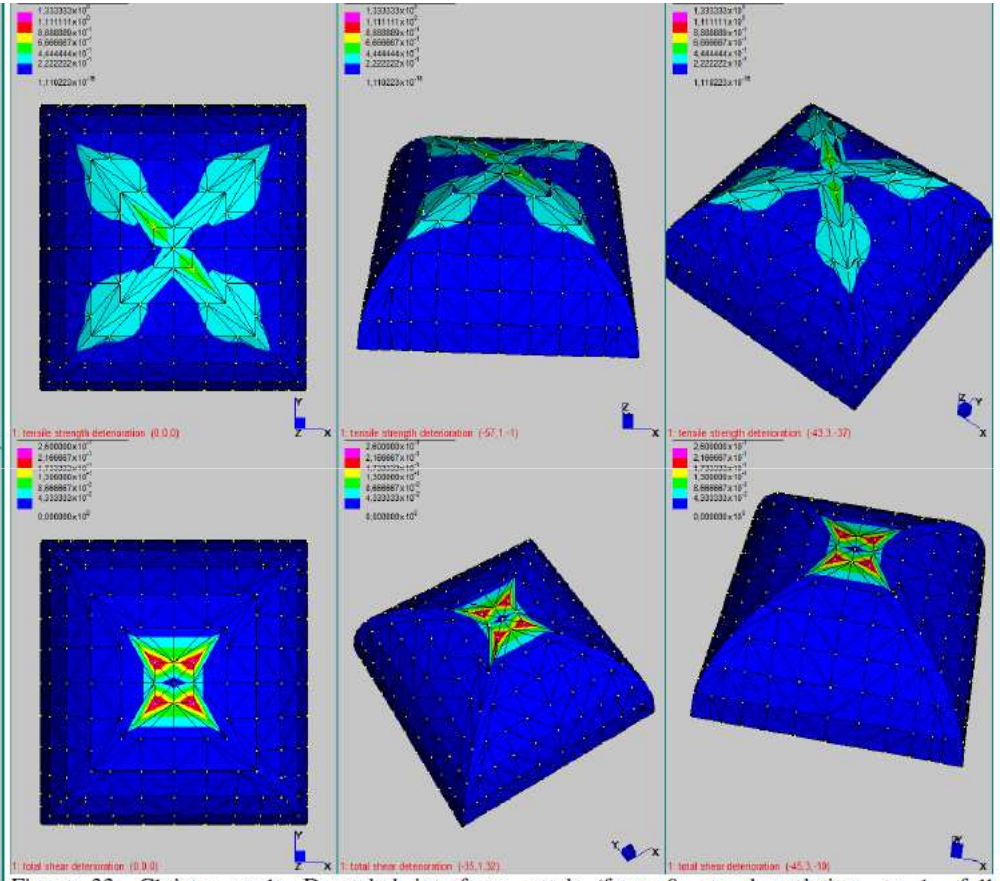

Figure 33: Cloister vault. Degraded interfaces patch (from 0 -no degradation- to 1 –full degradation) obtained through the non-linear homogenized FE code proposed. Top: positive normal stress. Bottom: in- and out-of-plane shear damage map.

Recent papers

The influence of fill :a case study

G. MILANI, M. SIMONI, A. TRALLI "Advanced numerical models for the analysis of masonry cross vaults: a case-study in Italy" ENGINEERING STRUCTURES,76,(October), pp. 339-358, 2014.

A 3D analysis of a masonry bridge

E. RECCIA, G. MILANI, A. CECCHI, A. TRALLI "Full 3D homogenization approach to investigate the behavior of masonry arch bridges: the Venice trans-lagoon railway bridge"JCBM, 66, pp. 567-586, 2014

A Medieval tower damaged by Emilia earthquake

G. MILANI, S. MARZOCCHI, F. MINGHINI; A. TRALLI - IX IBMC 2014

S. CATTARI, S. LAGOMARSINO, G. MILANI, M. ROSSI, M. SIMONI. A. TRALLI- SACH 2014

A software for practitioners

A. CHIOZZIM. MALAGU, A. CAZZANI; A. TRALLI "ArchNURBS: a NURBS-Based Tool for the Structural Safety Assessment of Masonry Arches in MATLAB" accepted on ASCE *J. of Computing in Civil Engineering (CPENG).*

A case study

CITTA' DI LUCCA

INTERVENTO DI RESTAURO
DELL' EX CONVENTO DI SAN ROMANO
EX CASERMA LORENZINI

PIUSS
LUCCA
DENTRO

Valutazione comportamento statico delle volte a crociera: stato di fatto

G. MILANI, M. SIMONI, A. TRALLI "Advanced numerical models for the analysis of masonry cross vaults: a case-study in Italy" ENGINEERING STRUCTURES,76,(October), pp. 339-358, 2014

A case study

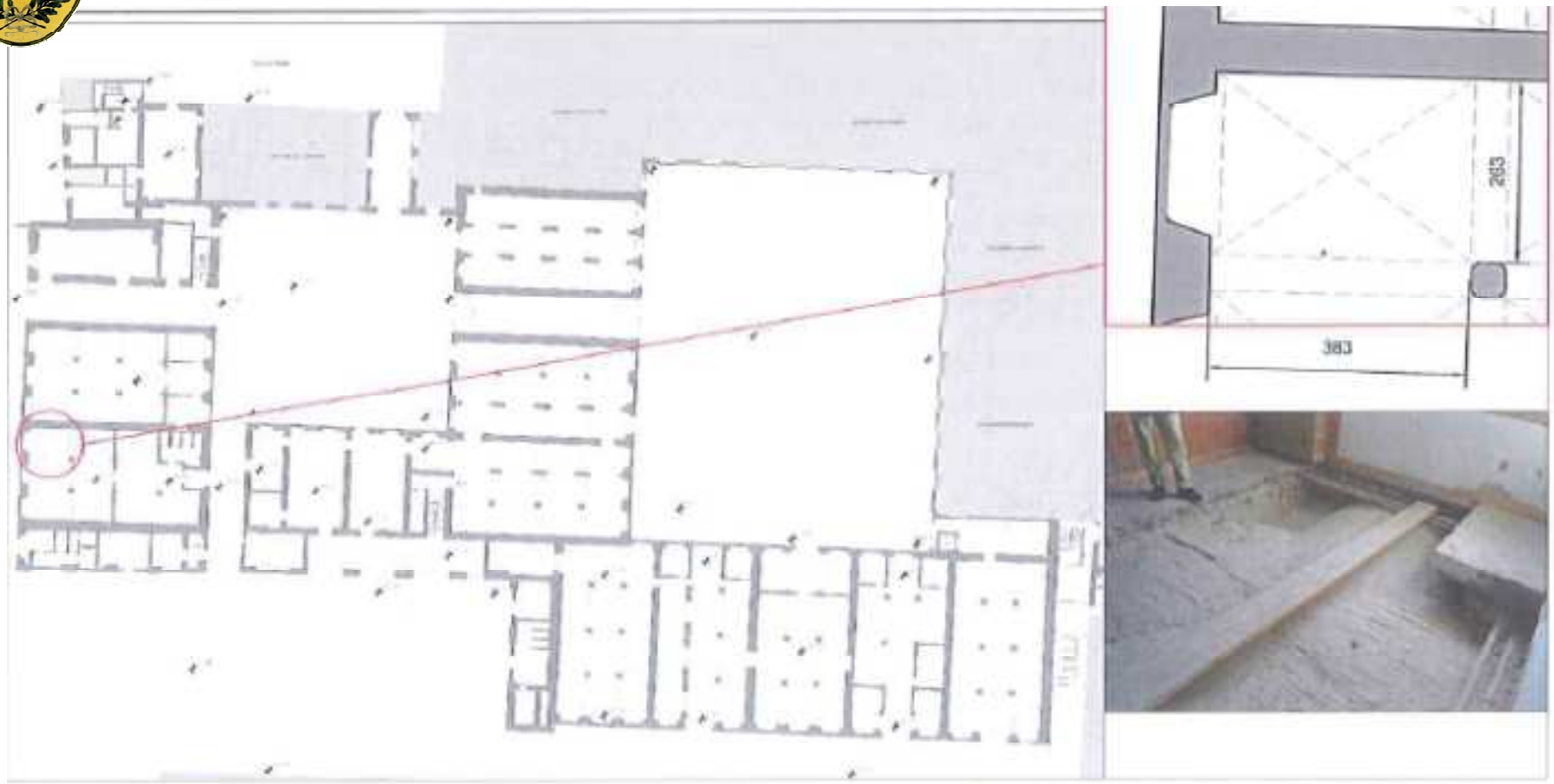

Figura 1: Pianta del piano terra e posizione della volta studiata

In this convent, built again about 1850, are present more than 100 cross vaults , completey surrounded by other vaults, along the boundary and in a hedge. In the different case the contribution of back fill on the collapse load , can be different

A case study

A case study

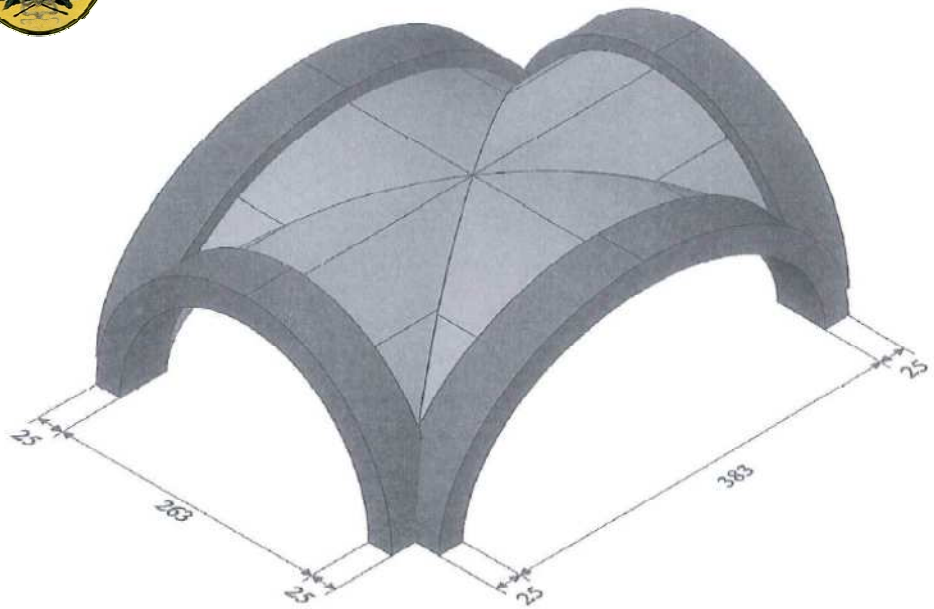

Figura 2: Assonometria (quote in cm)

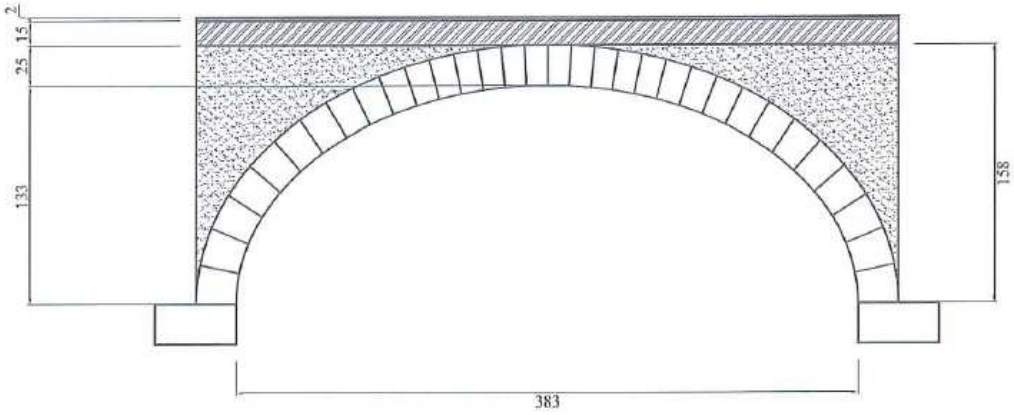

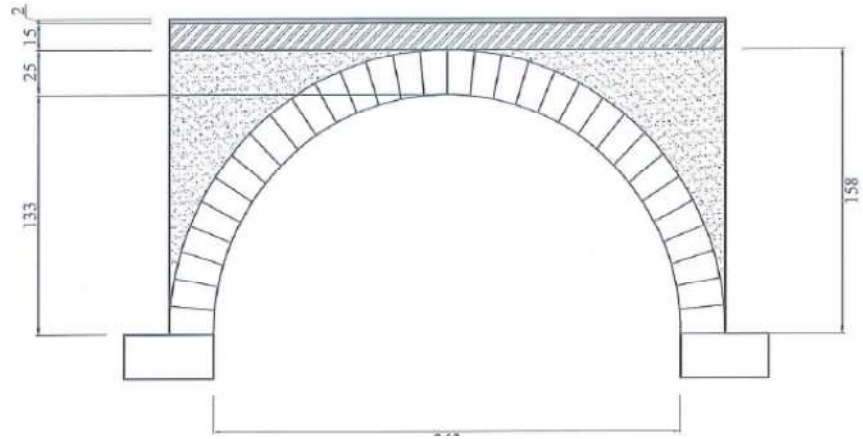

In-plane behavior

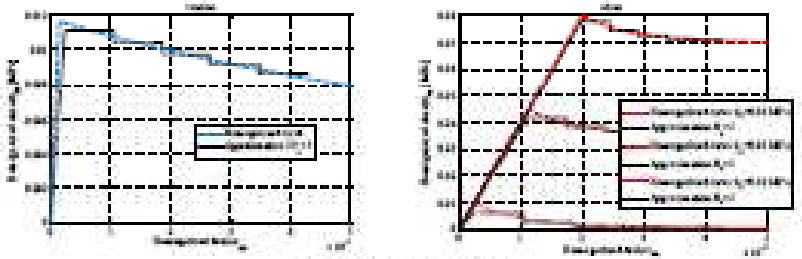

Out-of-plane behavior

Figure 5: Homogenized stress strain curves used in the non-standard FE approach proposed and their approximation by means of linear-piecewise constant functions.

A case study

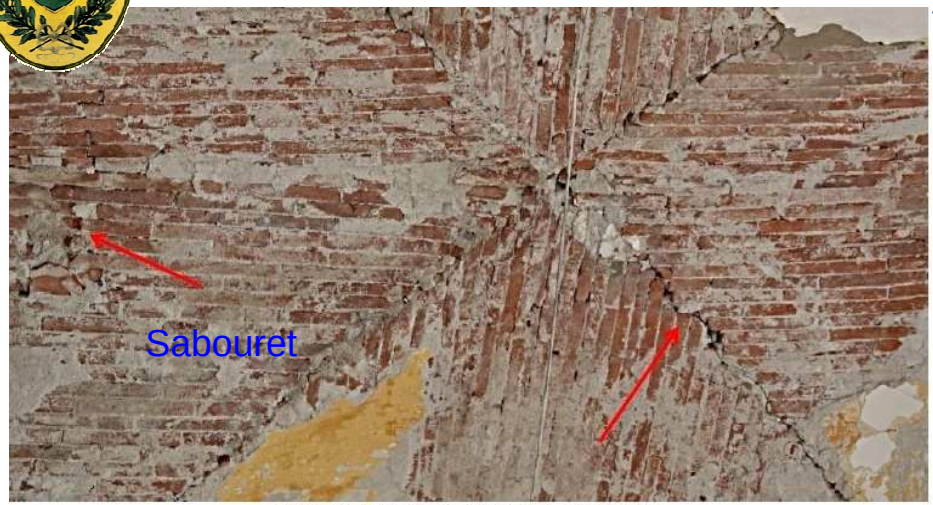

Figura 4: Lesioni archi diagonali, intradosso.


Figura 3:Lesione arco diagonale, estradosso


Figura 5: Distacco arcone di bordo della volta a crociera

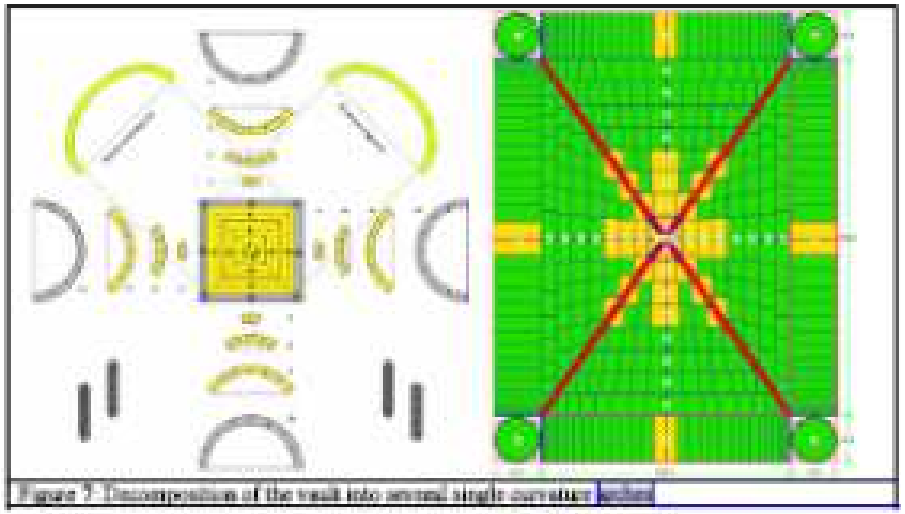

A case study

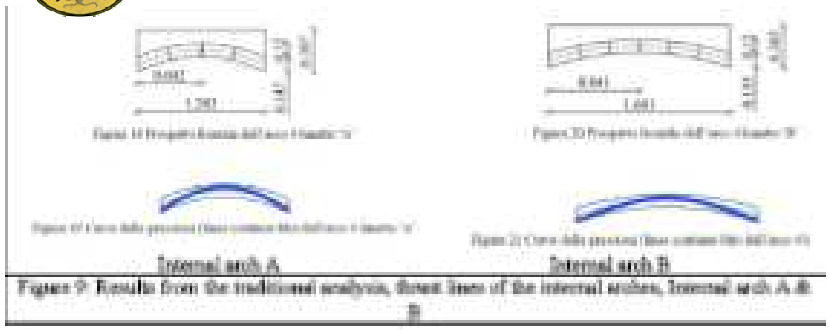

Figure 9: Results from the traditional analysis, thrust lines of the internal arches, Internal arch A & B

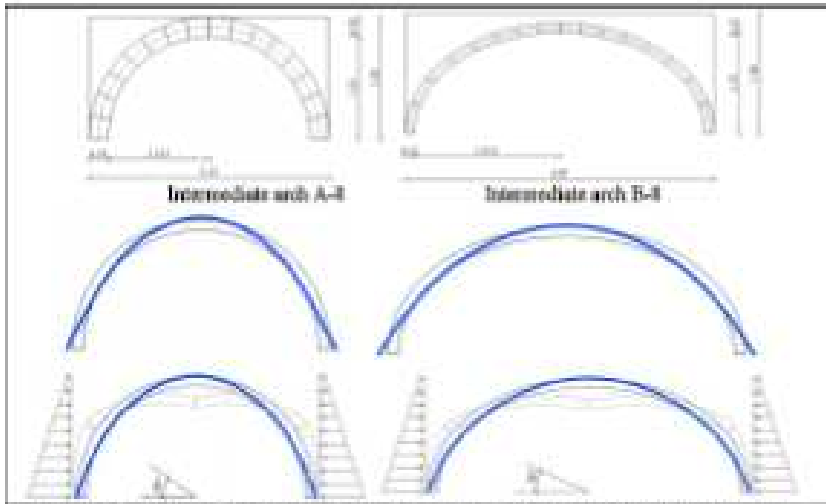

Figure 10: Results from the traditional analysis, thrust lines of the internal arches and kinematic limit analysis, intermediate arch A & B

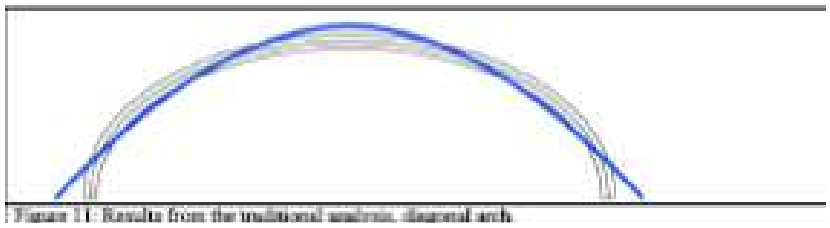

Figure 11: Results from the traditional analysis, diametral arch

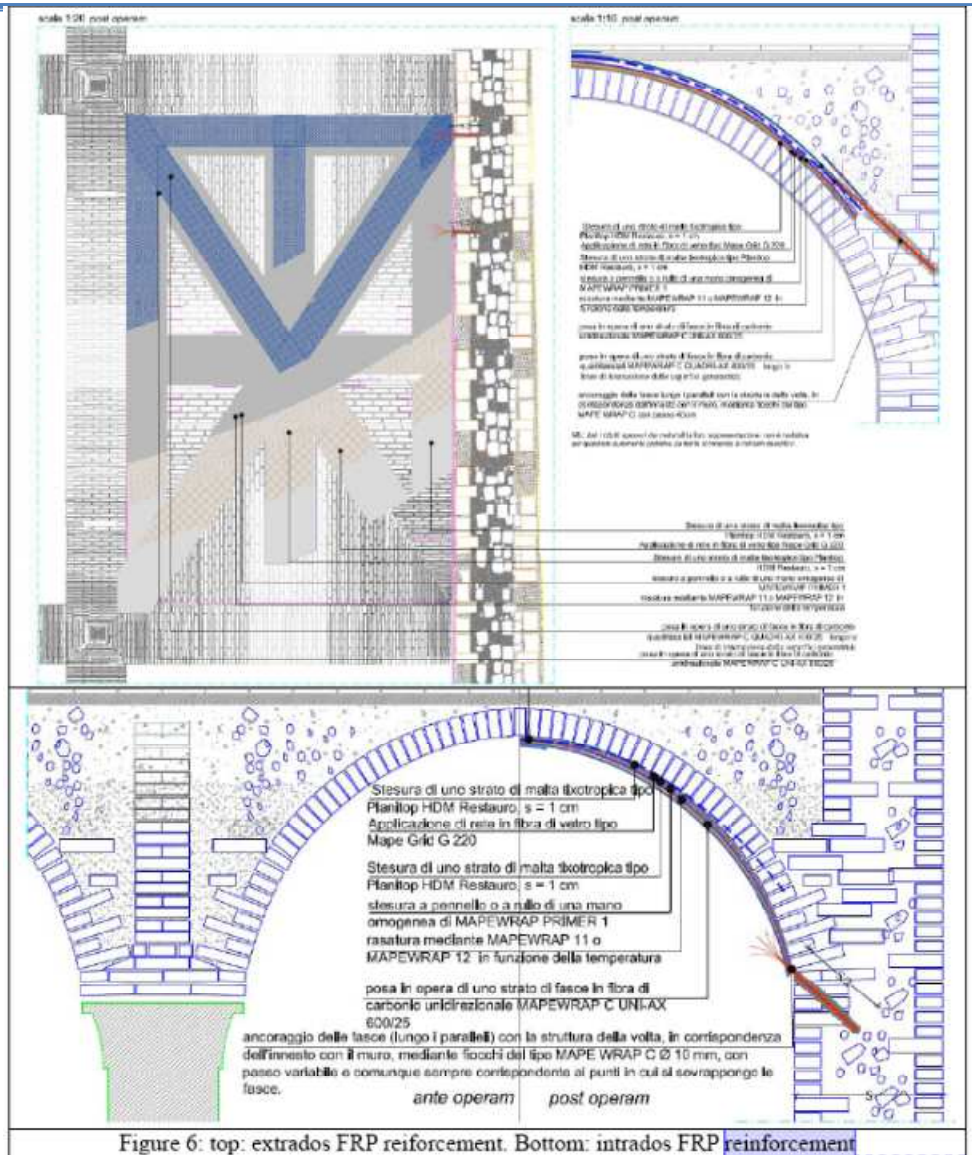

Figure 6: top: extrados FRP reiforcement. Bottom: intrados FRP reinforcement

A case study

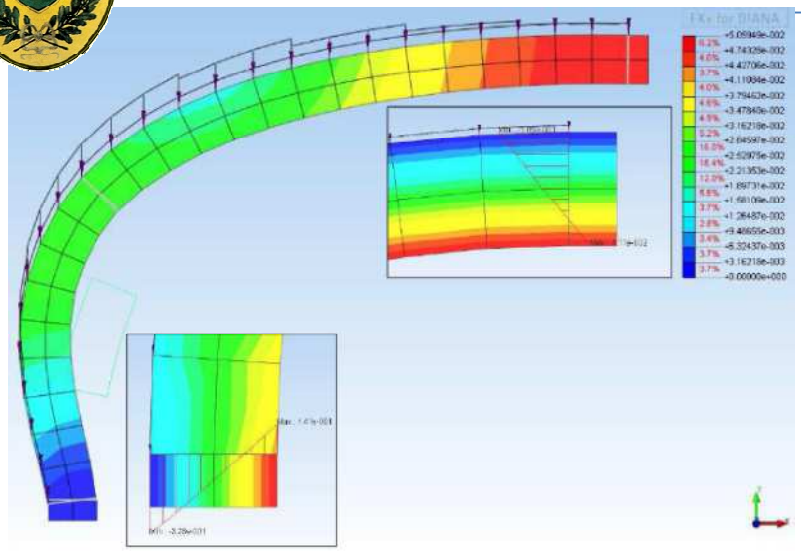

Figura 30 Analisi al elementi finiti dell'arco 8 in assenza di rinforzi in FRP

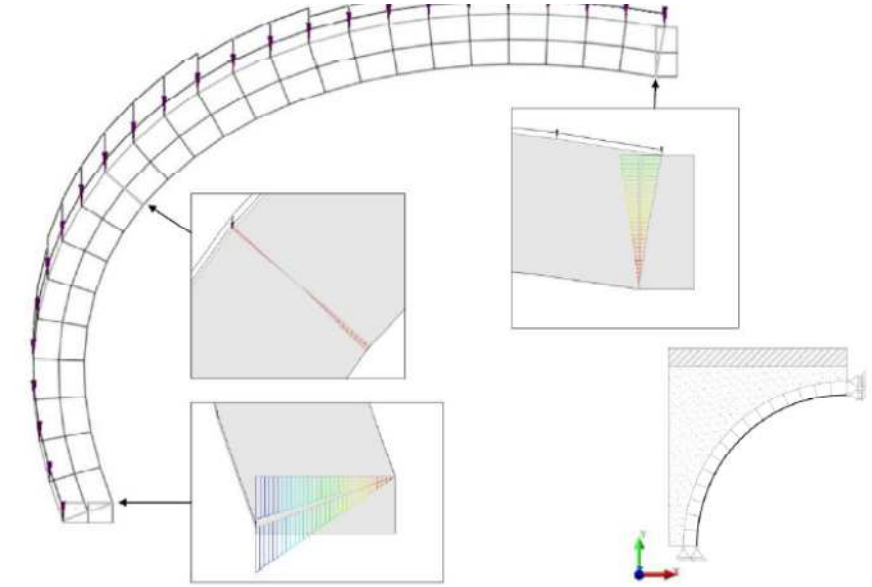

a 31 Analisi al elementi finiti dell'arco 8 con rinforzi in FRP all'intradosso

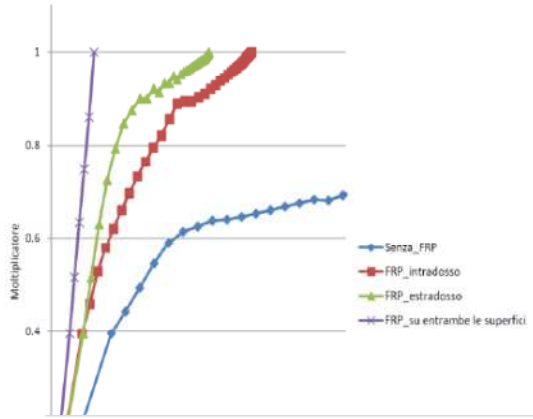

Figura 33 Analisi al elementi finiti dell'arco 8. Confronto fra i diversi tipi di rinforzo con FRP. Il valore 1 del moltiplicatore dei carichi corrisponde al carico massimo definito dalle NTC2008

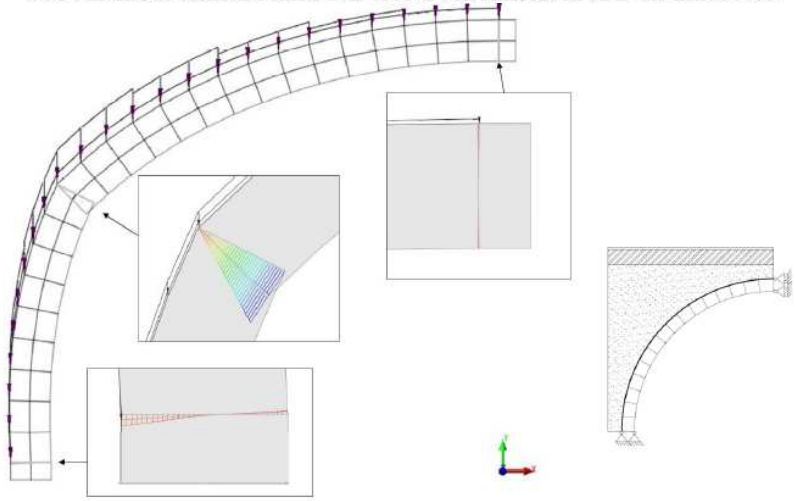

gura 32 Analisi al elementi finiti dell'arco 8 con rinforzi in FRP all'estradosso

A case study

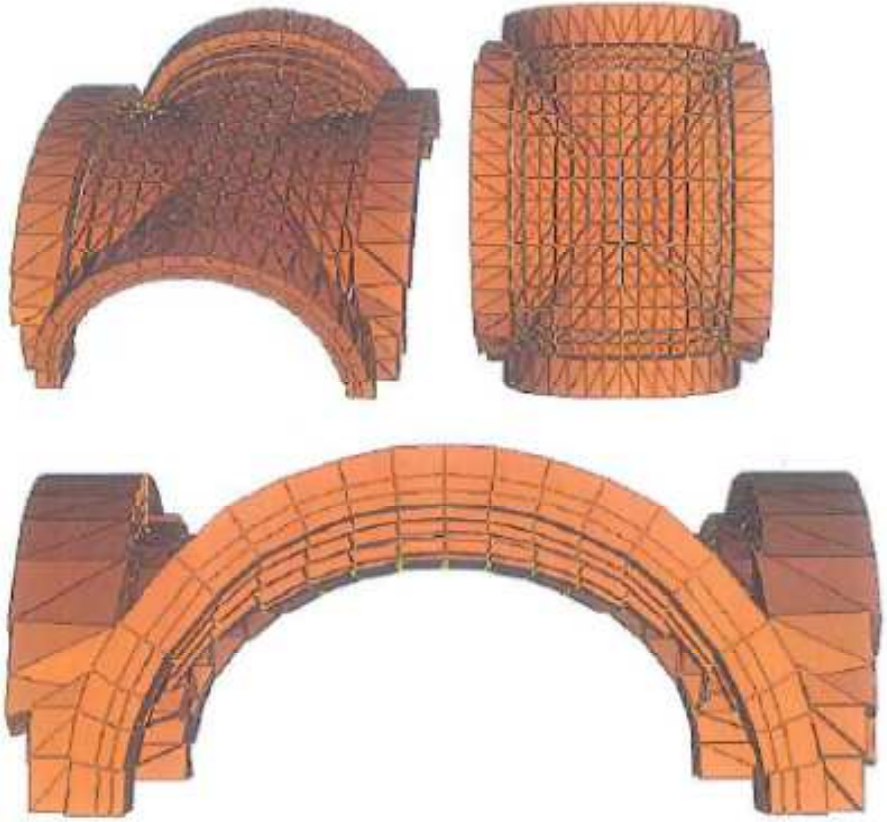

Figura 38: Meccanismo di collasso per la volta completamente isolata

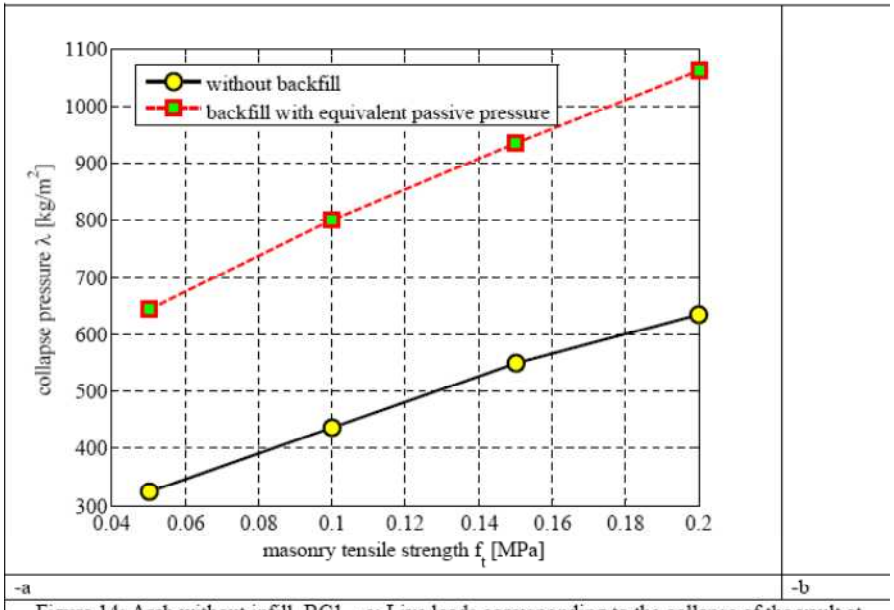

Figure 14: Arch without infill, BC1. –a: Live loads corresponding to the collapse of the vault at different values of mortar tensile strength and friction angle. –b: pressure-vertical displacement curves obtained with the non-linear code.

Andamento del carico di collasso al variare della resistenza a trazione della muratura per una volta isolata

A case study

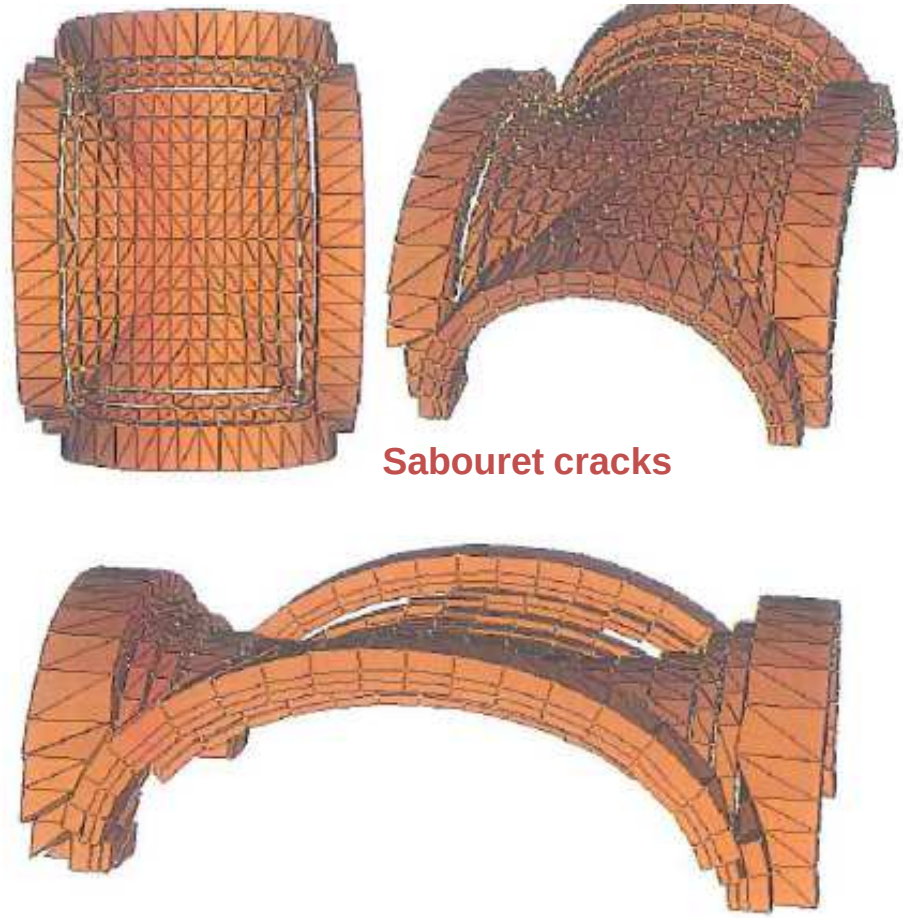

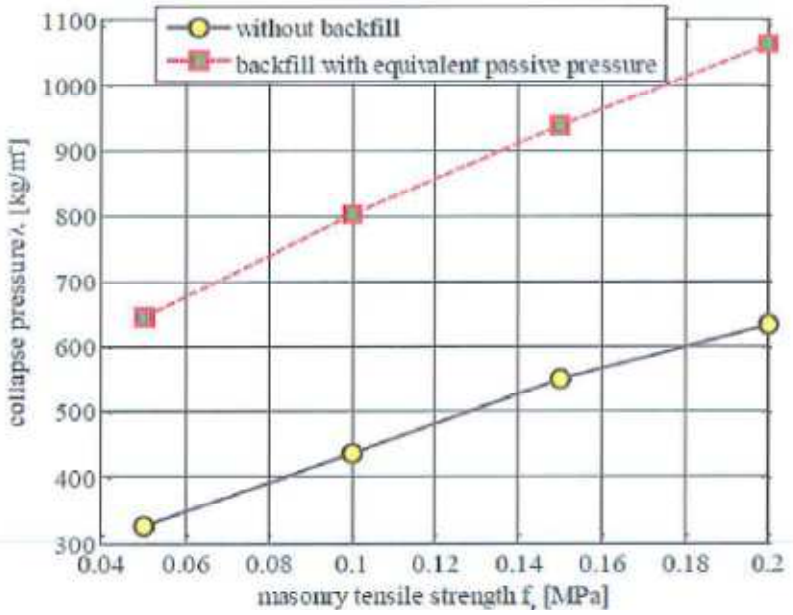

Figura 40: Meccanismo di collasso per la volta d'angolo
Andamento del carico di collasso al variare della resistenza a trazione della muratura per una volta d'angolo.

A case study

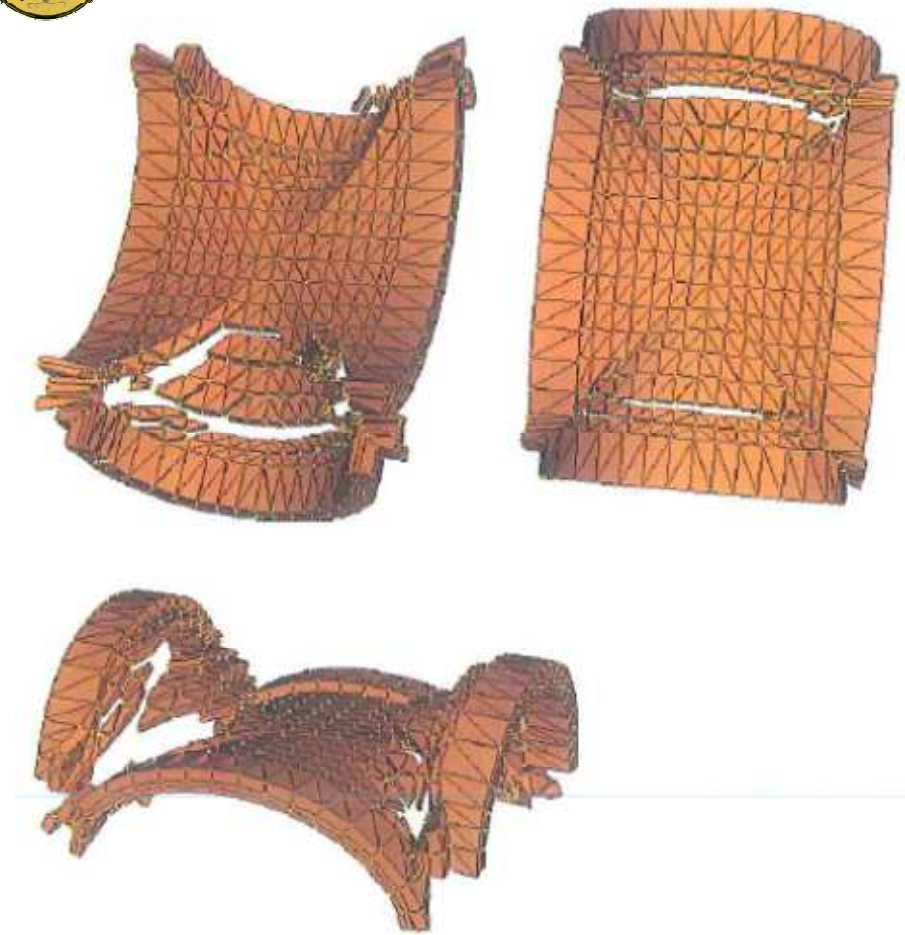

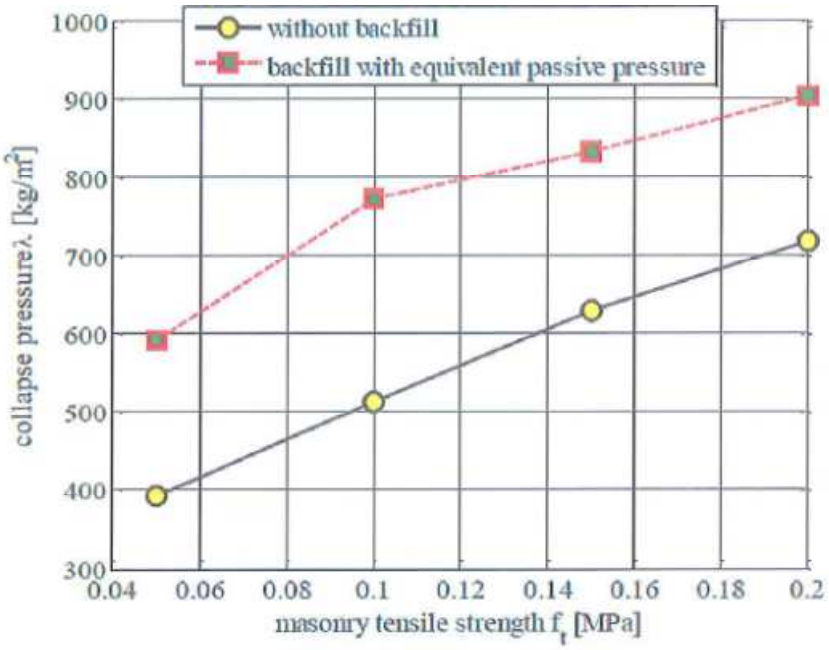

Figura 43: Meccanismo di collasso per una volta interna.

Figura 42: Andamento del carico di collasso al variare della resistenza a trazione della muratura per una volta interna, con resistenza a compressione 50 kgm^{-2}.

A case study

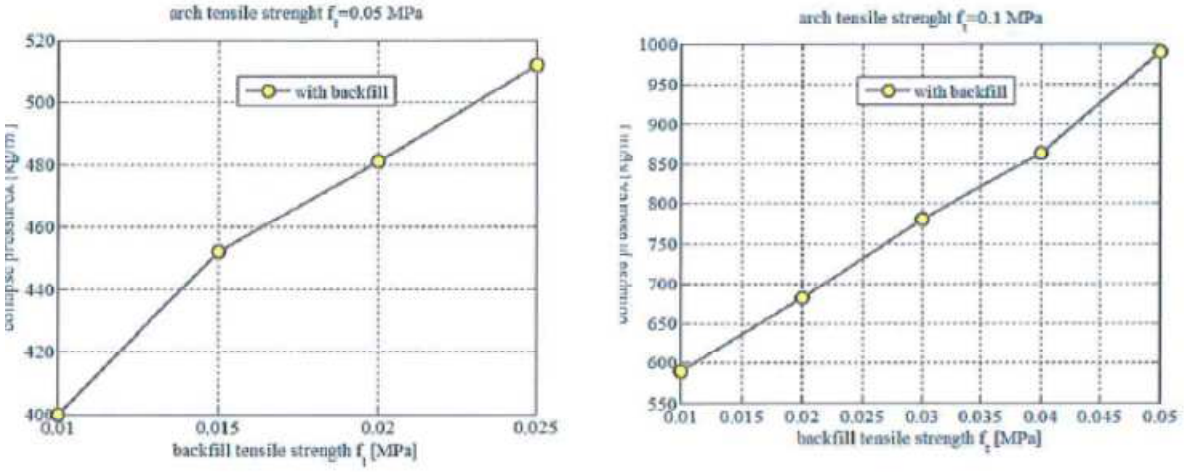

igura 44: variazione del moltiplicatore di collasso dalla resistenza a trazione del riempimento per 2 diversi valori della resistenza a trazione della muratura.

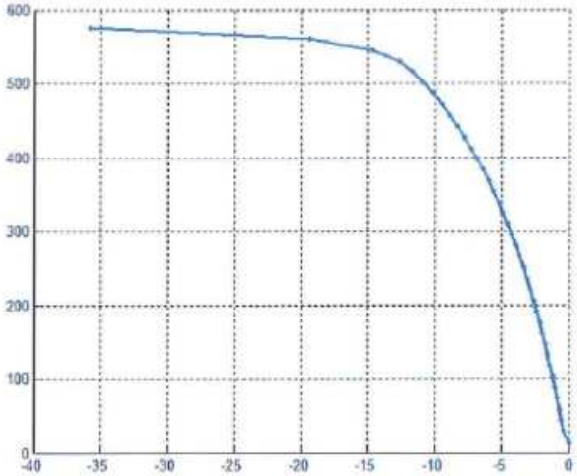

45: Curva carico spostamento per una volta d'angolo (muratura ft = 0,1 MPa e fc = 3 MPa, riempimento ft = 0,05 MPa)

A case study

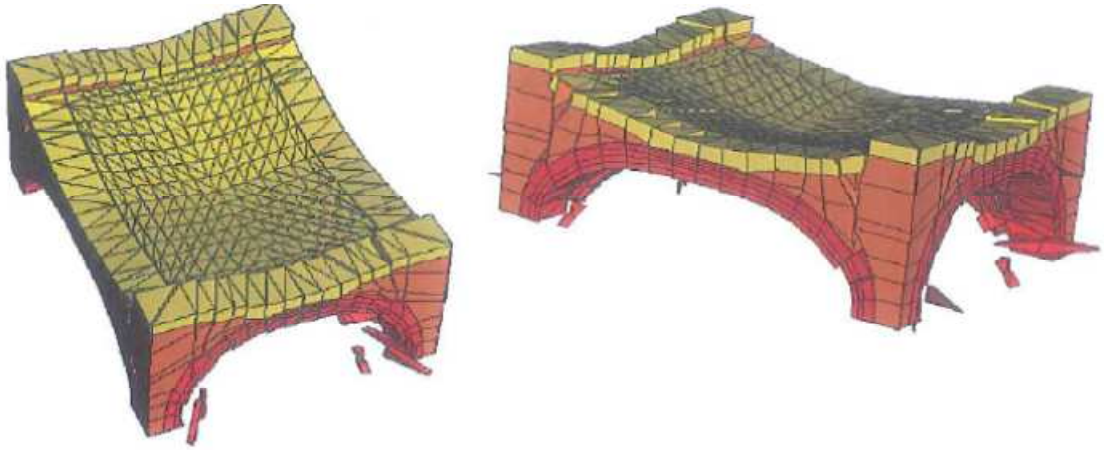

Figura 46: Meccanismo di collasso incipiente visto dall'estradosso

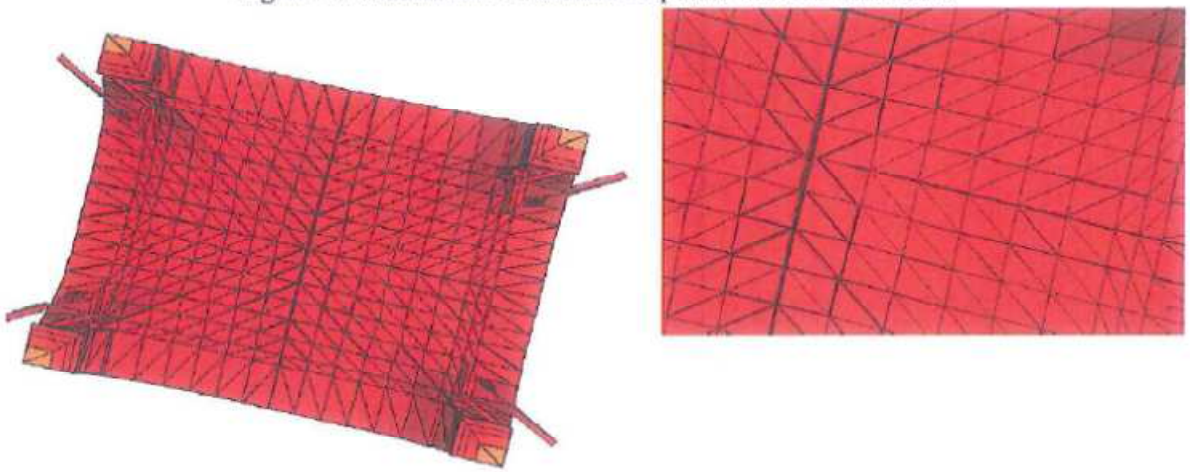

Figura 47: Meccanismo di collasso incipiente visto dall'intradosso

Venice trans lagoon bridge

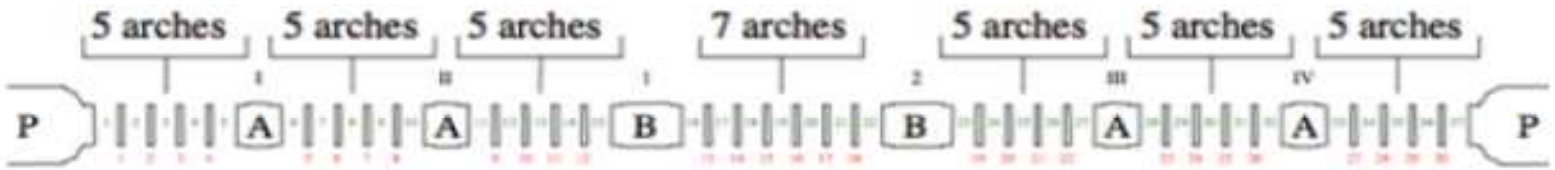

Figure 6: Historical photograph of the Venetian trans-lagoon bridge. One "stadio" of the bridge with artificial islands on the left and right (P).

Venice trans lagoon bridge

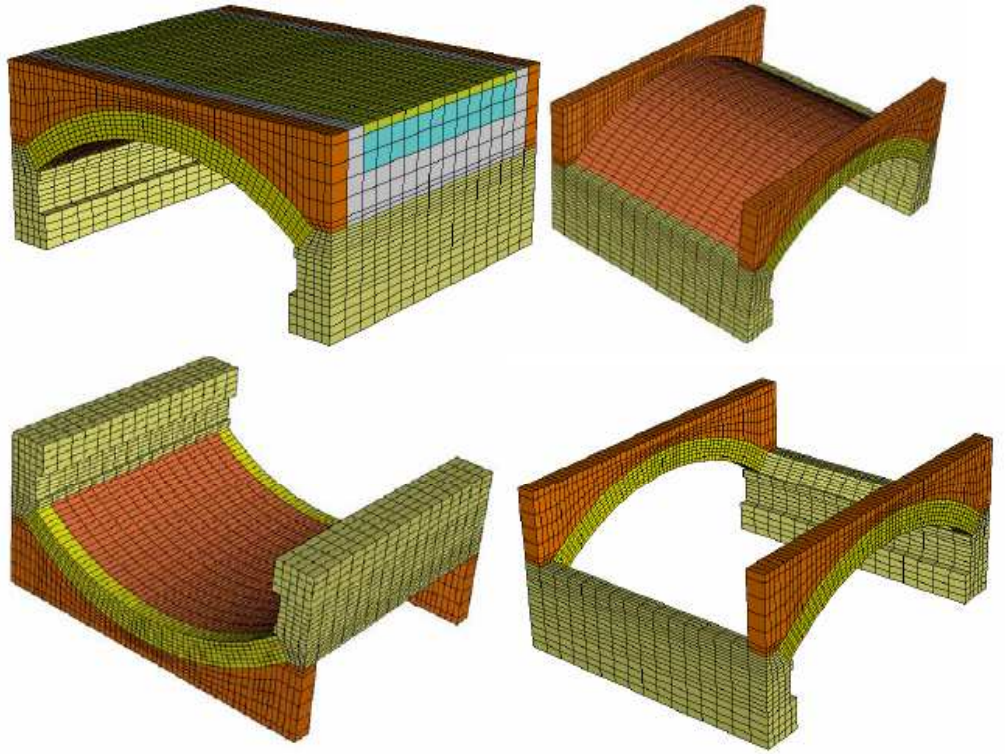

Figure 2: Typical configuration of an arch barrel, adapted from Torre [31] and FE discretization of the Venice trans-lagoon bridge with identification of external stone arches (14688 nodes and 12224 bricks)

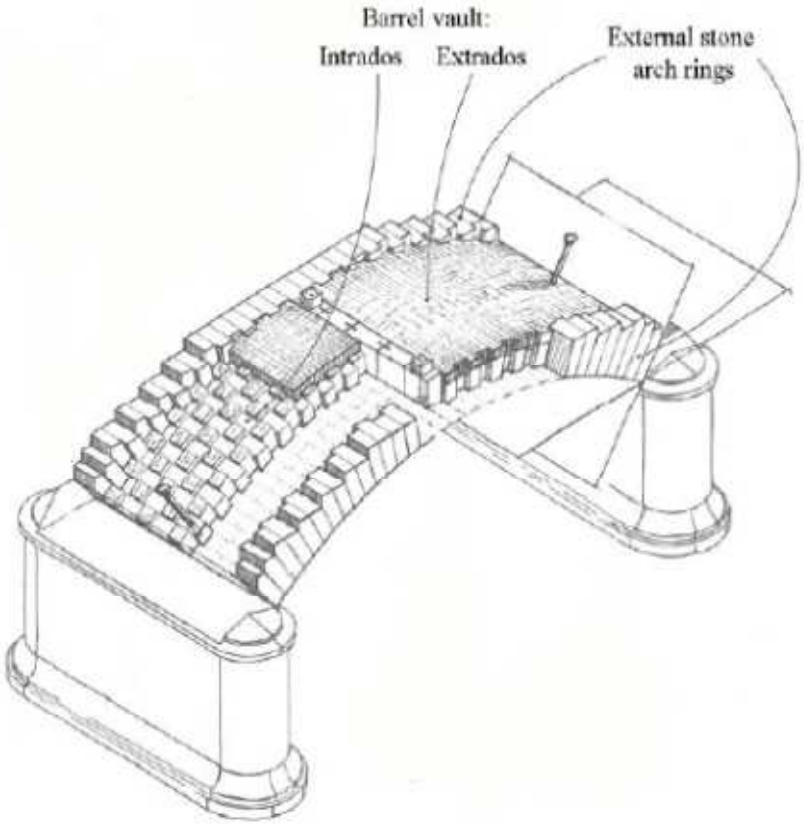

E. RECCIA, G. MILANI, A. CECCHI, A. TRALLI "Full 3D homogenization approach to investigate the behavior of masonry arch bridges: the Venice trans-lagoon railway bridge" J. Construction Building Materials (JCBM), 66, pp. 567-586, 2014

Venice trans lagoon bridge

Figure 7: The texture of masonry barrel vault

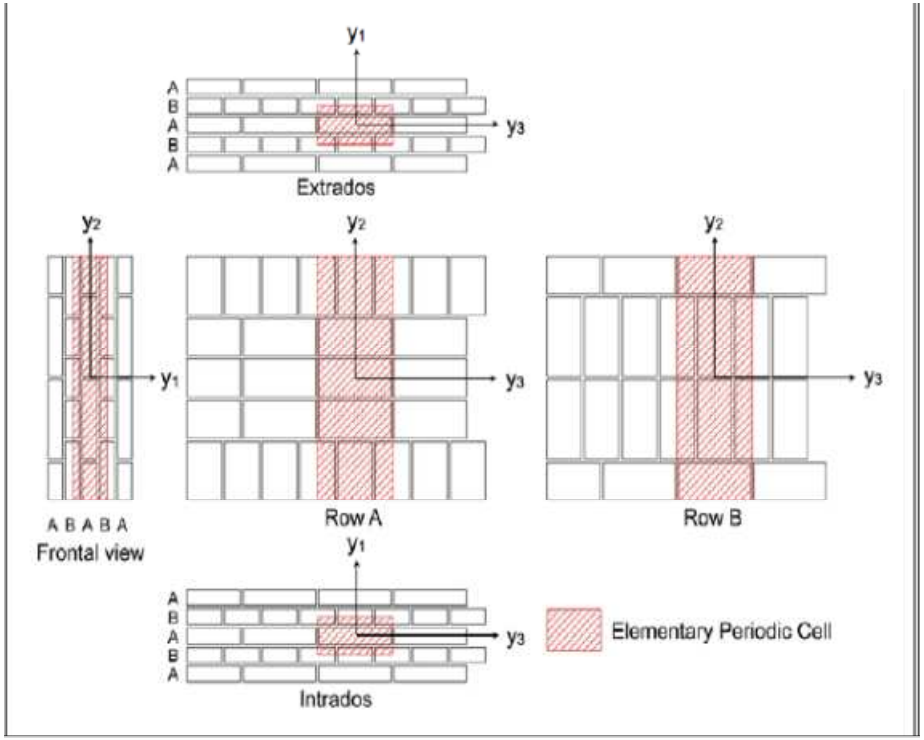

Figure 8: The elementary cell for the homogenization of barrel vault.

Venice trans lagoon bridge

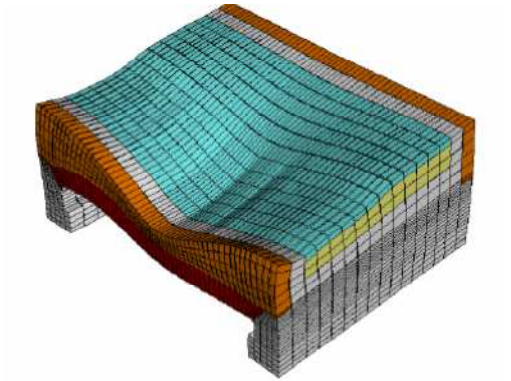

-a

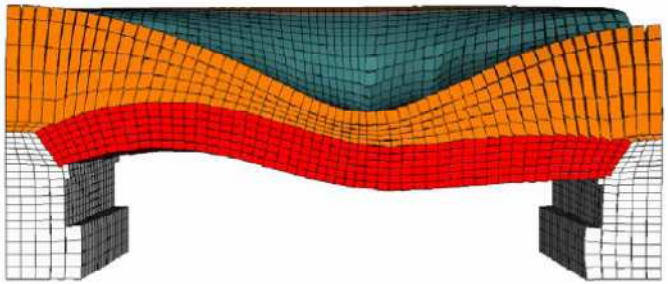

-b

Figure 20: LM71 load on single track. –a: Deformed shape obtained with the non-commercial FE code. –b: formation of plastic hinges on the lower arch.

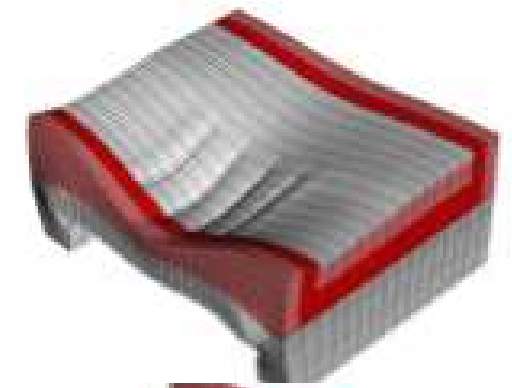

Deformed shape obtained with commercial code –Elastic plastic material Mohr-Coulomb yield surface

Venice trans lagoon bridge

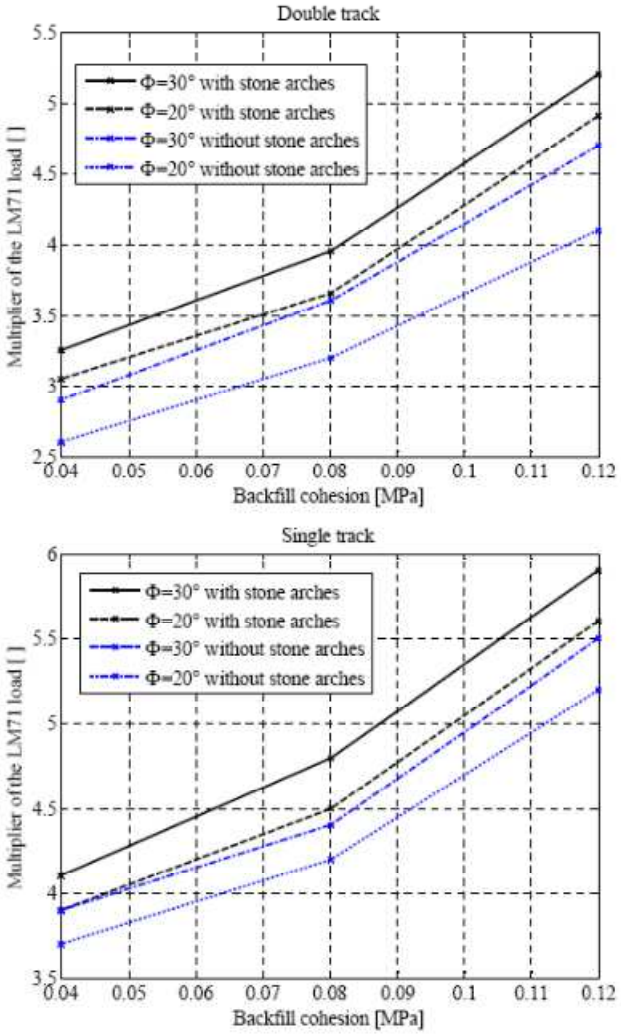

-a

-b

Figure 22: Synopsis of failure loads obtained with limit analysis. –a: LM71 load on both tracks. –b: LM71 load on single track.

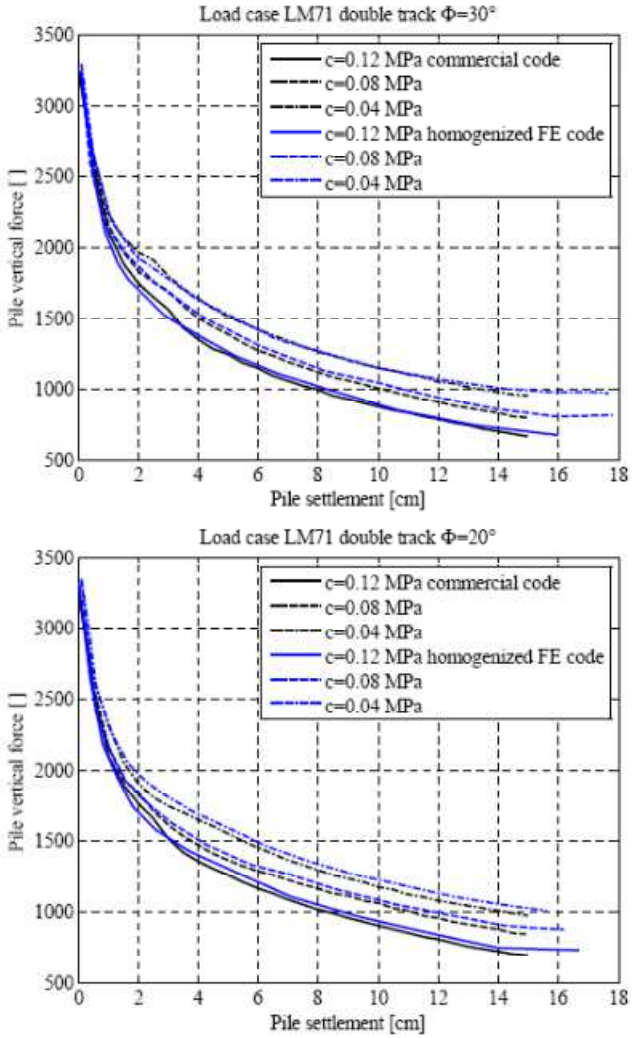

e 23: Right pile settlement. Load displacement curves at different values of infill cohesion at two different friction angles: (-a) 30°, (-b) 20°

Venice trans lagoon bridge

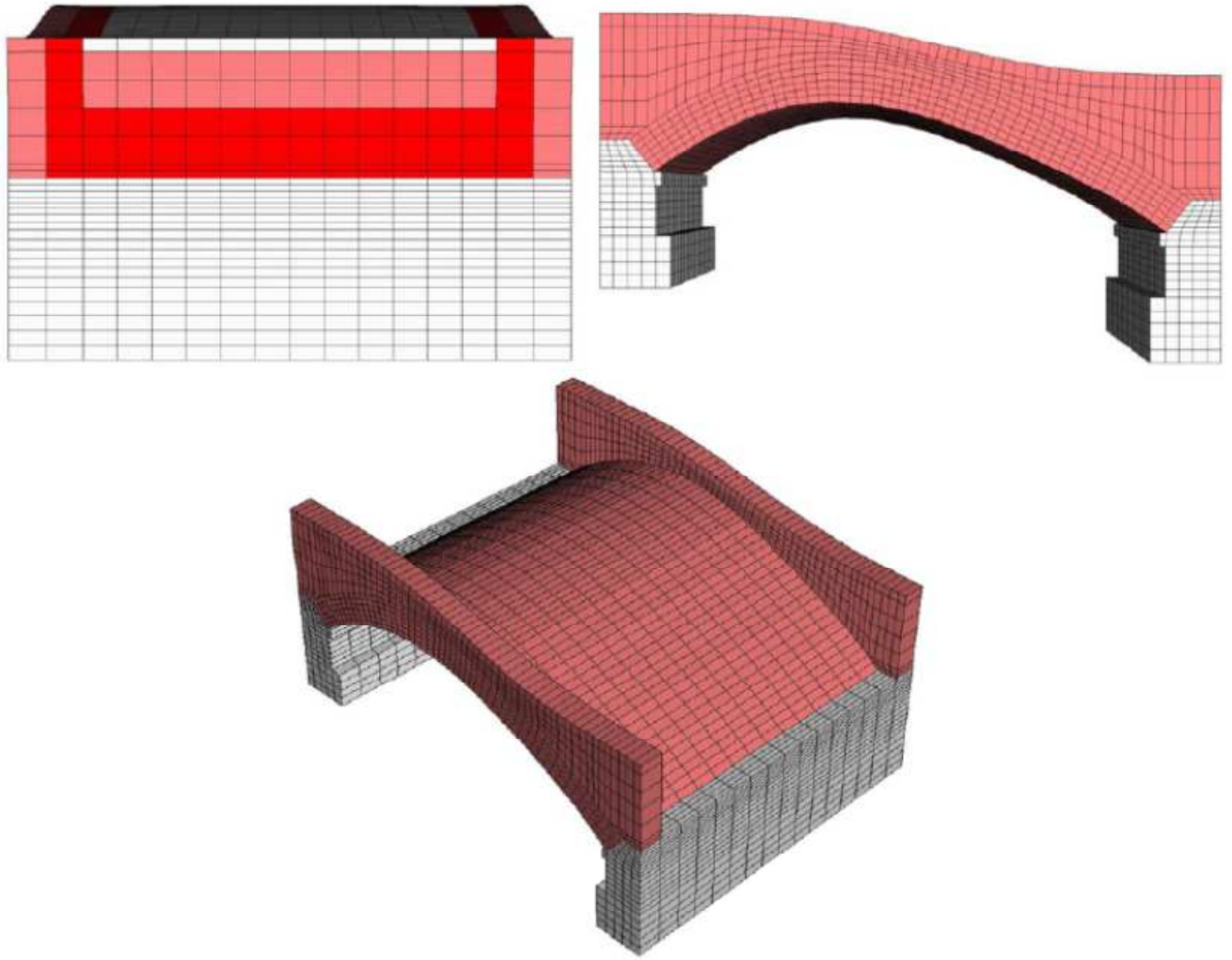

Figure 25: right pile settlement. –a: Deformed shape obtained with the non-commercial FE code. –b: formation of plastic hinges on the lower arch.

Torre Fornasini, XIII century, Poggio Renatico

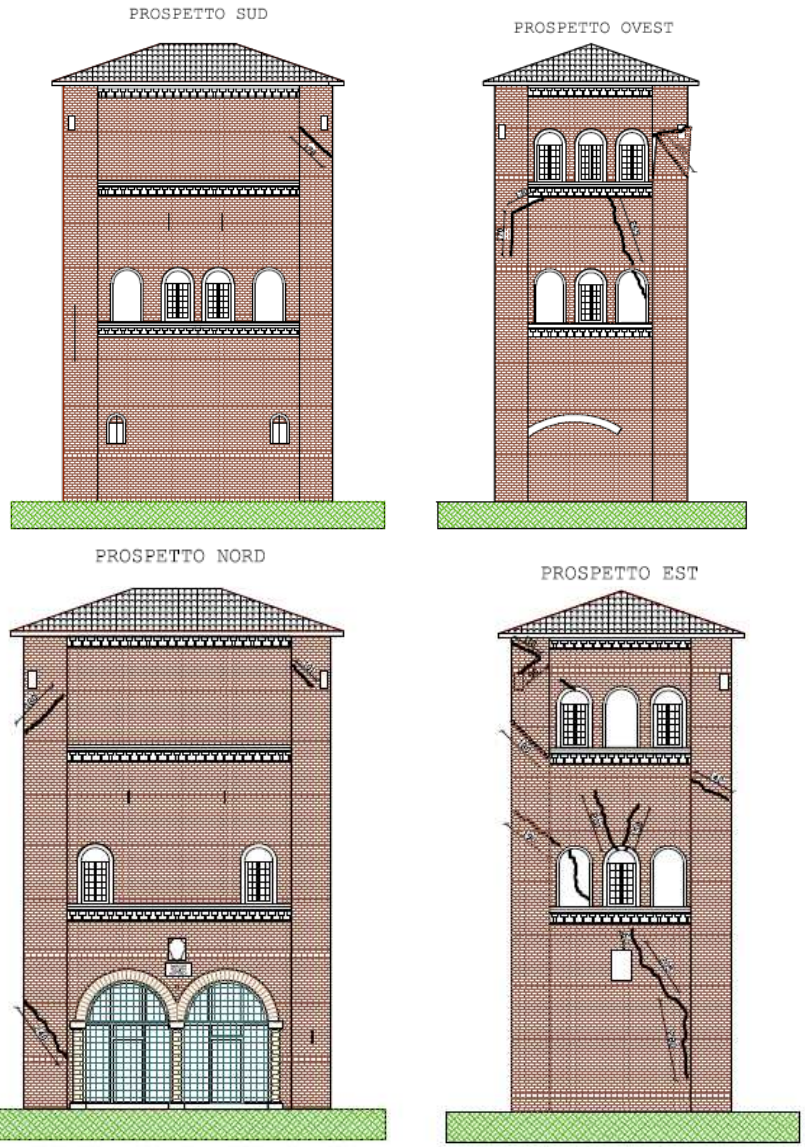

Torre Fornasini, XIII century, Poggio Renatico

Torre Fornasini, XIII century, Poggio Renatico

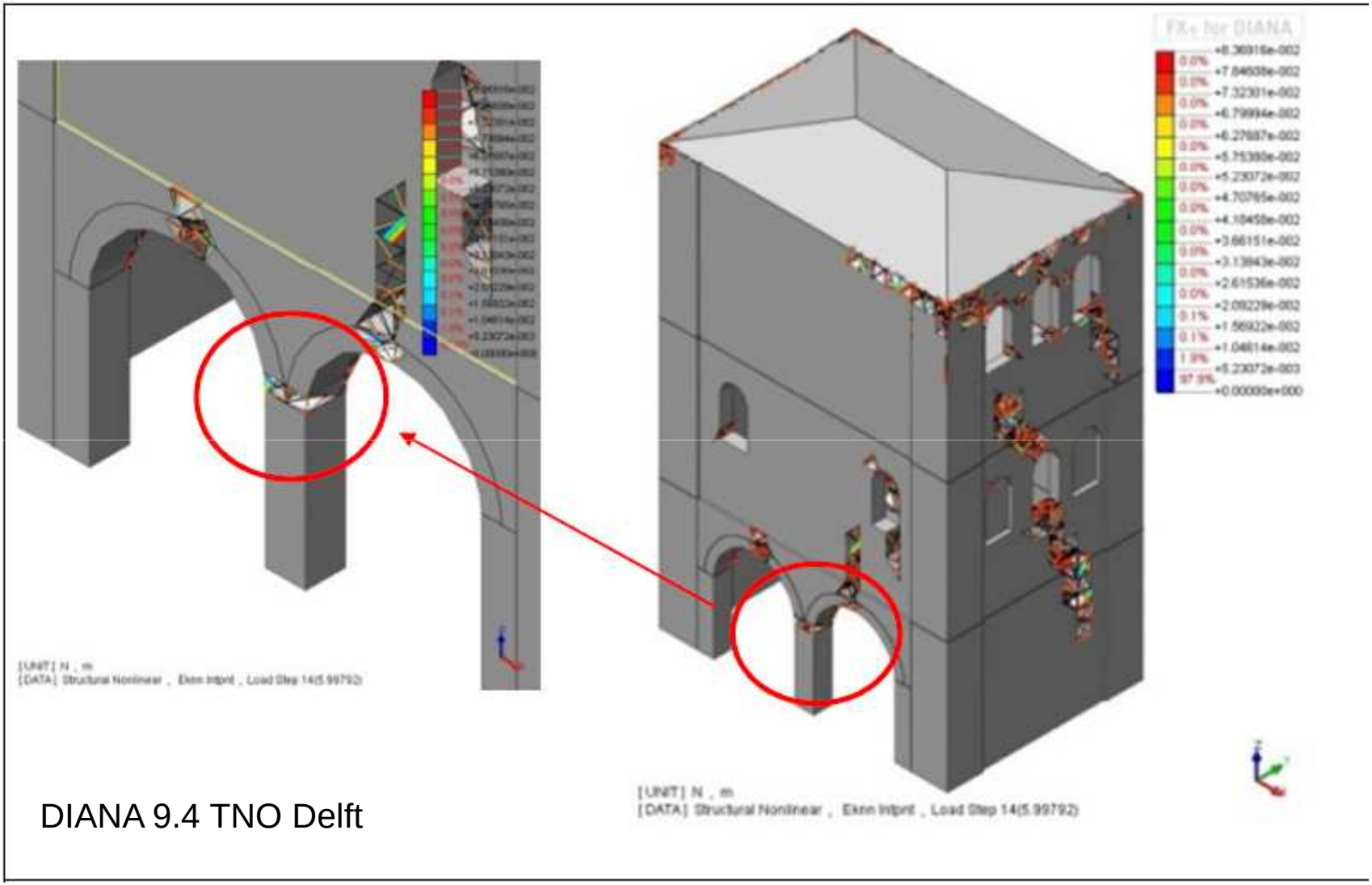

DIANA 9.4 TNO Delft

Torre Fornasini, XIII century, Poggio Renatico

Fig. 4. 51: Crack Pattern Direzione: -Y, Eccentricità: e >0, Materiale: Total Strain Crack Model, Taglio alla base: 827 kN; Spostamento: 10 mm

Torre Fornasini, XIII century, Poggio Renatico

Torre Fornasini, XIII century, Poggio Renatico

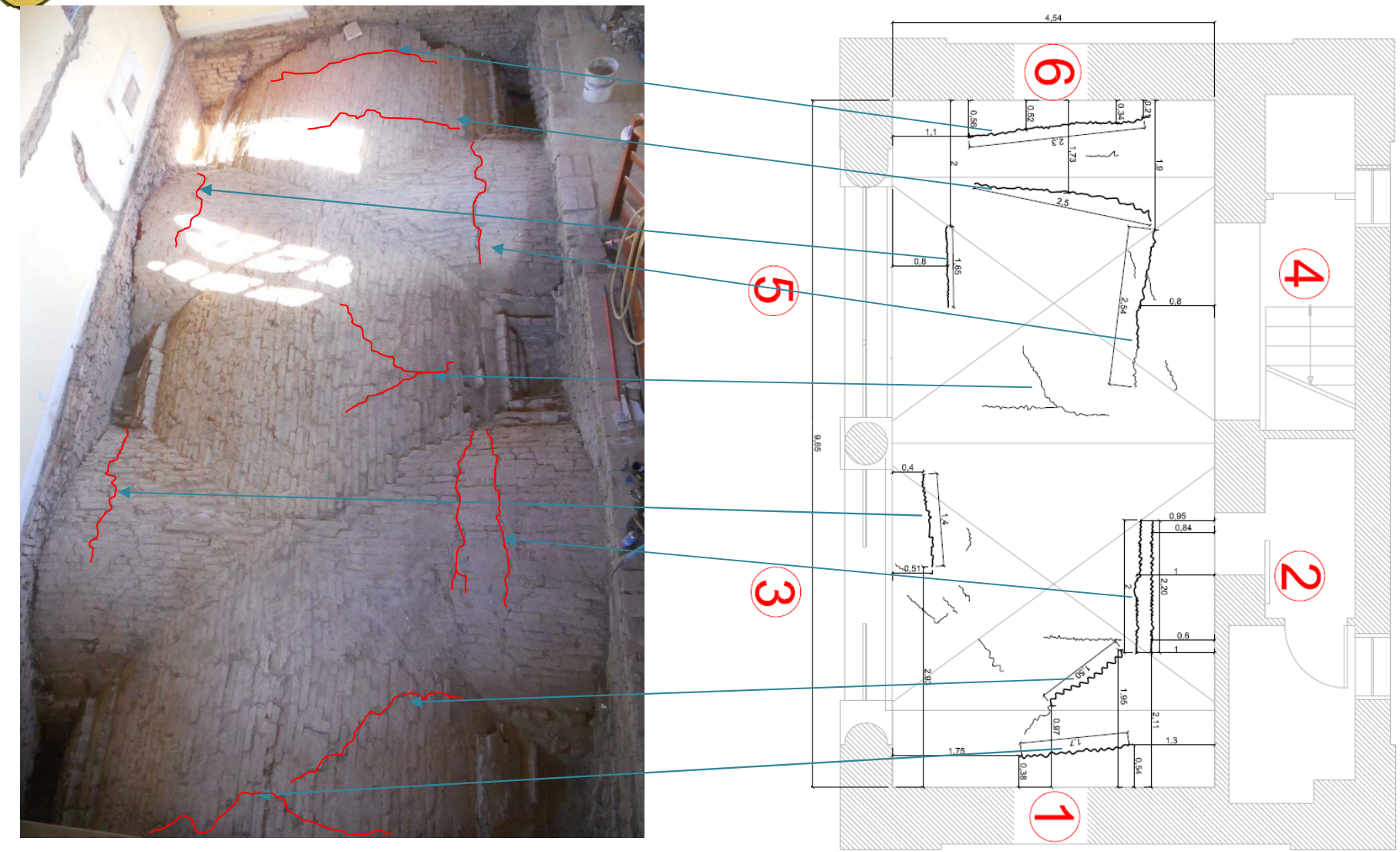

Torre Fornasini, XIII century, Poggio Renatico

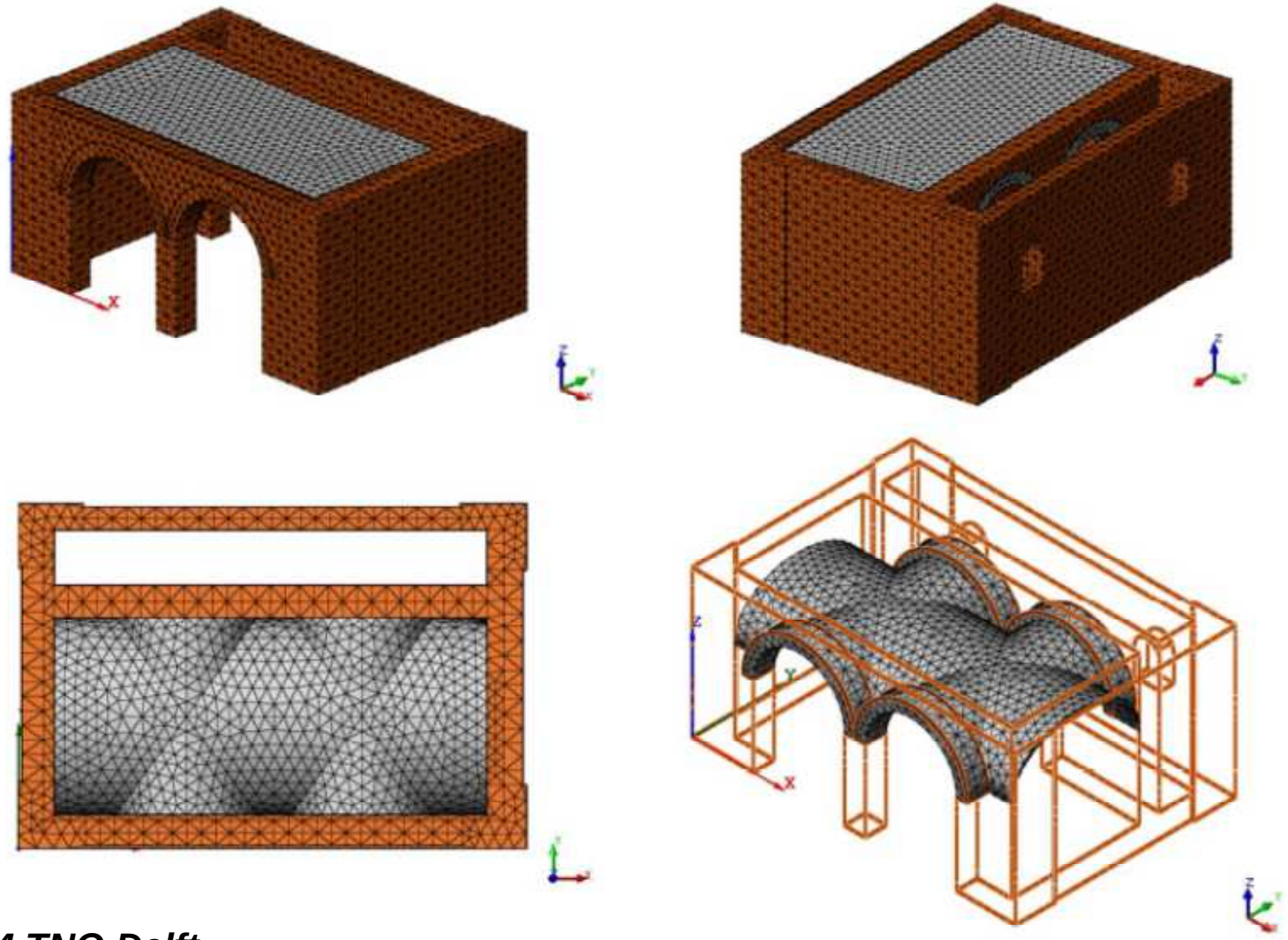

DIANA 9.4 TNO Delft

Fig. 5. 1: Discretizzazione mesh

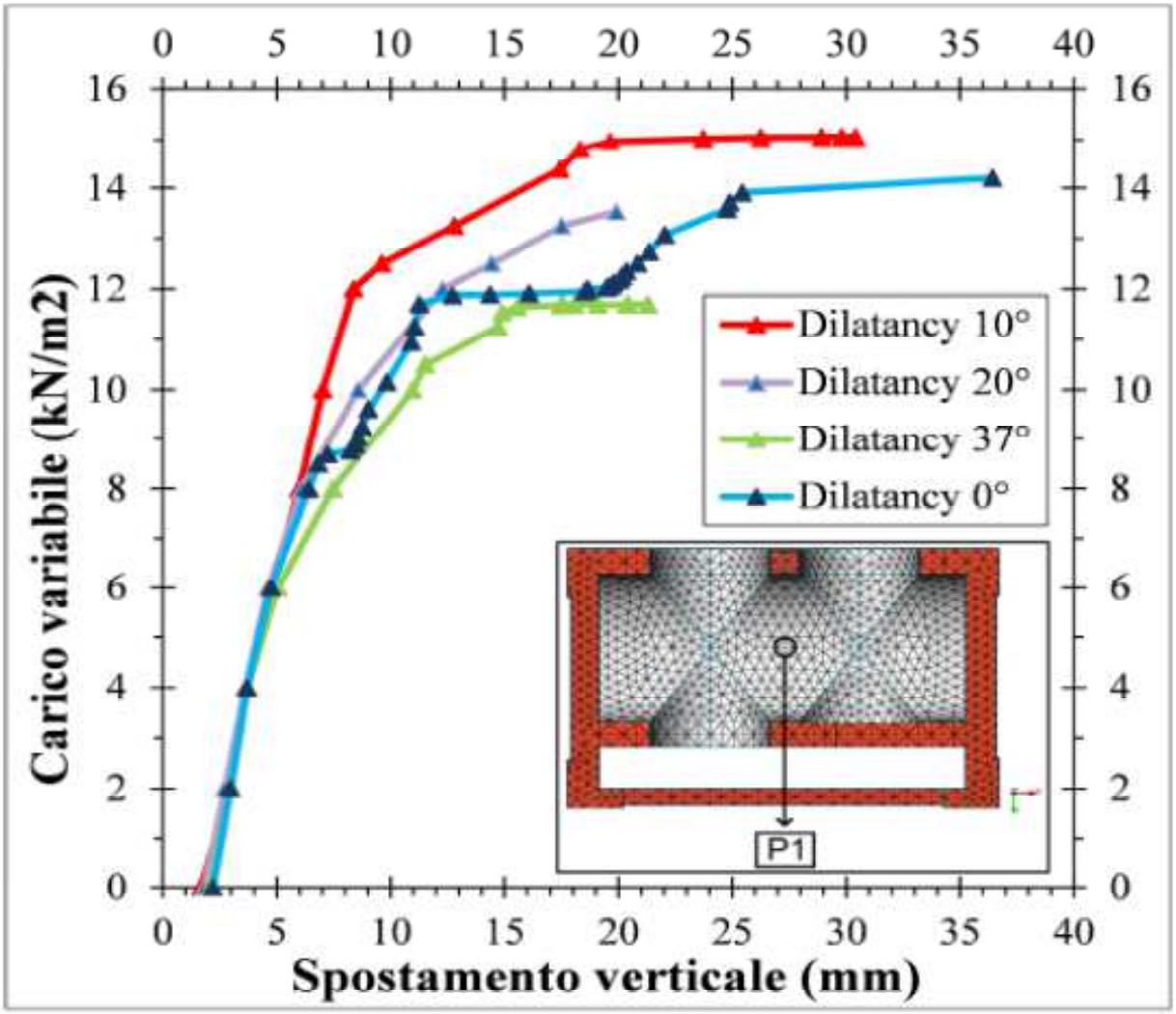

): Analisi incrementale ai carichi verticali. Confronto tra i vari angoli di dilatanza indagati per il punto di controllo P1.

Torre Fornasini, XIII century, Poggio Renatico

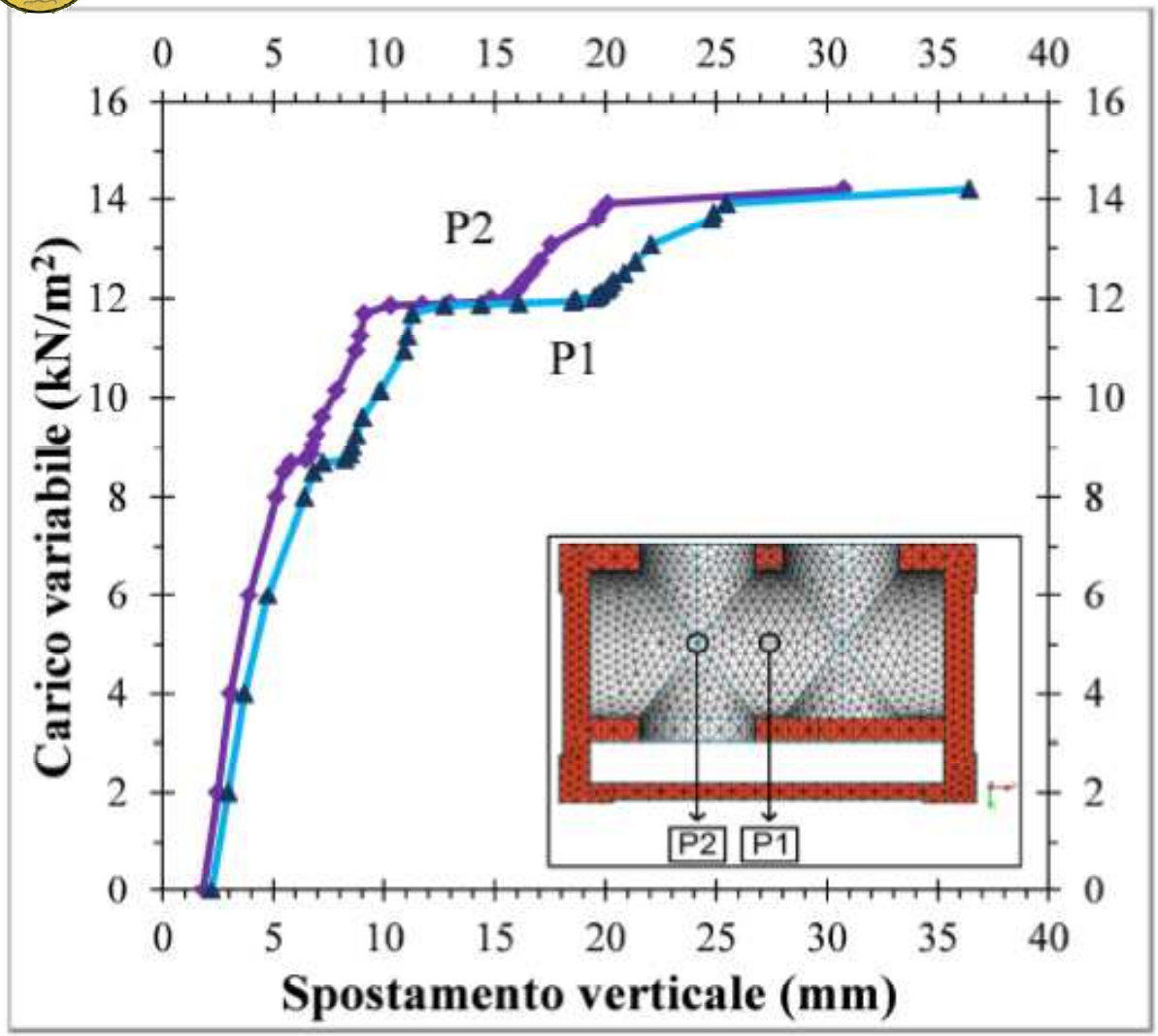

Fig. 5. 2: Analisi incrementale ai carichi verticali. Angolo di dilatanza 0°

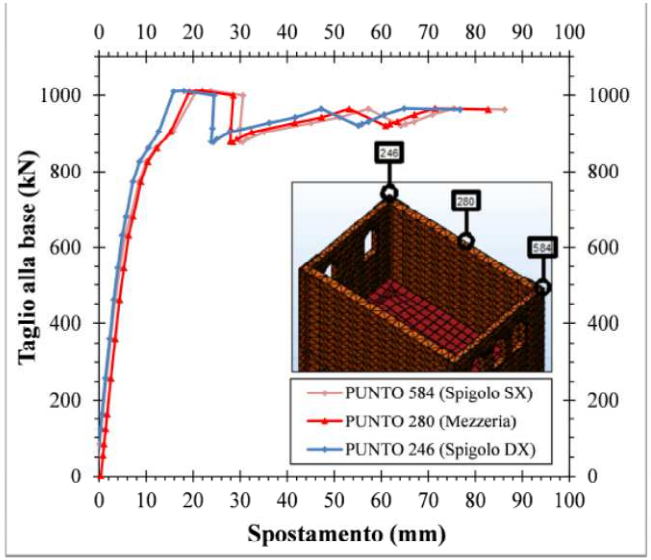

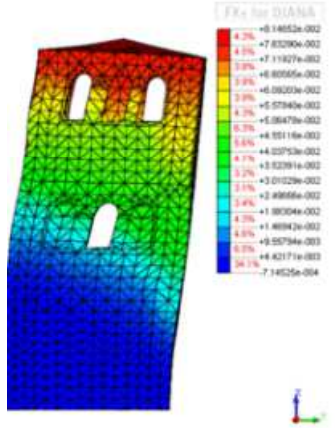

Fig. 4. 33: Spostamenti dY
listribuzione di forze principale, Base
shear: 922 kN, dY: 80,19 mm

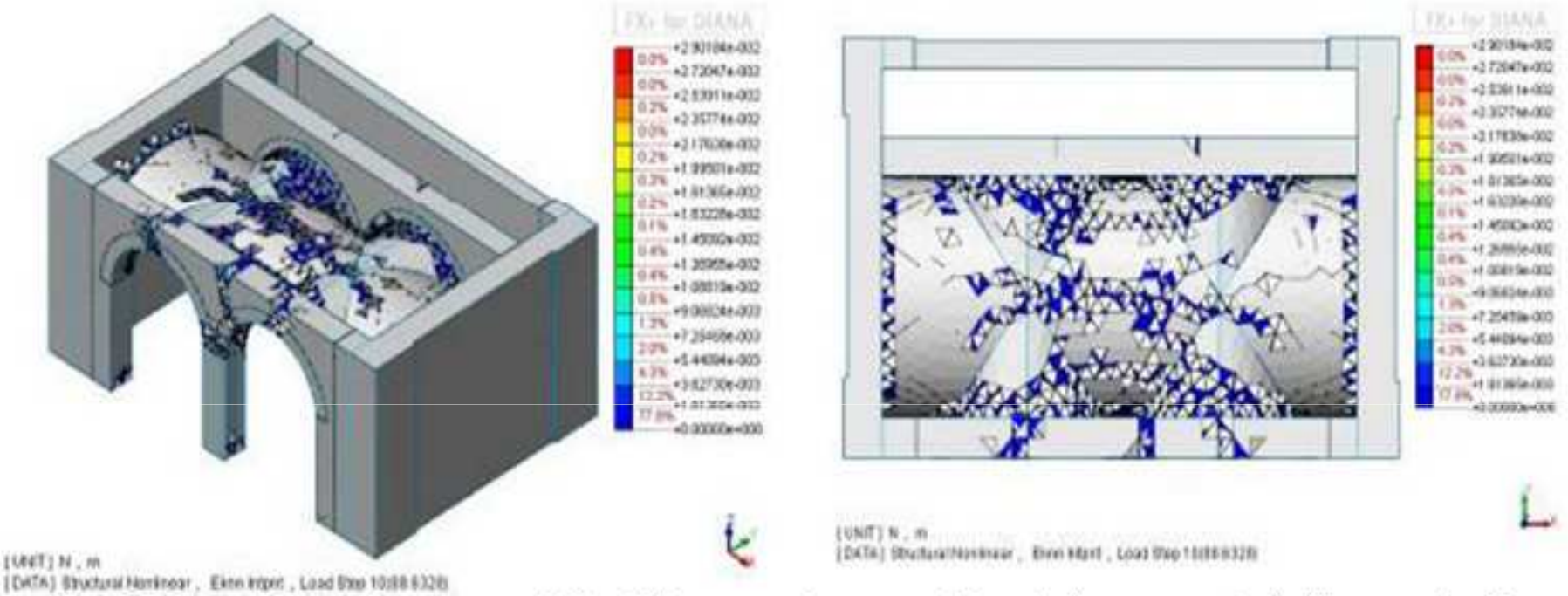

Fig. 5. 7: Stato di fessurazione ottenuto dall'analisi incrementale sotto carichi verticali per un angolo di dilatanza pari a 0°.

Torre Fornasini, XIII century, Poggio Renatico

Fig. 7. 4: Consolidamento delle volte mediante fibre di vetro e di carbonio all'estradosso

Fig. 7. 5: Particolare posa in opera delle fibre di carbonio

Torre Fornasini, XIII century, Poggio Renatico

Fig. 7. 7: Ripristino del riempimento originario delle volte

Fig. 7. 6: Particolare cerchiatura del primo solaio mediante UPN 80

A software for practitioners: ArchNURBS

ArchNURBS is distributed as an open-source project
(*http://sourceforge.net/projects/archnurbs/*).

ArchNURBS

Main features:

1. *Arch geometry fully described via NURBS functions*
2. *AutoCAD® geometry import function*
3. *Circular, lancet, elliptic, parabolic arch preset shapes*
4. *Wide choice of load conditions (backfill, vertical and horizontal load distr.)*
5. *Elastic analysis with a NURBS-based finite element method*
6. *"Heyman" limit analysis of the arch (taking into account the limited strength in compression)*
7. *Accounts for intrados and extrados FRP arch reinforcement*
8. *Plot of the collapse mechanism*
9. *Elastic analysis of cracked arch (not yet)*

ArchNURBS - the Graphical User Interface

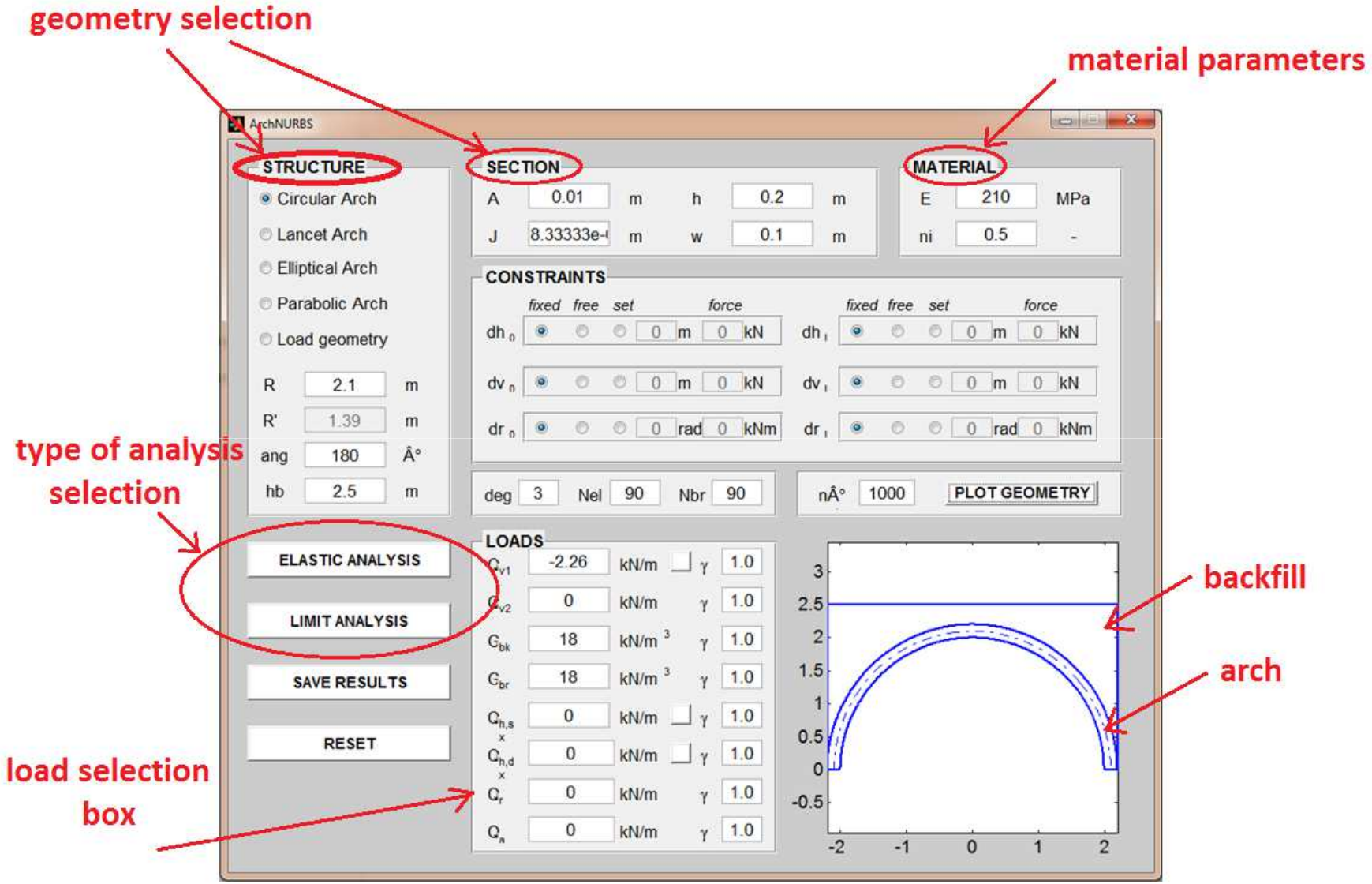

Example 1: uniformly loaded circular arch - ELASTIC ANALYSIS

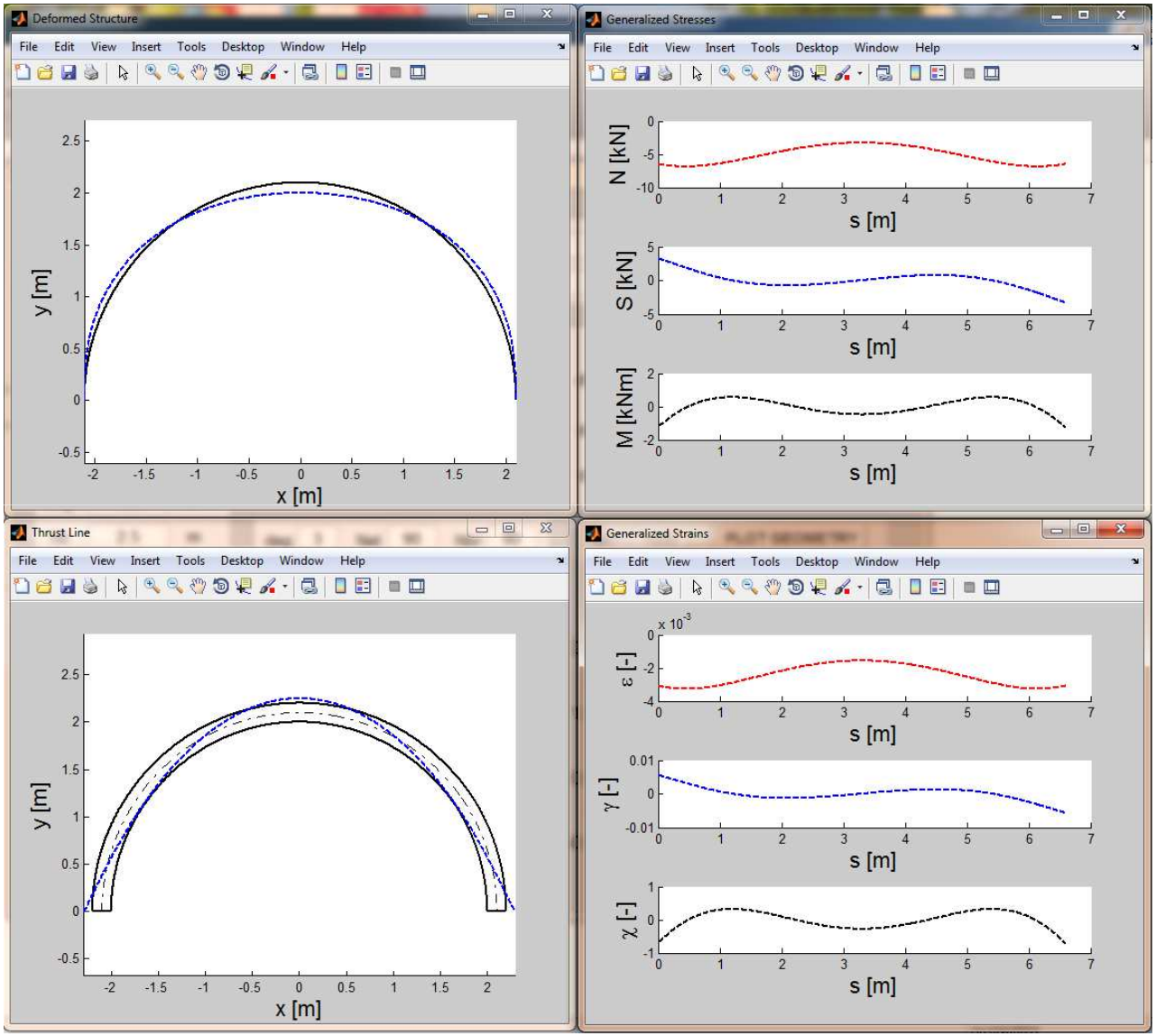

Example 1: uniformly loaded circular arch - LIMIT ANALYSIS

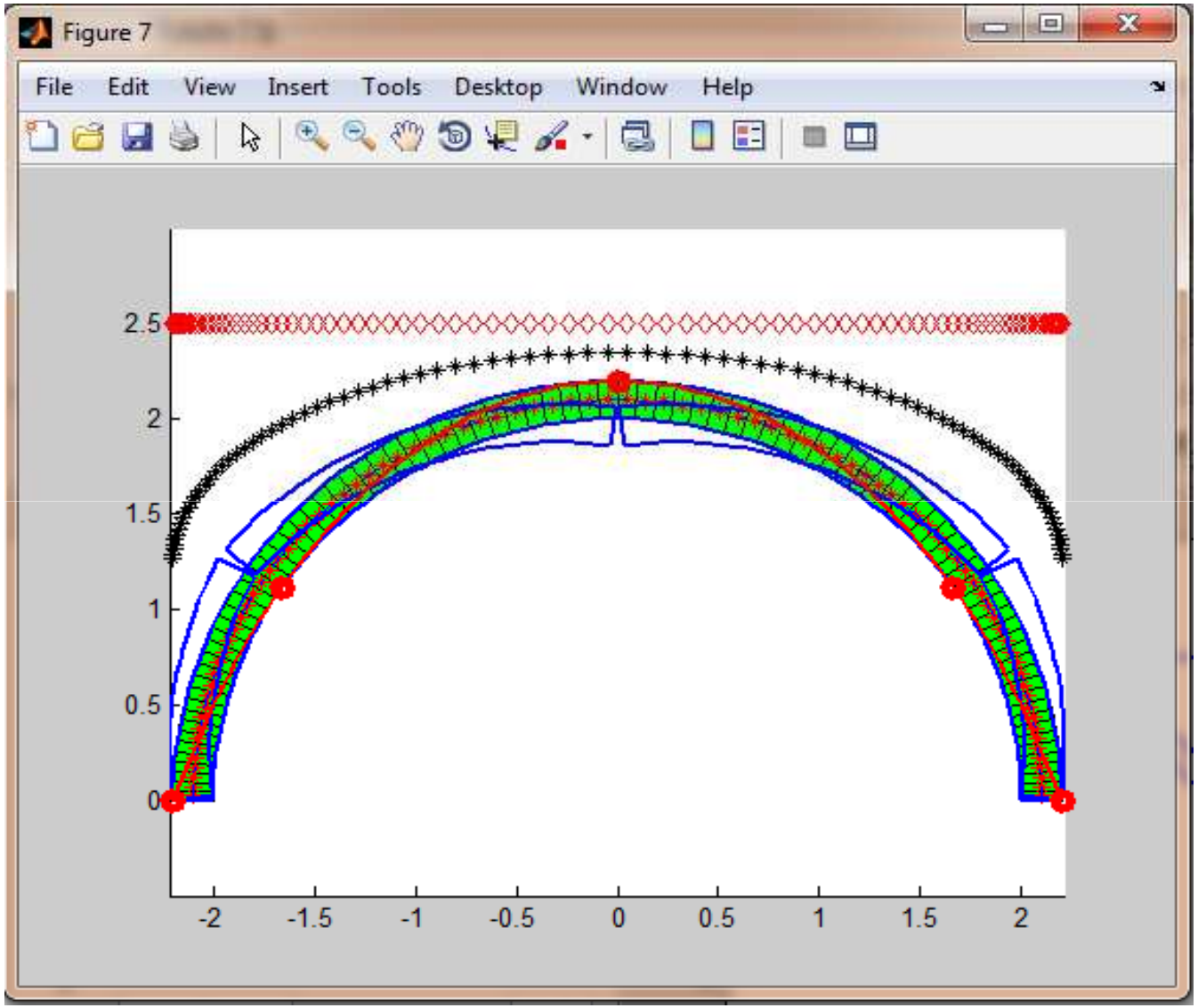

Example 2: uniformly loaded elliptic arch - LIMIT ANALYSIS

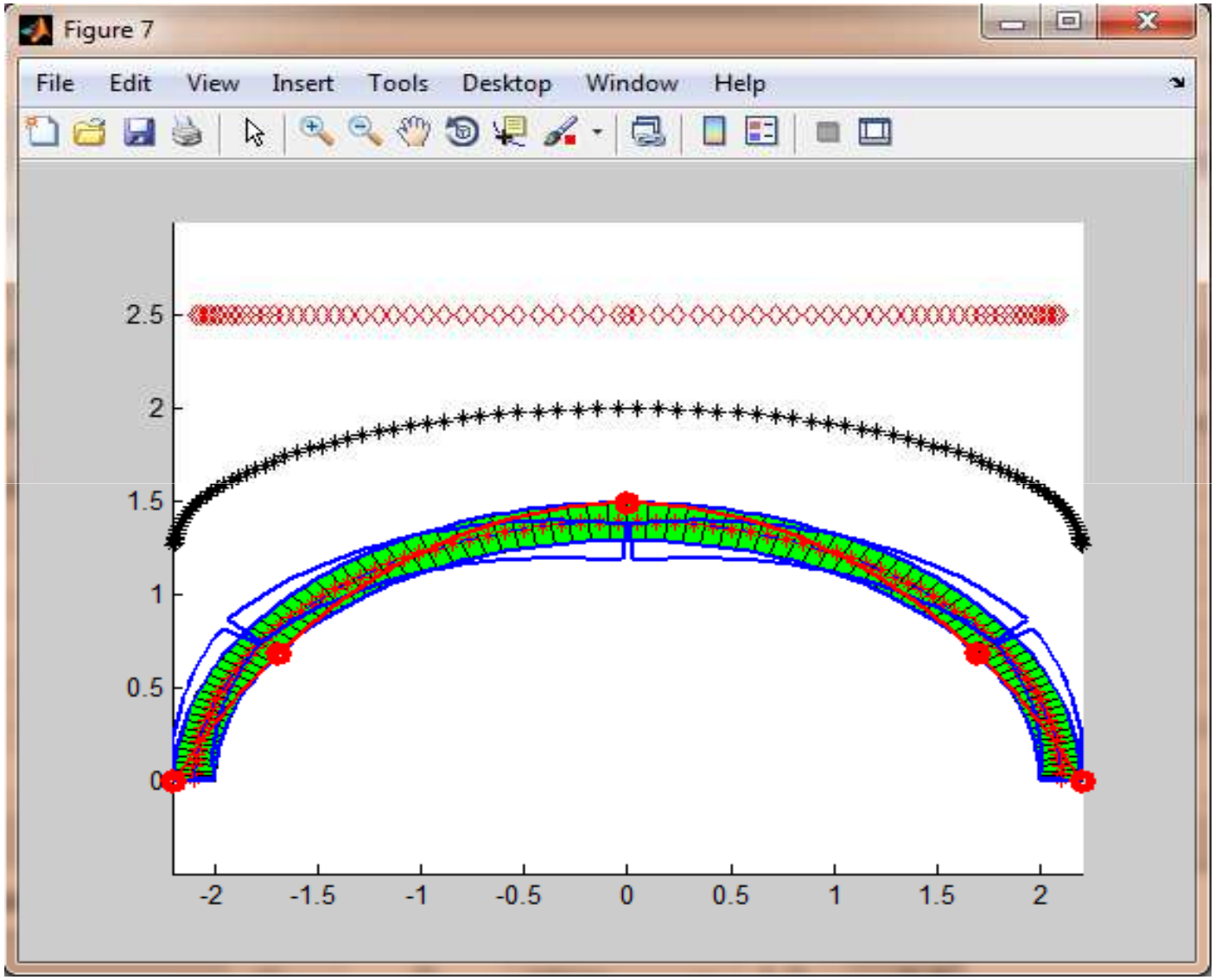

Arco policentrico

Llanelltid Bridge-94 Wales

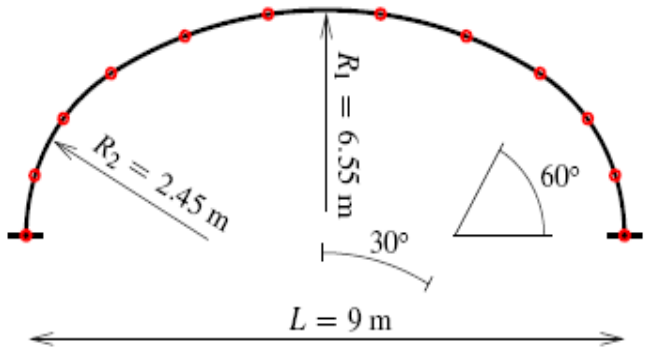

FIG. 2: Polycentric arch (red circles denote the interpolating points P_i)

n° of P_i	10	20	40
E_∞ [m]	1.34e-2	0.79e-2	0.39e-2
E_2 [m]	1.64e-3	3.73e-4	2.74e-5

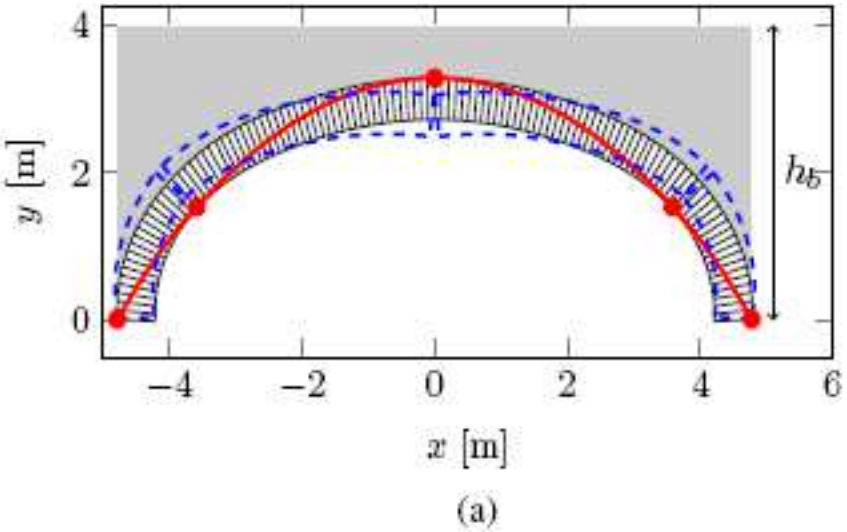

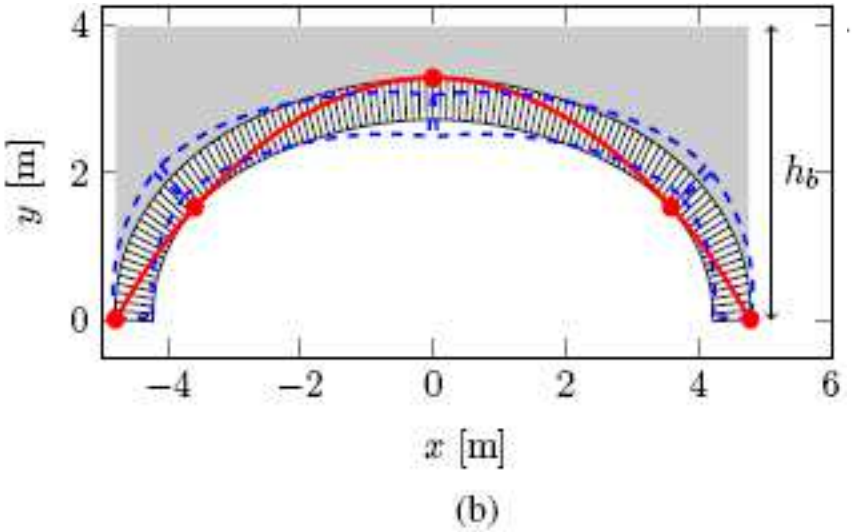

(a) Moltiplicatore 0,78 senza back-fill, (b) moltiplicatore con back-fill 21,62

Rounded voussoirs – semicircular arch

Porta Asinaria -Rome

Comparison
R=0,2125. t= 0,25m
Backfill 3m
Poligonal λ =8,9
Rounded λ = 9,8

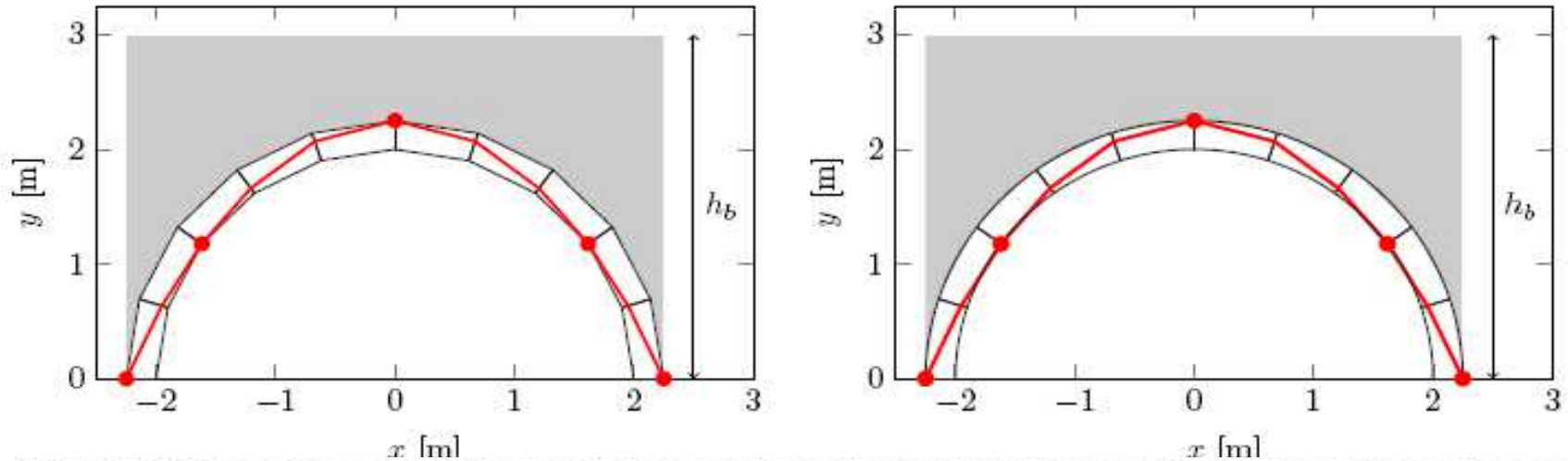

FIG. 4: Thrust lines computed with (a) quadrangular voussoirs and (b) rounded voussoirs example arch models.

Torre Fornasini, XIII century, Poggio Renatico

Torre Fornasini, XIII century, Poggio Renatico

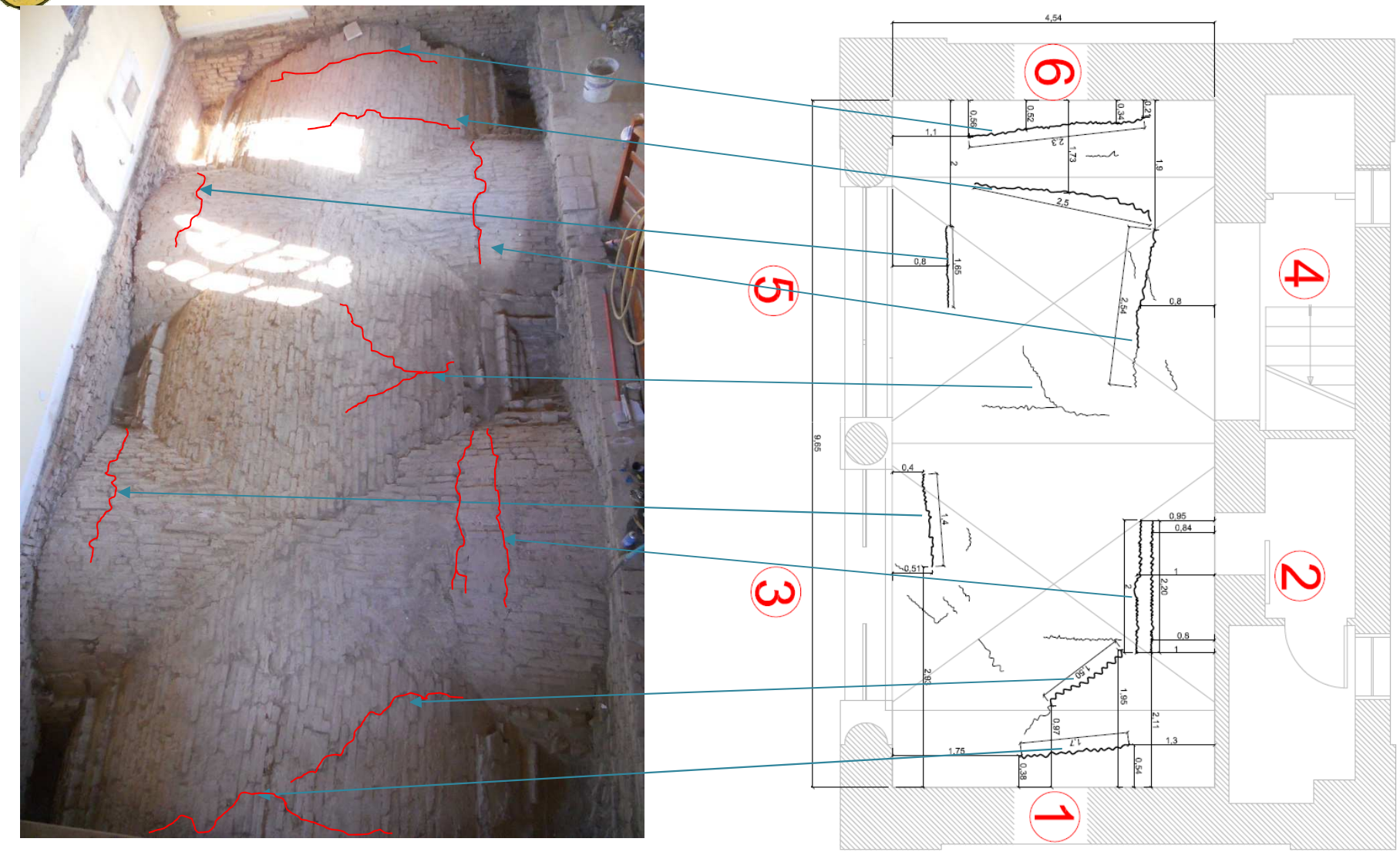

Torre Fornasini, XIII century, Poggio Renatico

Fig. 7. 4: Consolidamento delle volte mediante fibre di vetro e di carbonio all'estradosso

Fig. 7. 5: Particolare posa in opera delle fibre di carbonio

Torre Fornasini, XIII century, Poggio Renatico

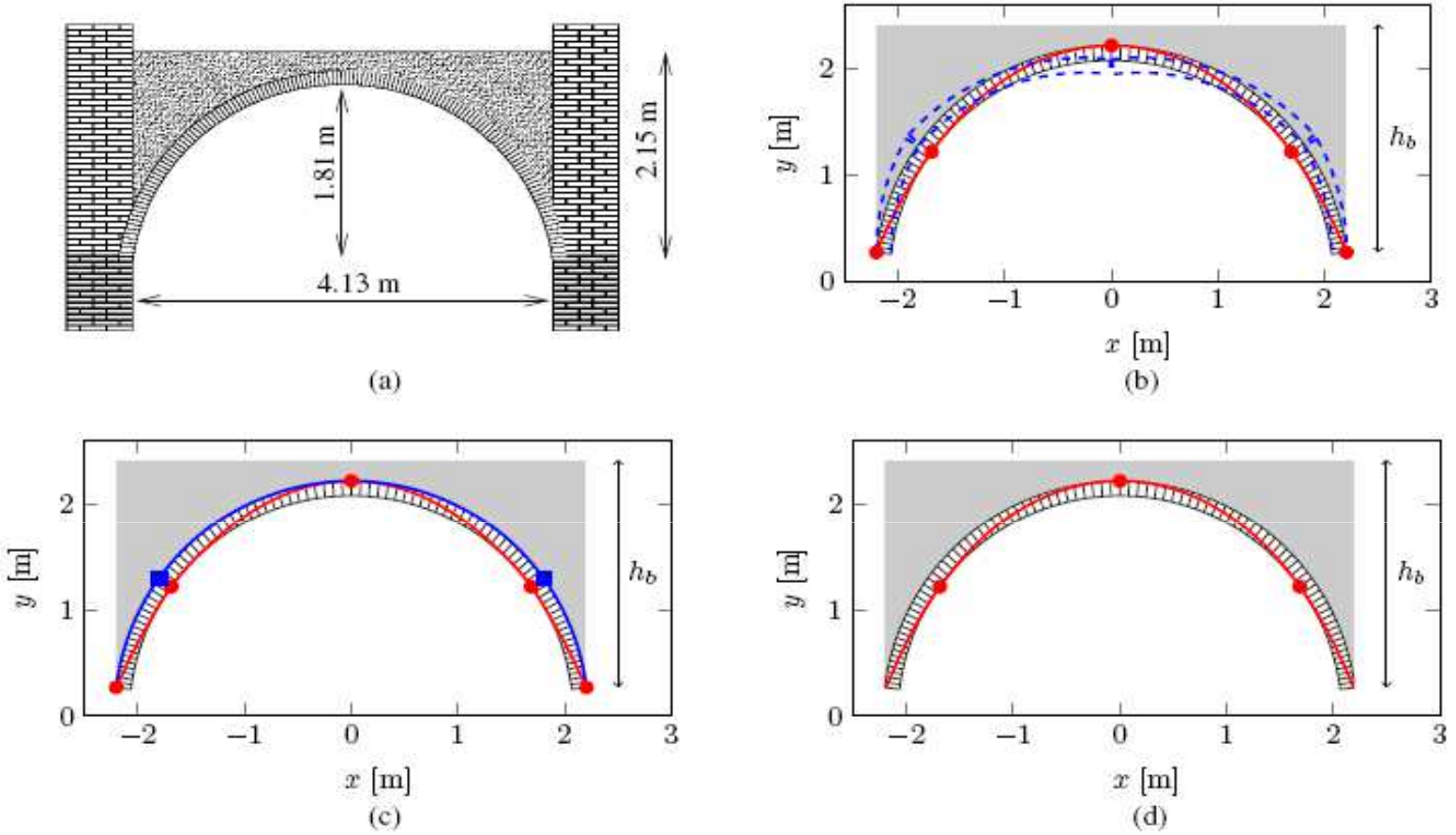

FIG. 7: A masonry arch from *Torre Fornasini* in Poggio Renatico, (Ferrara, Italy) and represented in (a) has been examined. The thrust line (solid red line) and the position of the hinges (red circles) at collapse are illustrated in (b). Moreover, the solution of the limit analysis has been studied by considering (c) the FRP reinforcement indicated with a solid blue line (blue solid squares denote the FRP delamination points) and (d) sliding between blocks (with $\mu = 0.275$).

Torre Fornasini, XIII century, Poggio Renatico

	Arch Configuration	Collapse Load Multiplier λ
without FRP	no backfill and unlimited masonry compressive strength	-
	backfill and unlimited masonry compressive strength	1.43
	backfill and limited masonry compressive strength	0.86
	backfill, unlimited masonry compressive strength and limited friction between blocks ($\mu = 0.3$)	1.43
	backfill, unlimited masonry compressive strength and limited friction between blocks ($\mu = 0.275$)	1.02
with FRP	backfill and unlimited masonry compressive strength	5.94
	backfill and limited masonry compressive strength	3.44

TABLE 3: Collapse load multipliers resulting from limit analysis of the arch analyzed in Section 5.3, belonging to Torre Fornasini (Poggio Renatico, Italy) groin vault, under different assumptions

A general method for determining collapse mechanism of masonry vaults

A general method for collapse mechanisms

PARABOLIC ARCH BRIDGE: NURBS MODEL

Rhinoceros®
NURBS modeling for Windows

IGES STANDARD

NURBS SURFACE MESHING

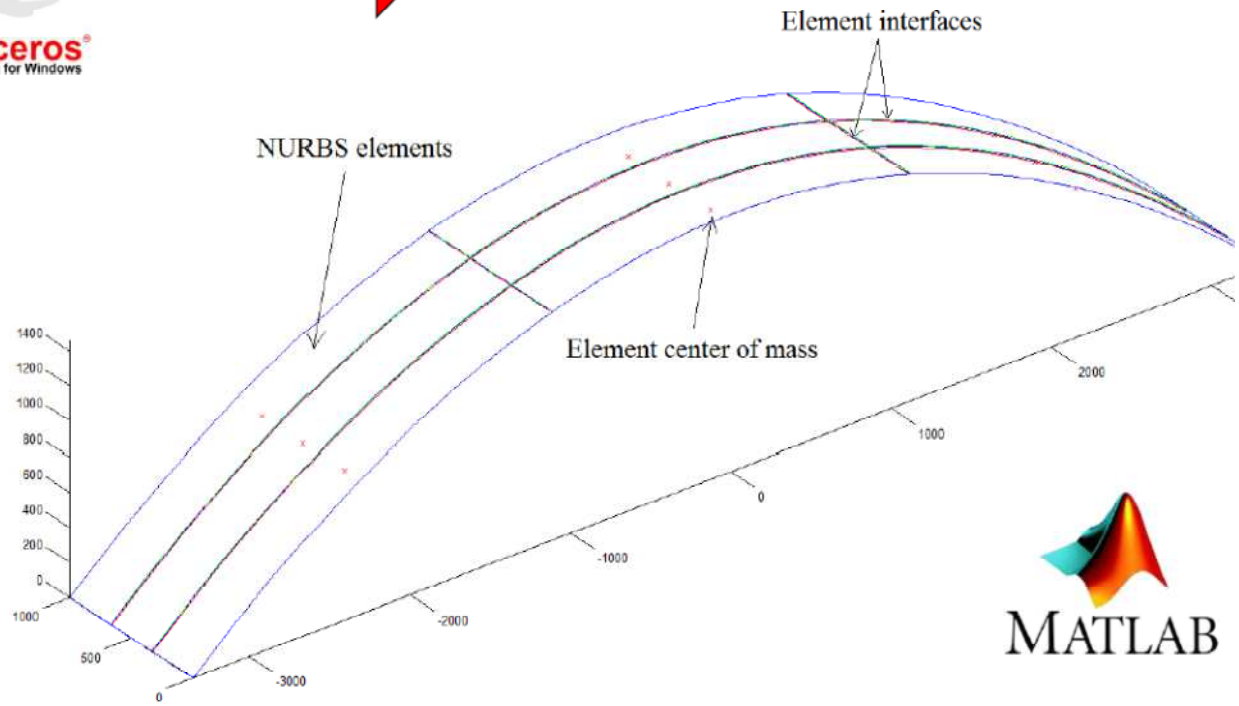

MATLAB

KINEMATIC APPROACH

- ***Sequencial limit analysis,***
- ***genetic algorithms***
- ***Discontinuity layout optimization (Gilbert)***

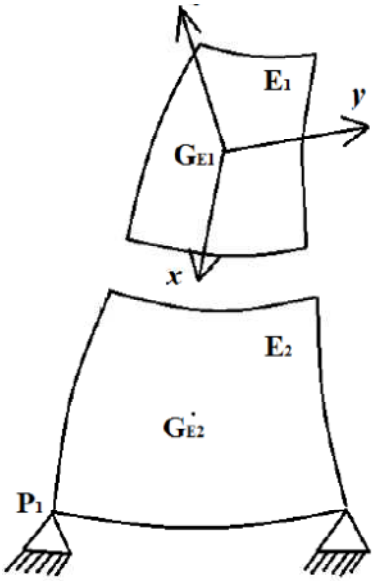

The structure is loaded by both *dead* (F_0) and *live* (Γ) external loads. Six unknown *generalized velocities* (three translations and three rotations) in the center of mass of each element are defined in a global reference system xyz:

$$\left\{u_x^{E_1}, u_y^{E_1}, u_z^{E_1}, \Phi_x^{E_1}, \Phi_y^{E_1}, \Phi_z^{E_1}\right\}$$

The ***optimization problem*** is written as follows:

$$\min\left\{D_{\text{int}} - P_{F_0}\right\}$$

where D_{int} is the internal dissipation (assumed to happen only on interfaces) and P_{F0} is the power of external dead loads. The interfaces have been discretized in a given number of slices which are identified by points P_i on the border of each interface. D_{int} is defined as follows:

$$D_{\text{int}} = \sum_{i=1}^{N_{interfaces}} \int_{A_i} \boldsymbol{\sigma} \cdot \Delta\tilde{u}\ dA_i$$

where $\boldsymbol{\sigma}$ is the local stress vector and Δu is the velocity difference on each point of the interface in a local reference system defined on the interface.

Thank you for your attention